Magnetic field sensors

Magnetic field sensors

- Hall effect devices
- Anisotropic magneto resistance (AMR) devices
- Giant magneto-resistance (GMR) devices
- Giant magneto-impedence (GMI) devices
- Fluxgates
- SQUIDs
- others….

Magnetic field sources

Charges in motion
Intrisic magnetic moments of particules (electrons, protons, neutrons ...)


Current in wire

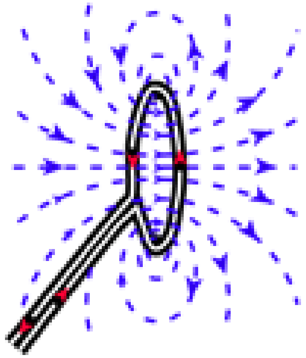
Loop of wire

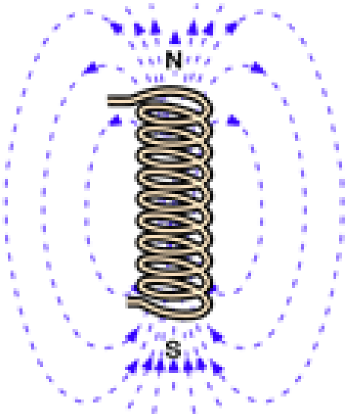
Solenoid

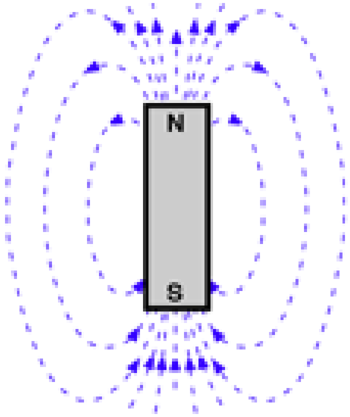
Bar Magnet

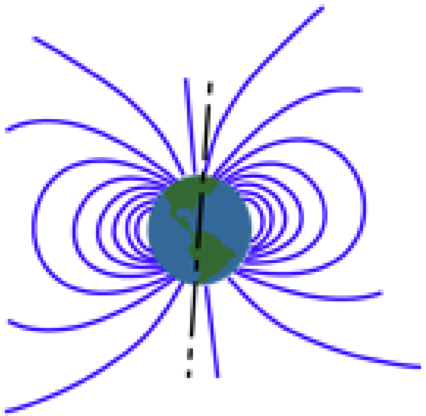
The Earth

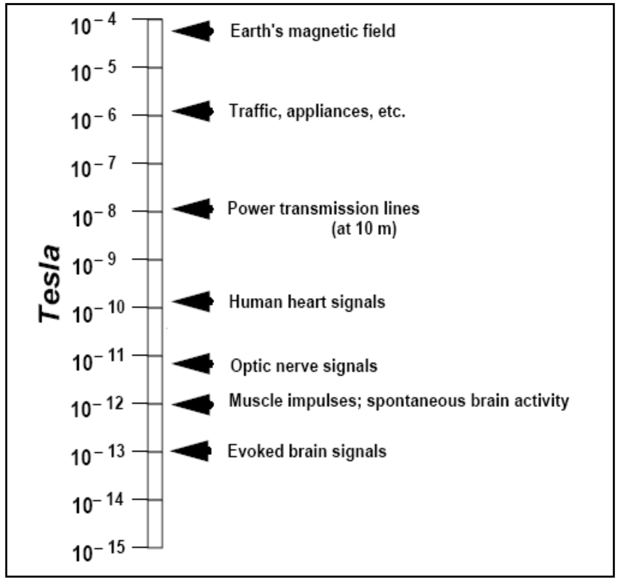

Coils with currents
< 100 T typ.

Permanent magnets
< 10 T typ.

Earth (on the surface)
~ 0.1 mT

Sources of «weak» magnetic fields (down to fT)

A distribution of static electric charges produces a static electric field.

A distribution of steady electric currents produces a static magnetic field.

Magnetic field sensors

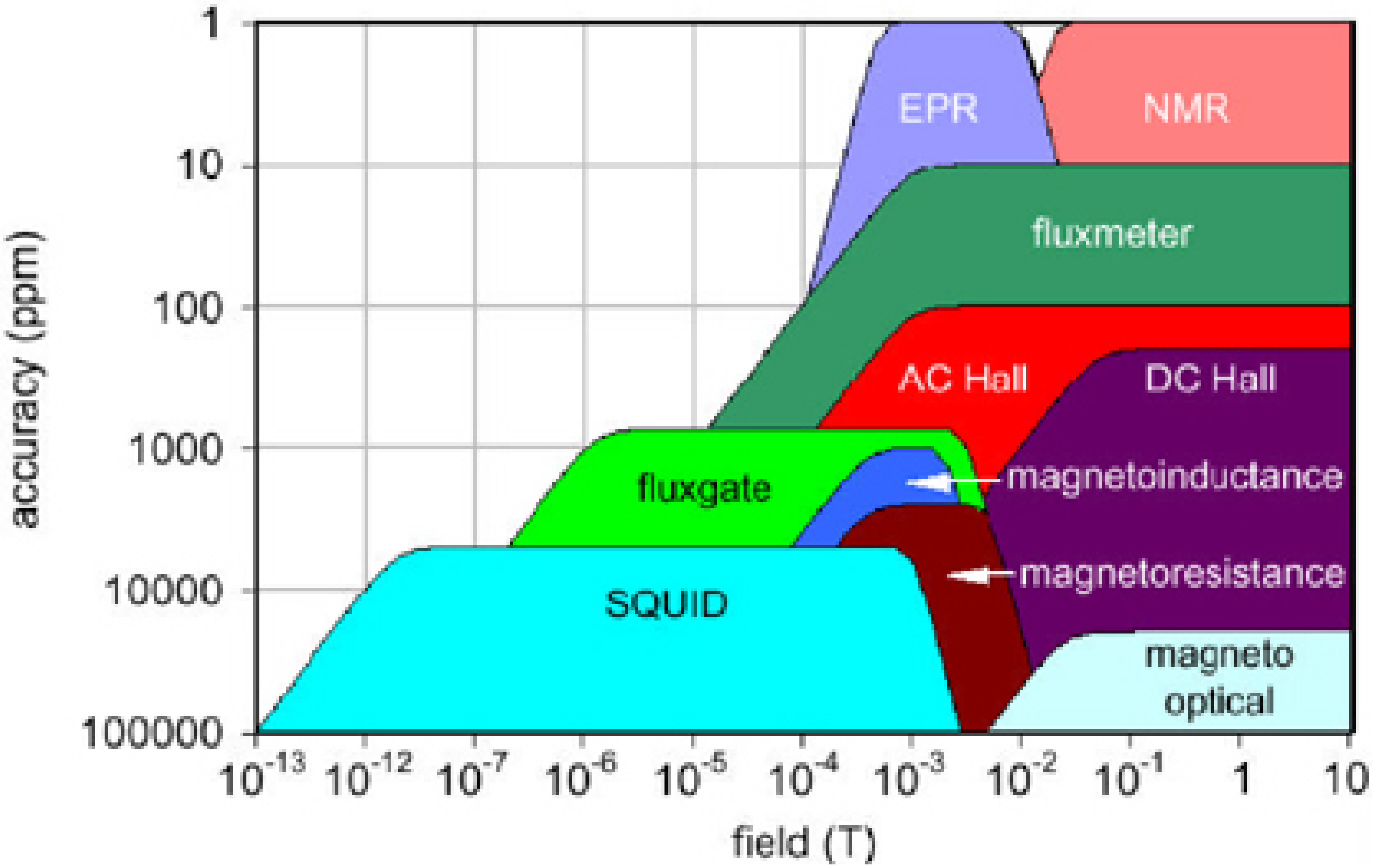

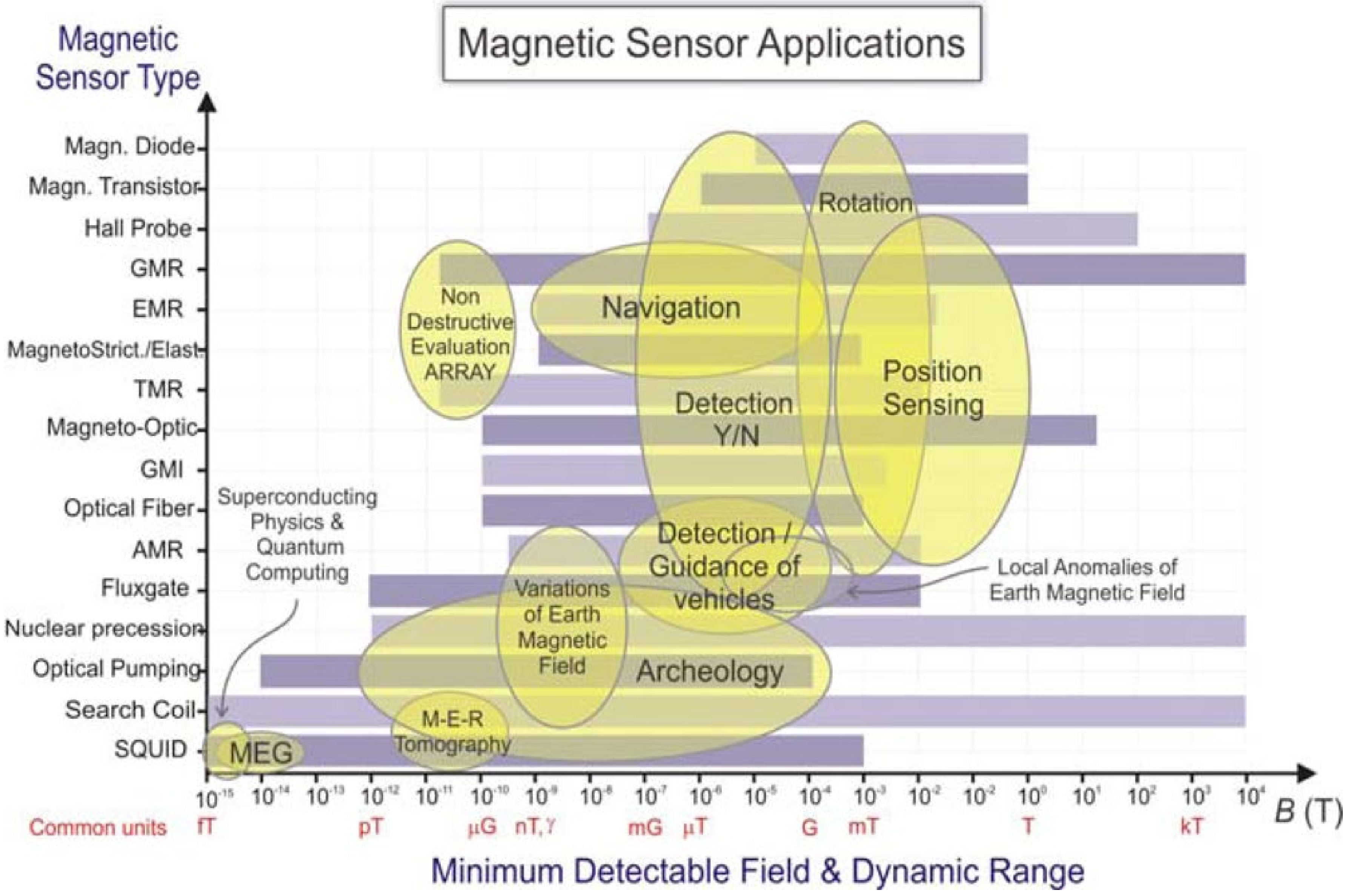

Magnetic Sensor Applications
Magnetic Sensor Type
Magn. Diode
Magn. Transistor
Hall Probe
GMR
EMR
MagnetoStrict./Elast.
TMR
Magneto-Optic
GMI
Optical Fiber
AMR
Fluxgate
Nuclear precession
Optical Pumping
Search Coil
SQUID
Rotation
Navigation
Non Destructive Evaluation ARRAY
Position Sensing
Detection Y/N
Detection / Guidance of vehicles
Superconducting Physics & Quantum Computing
Local Anomalies of Earth Magnetic Field
Variations of Earth Magnetic Field
Archeology
M-E-R Tomography
MEG
B (T)
Common units
fT
pT
µG
nT, γ
mG
µT
G
mT
T
kT
Minimum Detectable Field & Dynamic Range

Magnetic field sensors market

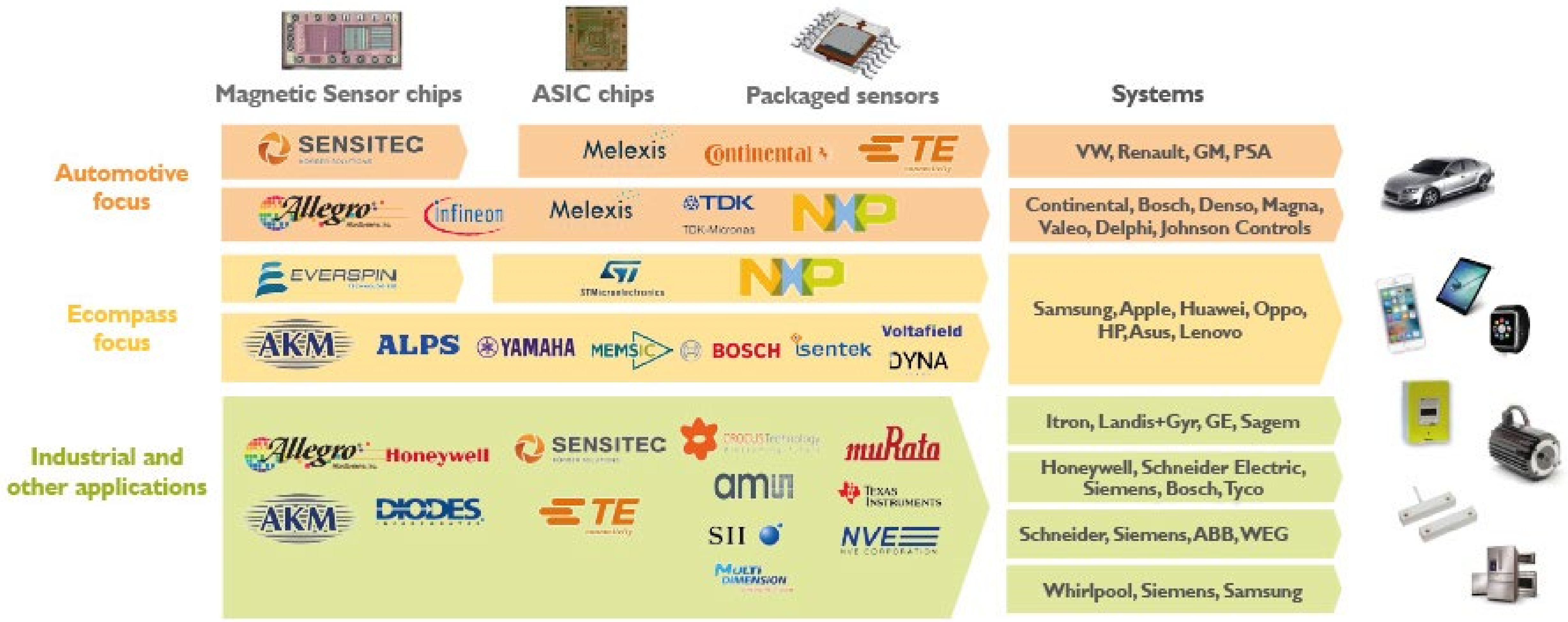

*Non-exhaustive list of the magnetic sensor supply chain and its key players

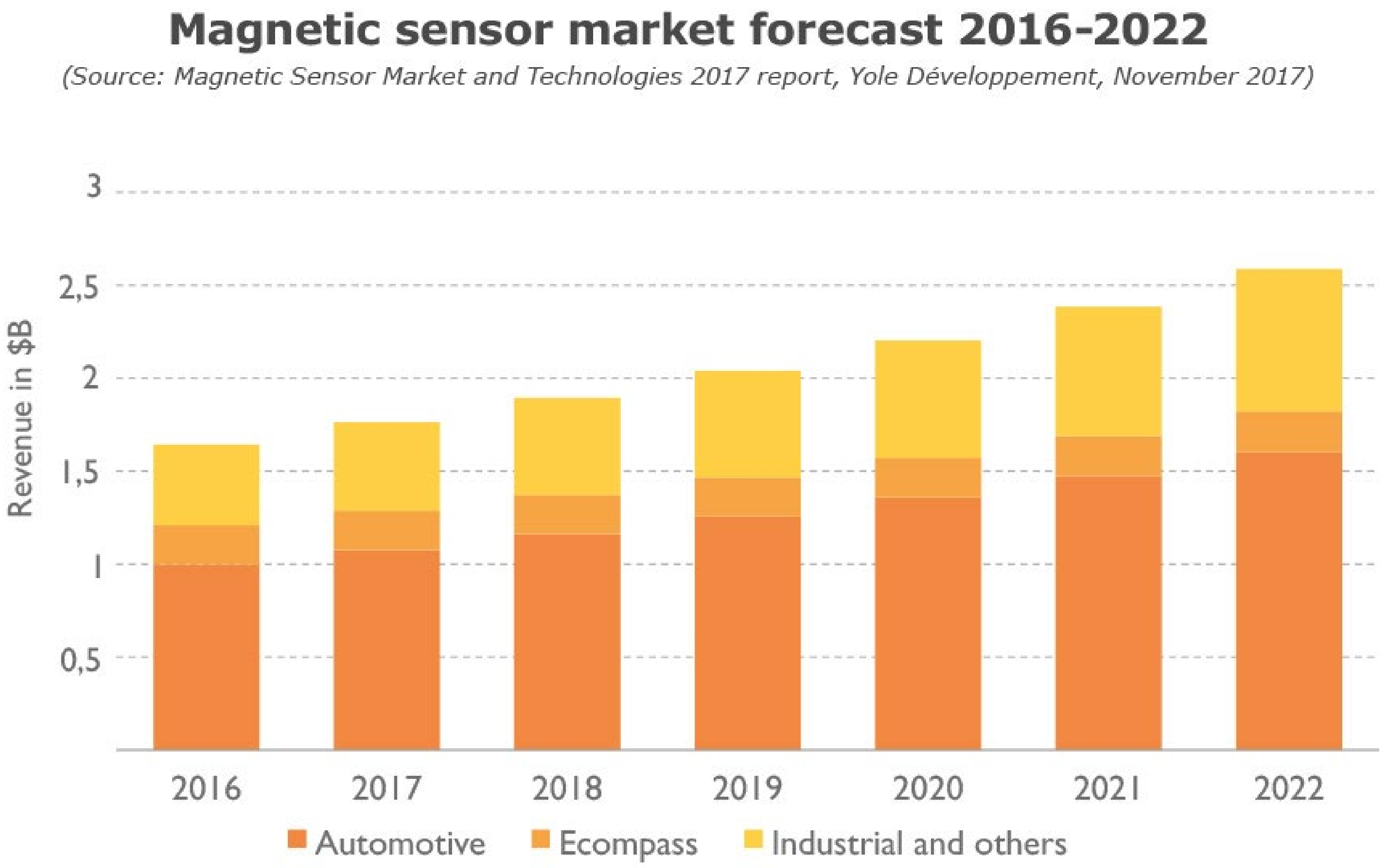
Magnetic sensor market forecast 2016-2022
(Source: Magnetic Sensor Market and Technologies 2017 report, Yole Développement, November 2017)
Revenue in $B
3
2,5
2
1,5
1
0,5
2016
2017
2018
2019
2020
2021
2022
Automotive
Ecompass
Industrial and others

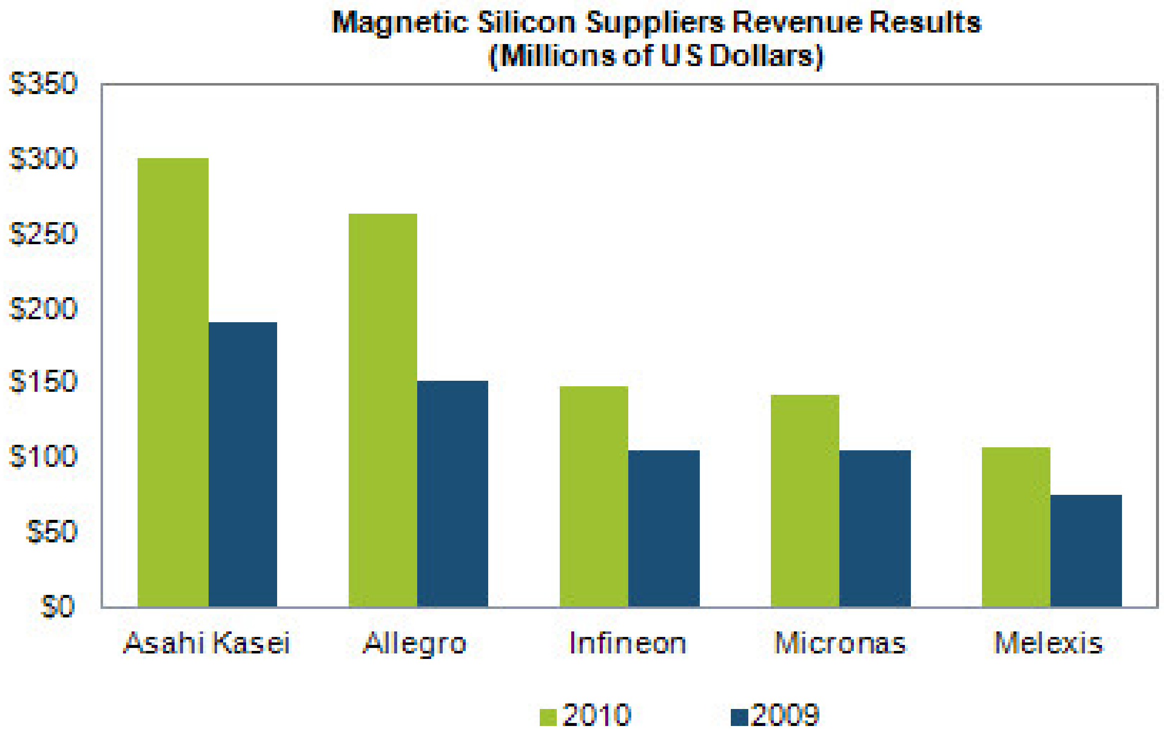

"With a production volume of over
100 million Hall elements per month,
Asahi Kasei Co. serves the needs of some 70%
of the world market"

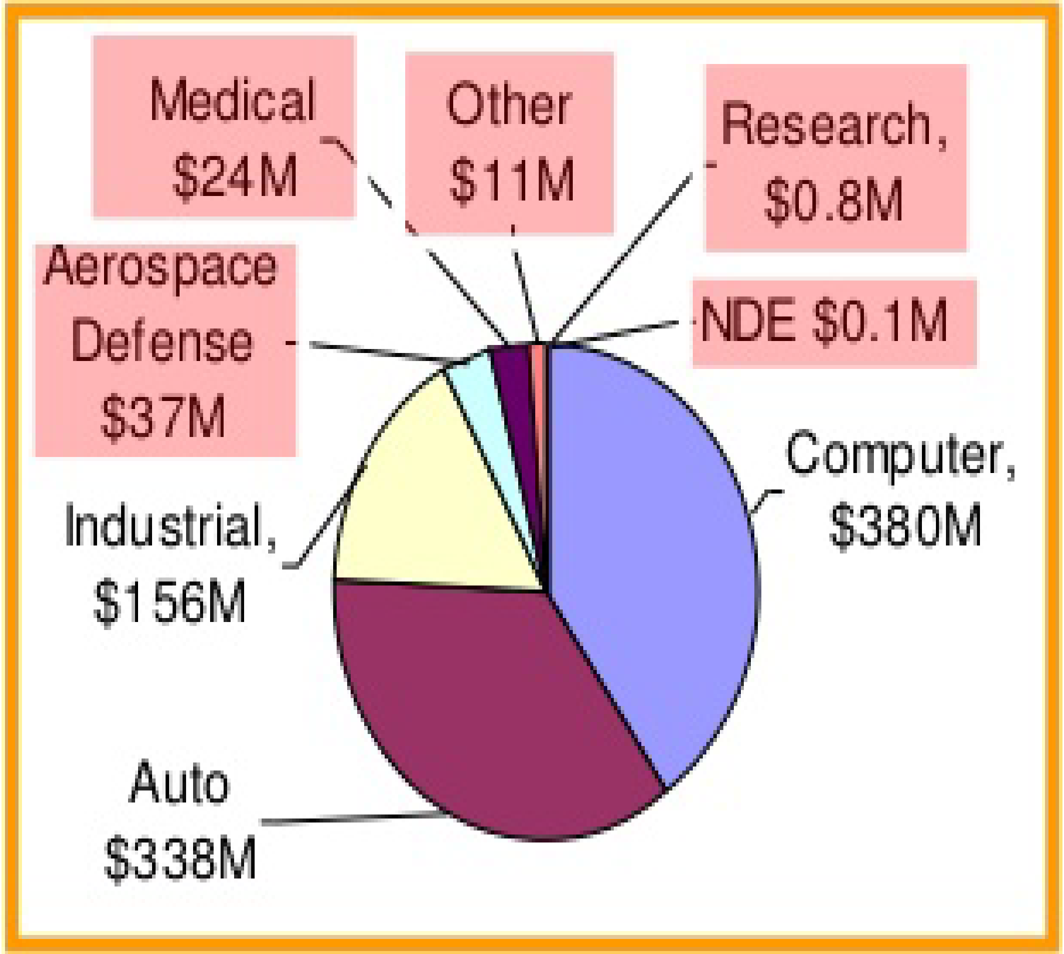

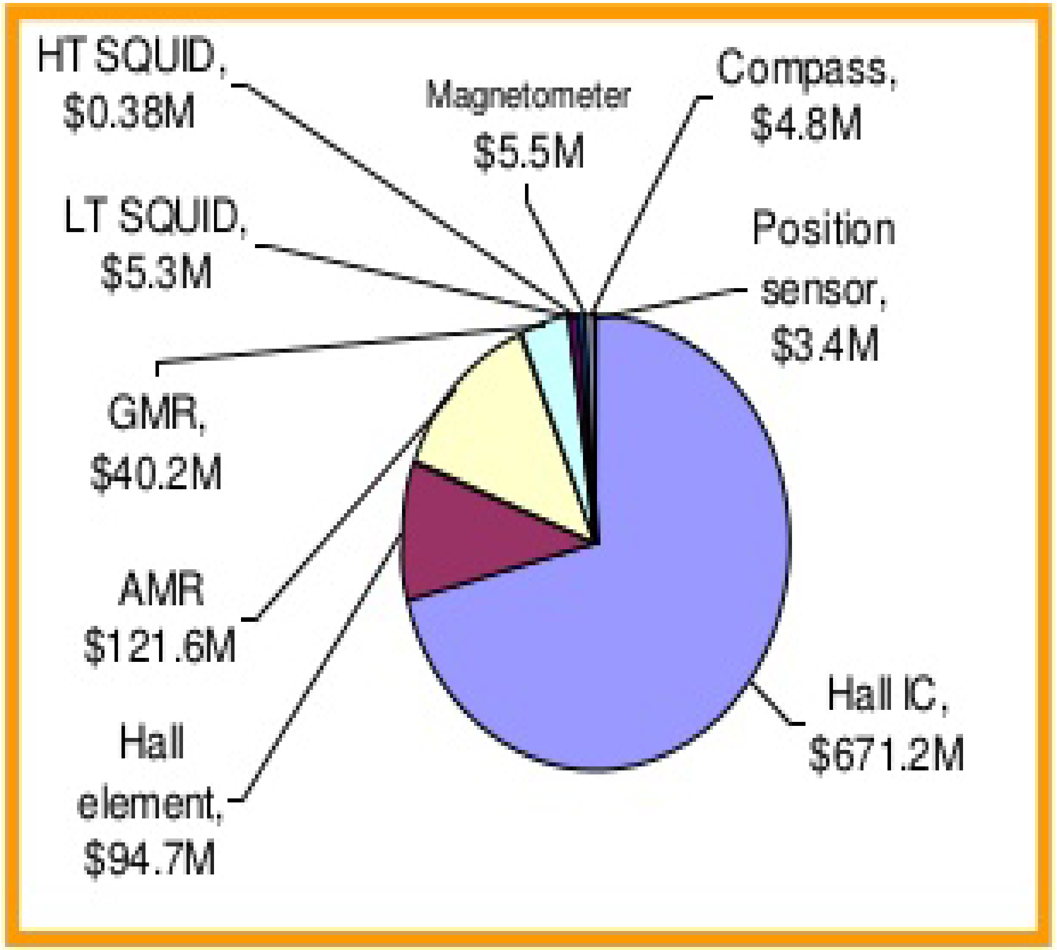

Application ***Sensor type***

World magnetic sensors components and module/subsystems markets (Frost & Sullivan 2005)

Technology	Hall Effect	AMR	GMR	TMR
Power Consumption (mA)	5 ~ 20	1 ~ 10	1 ~ 10	0.001 ~ 0.01
Die Size (mm^2)	1 × 1	1 × 1	1 × 2	0.5 × 0.5
Field Sensitivity (mV/V/Oe)	~ 0.05	~ 1	~ 3	~ 100
Dynamic Range (Oe)	~ 10000	~ 10	~ 100	~ 1000
Resolution ($nT/Hz^{1/2}$)	>100	0.1 ~ 10	1 ~ 10	0.1 ~ 10
Temperature Performance (℃)	< 150	< 150	< 150	< 200

Hall effect devices

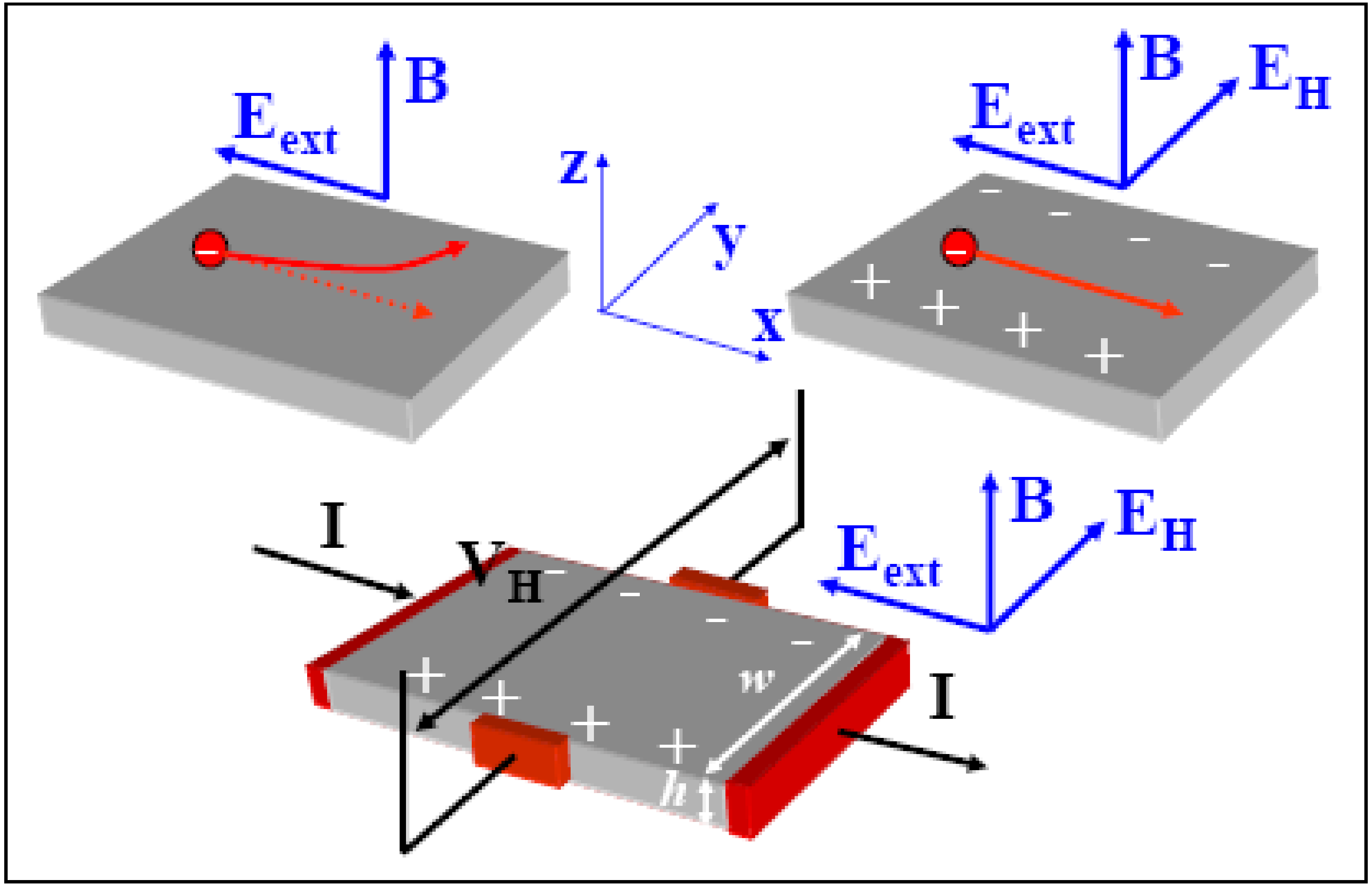

$$\mathbf{F} = e(\mathbf{E} + \mathbf{v} \wedge \mathbf{B})$$

Lorentz force :

$$\mathbf{F} = e\left(\mathbf{E} + \mathbf{v} \wedge \mathbf{B}\right)$$

$$F_x = e\left(E_x + v_y B_z - v_z B_y\right)$$

$$F_y = e\left(E_y - v_x B_z + v_z B_x\right)$$

$$F_z = e\left(E_z + v_x B_y - v_y B_x\right)$$

Scattering :

$$\mathbf{F} = m\dot{\mathbf{v}} = m\Delta\mathbf{v} / \Delta t \cong m\mathbf{v} / \tau$$

(τ: mean free path)
($\mathbf{v}$: drift velocity)

$$mv_x / \tau = e\left(E_x + v_y B_z - v_z B_y\right)$$

$$mv_y / \tau = e\left(E_y - v_x B_z + v_z B_x\right)$$

$$mv_z / \tau = e\left(E_z + v_x B_y - v_y B_x\right)$$

Zero current in y and z direction : $v_y \cong v_z \cong 0$

$$mv_x / \tau = eE_x$$

$$0 = e\left(E_y - v_x B_z\right)$$

$$0 = e\left(E_z + v_x B_y\right)$$

Hence :

$$v_x = \frac{em}{\tau} E_x$$

$$E_y = v_x B_z$$

Hall voltage : $$V_H = \int_{-w/2}^{w/2} E_y dy = v_x B_z w = \frac{1}{nqh} I B_z = \frac{\mu\rho}{h} I B_z$$

with the definitions :

w: width, h: thickness

$$\mu \equiv \frac{v_x}{E_x} = \frac{e\tau}{m} \qquad (\mu : \text{mobility})$$

$$\rho \equiv \frac{m}{en\tau} \qquad (\rho : \text{resistivity})$$

$$J \equiv env_x \qquad (J : \text{current density})$$

$$I \equiv Jwh \qquad (I : \text{current})$$

- V_H is large for small thickness, low doping, high mobility
- V_H indendent of sensor surface
- Low cost
- Fabricated in large quantities (>10^6/jour)

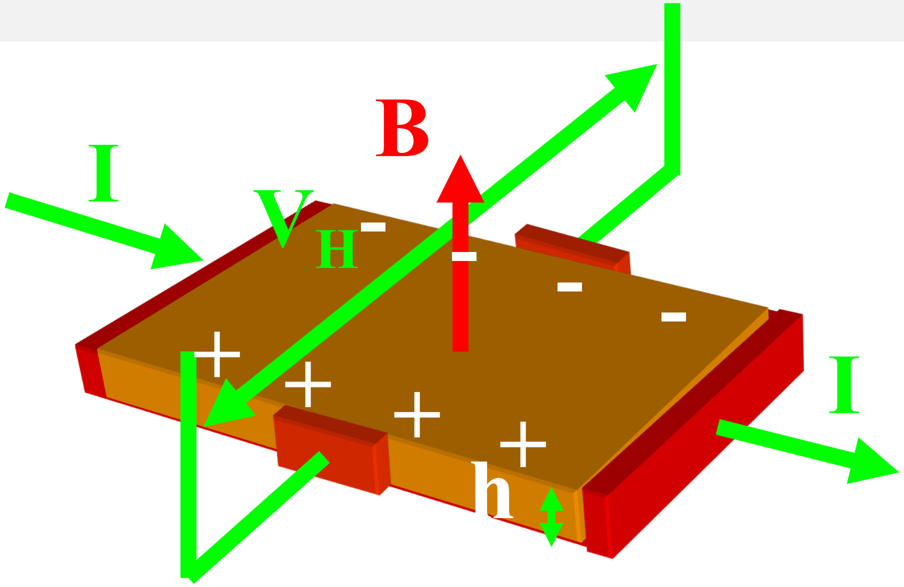

$$V_H = S_I I B$$

$$S_I = \frac{1}{neh}$$

Material	n (cm^{-3})	t (µm)	S_I (V/AT)
Si (doped)	10^{16}	2	300
Au	10^{22}	0.1	0.006

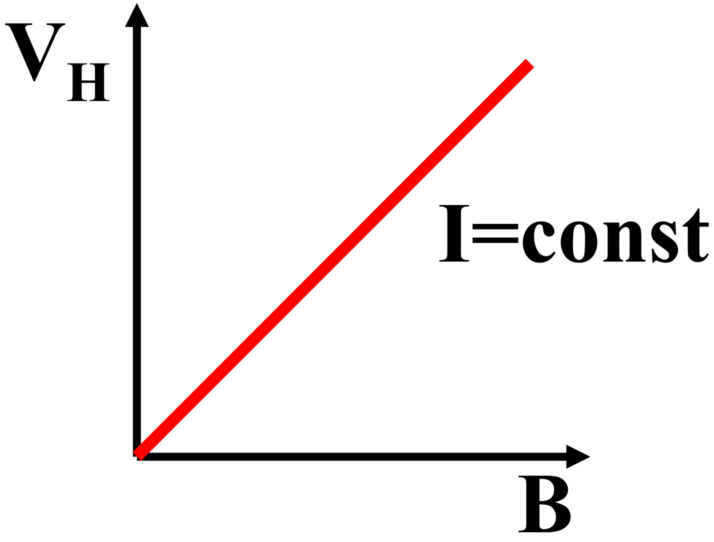

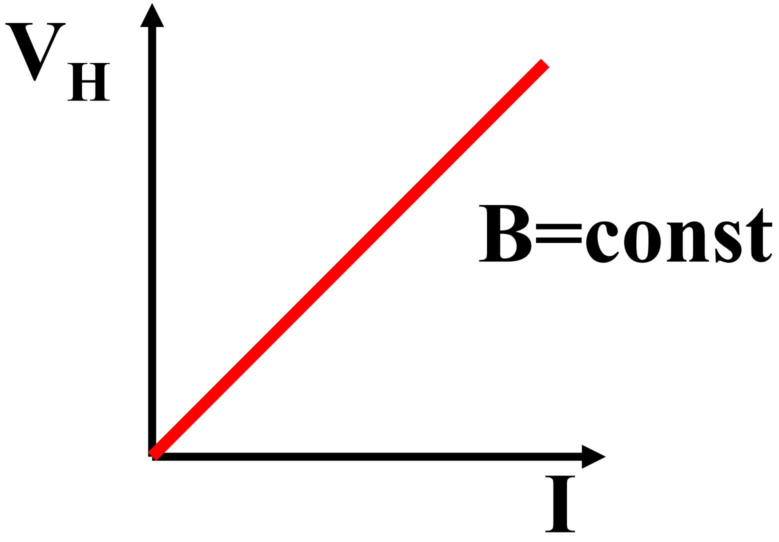

$$V_H = S_I I B$$

The current I is limited by:

- heating
- power available
- saturation of the carrier velocity
- 1/f noise (proportional to I)

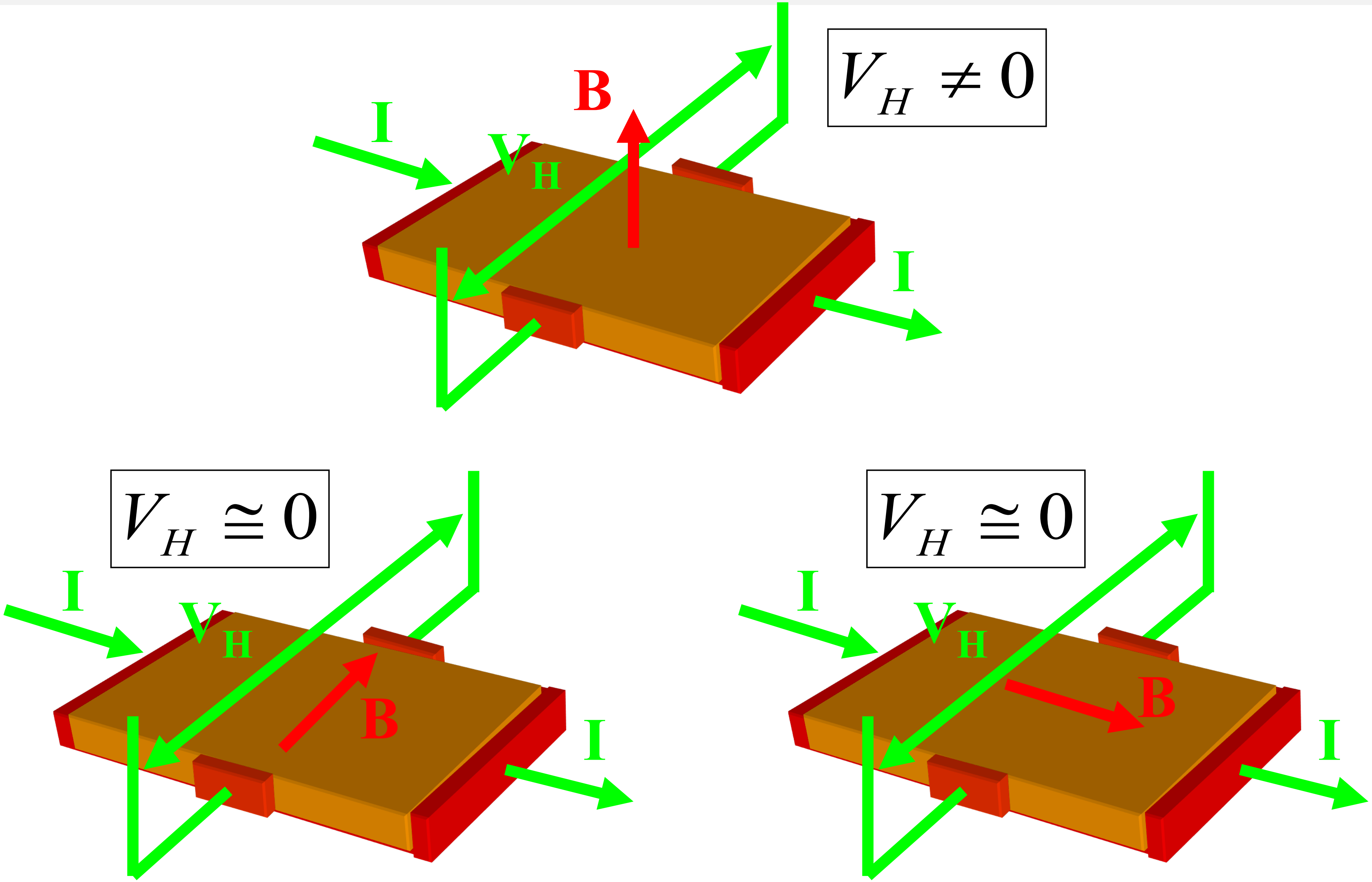

$V_H \neq 0$
I
V_H
B
I
$V_H \cong 0$
I
V_H
B
I
$V_H \cong 0$
I
V_H
B
I

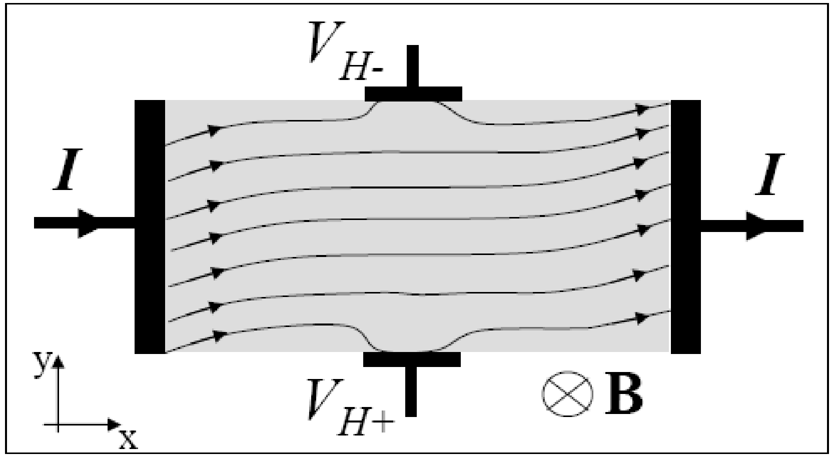

The actual Hall voltage is : $$V_H = G\frac{1}{nqh}IB_z$$

where G is dependent on the geometry (geometrical factor).

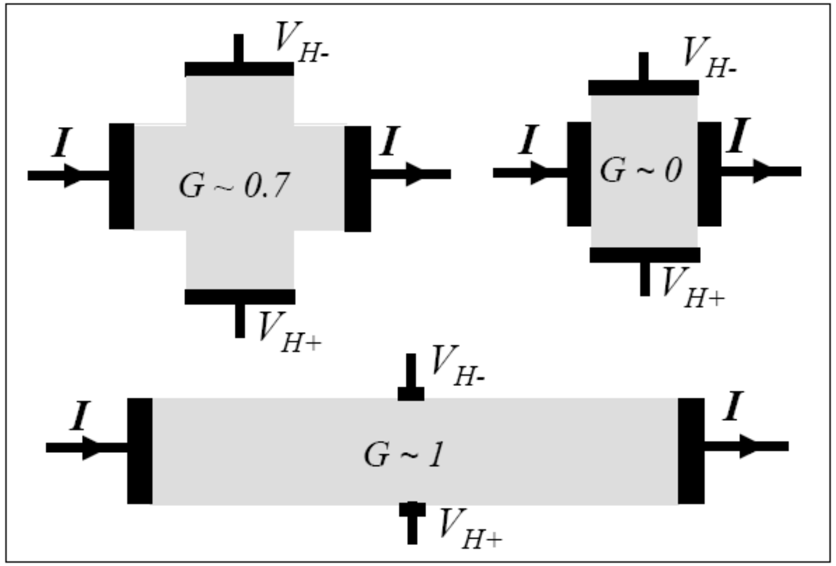

$$V_H \cong S_I I B$$

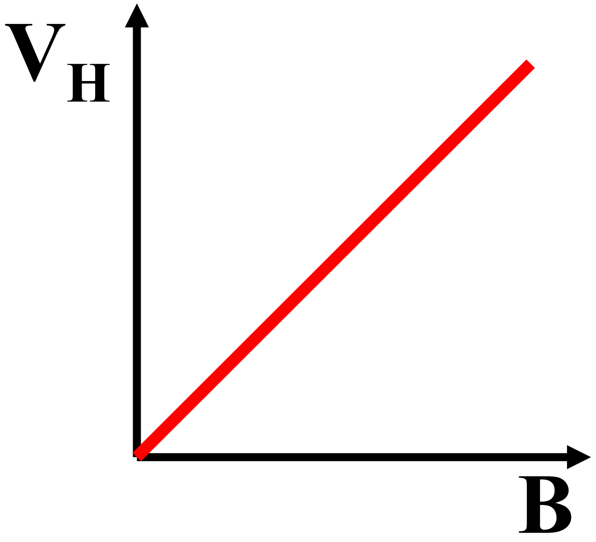

$S_I = 300$ V/AT
$I = 0.5$ mA

B	**V_H**
10 µT	1.5 µV
10 mT	1.5 mV
10 T	1.5 V

Hall devices: thermal noise

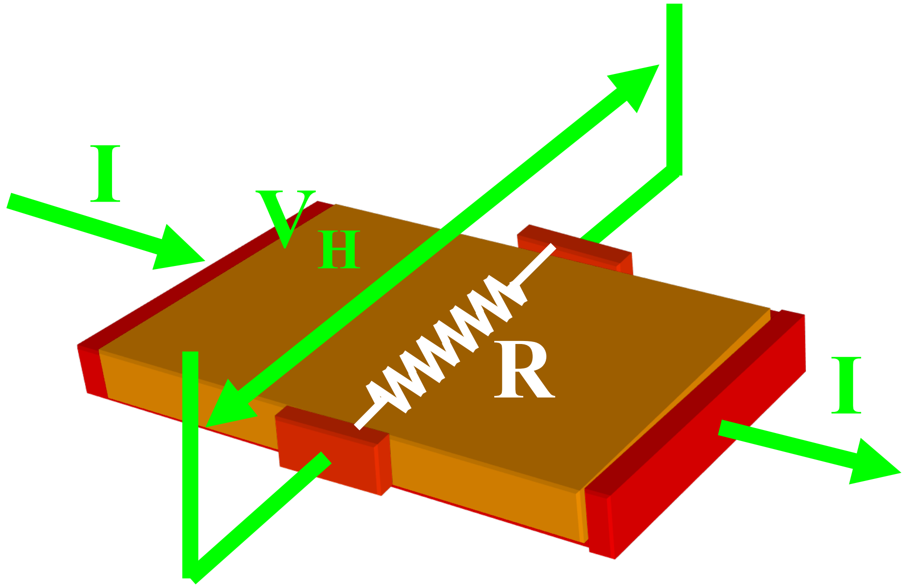

$$N = \sqrt{4\,k\,T\,R\Delta f}$$ [V]

R: output resistance

Signal : $$V_H = S_I IB$$ [V]

Resolution : $$B_{\min} \equiv \frac{N}{V_H / B} = \frac{\sqrt{4\,k\,T\,R\Delta f}}{S_I I}$$ [T]

Hall devices: magnetic field resolution

Si
n = 10^{16}
h = 2 µm
ρ = 1 Ω cm
T = 300 K
R = 15 kΩ
Δf = 1 Hz
S_I = 300 V/AT
I = 0.5 mA

$$B_{min} = \frac{\sqrt{4\,k\,T\,R\Delta f}}{S_I I}$$

$$B_{min} \cong 100 \text{ nT}$$

B	V_H
10 µT	1.5 µV
10 mT	1.5 mV

Other (intrinsic) noise source in Hall devices: 1/f noise

$$B_{\min} \propto \frac{\sqrt{4kRT\Delta f}}{S_I I} = \sqrt{4kT\Delta f \frac{\rho l}{wh}} \frac{enh}{I} = e\sqrt{4kT\Delta f} \sqrt{\frac{n}{\mu} \frac{hl}{w} \frac{1}{I}}$$

To achieve a good resolution :

1. material with a high mobility (large μ)
2. low doping (small n)
3. thin (small h)
4. large I

but I (and n and h) is limited by:

1. heating
2. available power
3. saturation of the charge carriers velocity (electrons or holes)
4. 1/f noise ($\propto I$)

If P is fixed : $P = RI^2$, $I = \sqrt{P/R}$, $B_{\min} \propto \frac{\sqrt{R}}{S_I I} = \frac{R}{S_I \sqrt{P}} = \frac{\rho l}{wh} \frac{neh}{\sqrt{P}} \propto \frac{1}{\mu} \frac{1}{\sqrt{P}}$

(hence μ is, at fixed power P, the important parameter to obtain a good resolution).

Hall devices: offset

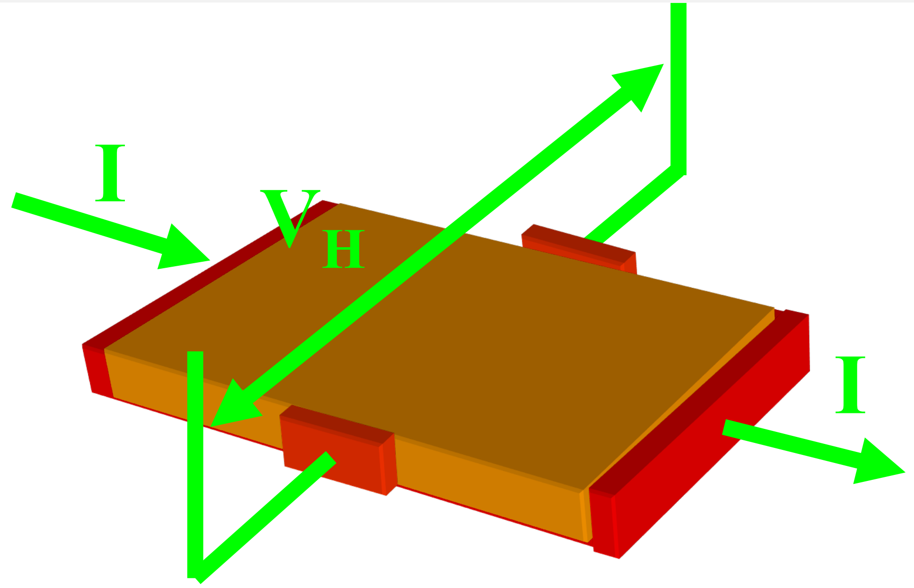

$V_H \neq 0$ even with B=0

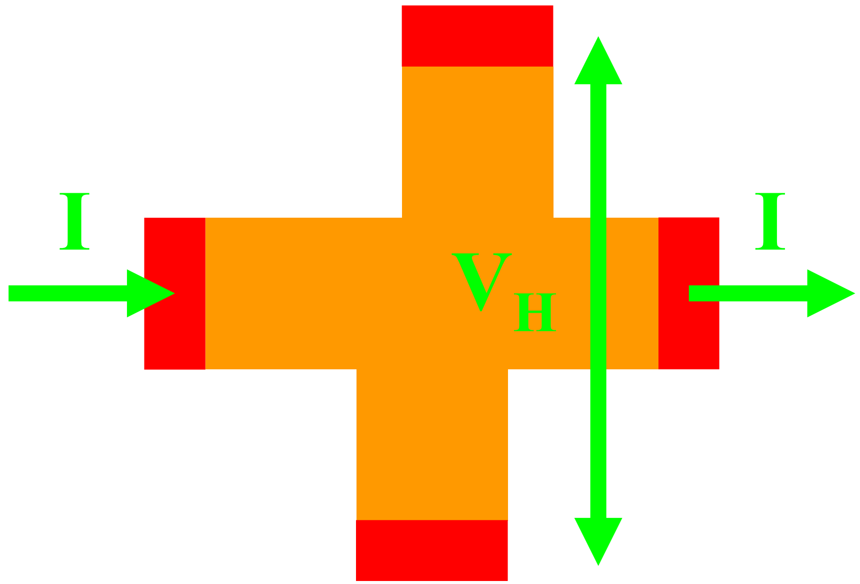

Possible reasons:

-Geometrical imperfections

- Non-uniform resistivity

Solution:

-Calibration

Hall devices: modeling

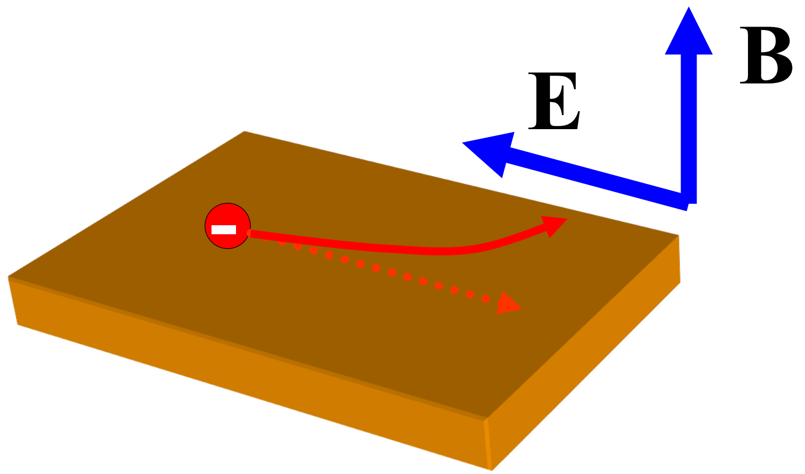

F

$$\frac{\Delta p}{\Delta t}$$

$$m\mathbf{v}/\tau = e(\mathbf{E} + \mathbf{v} \wedge \mathbf{B})$$

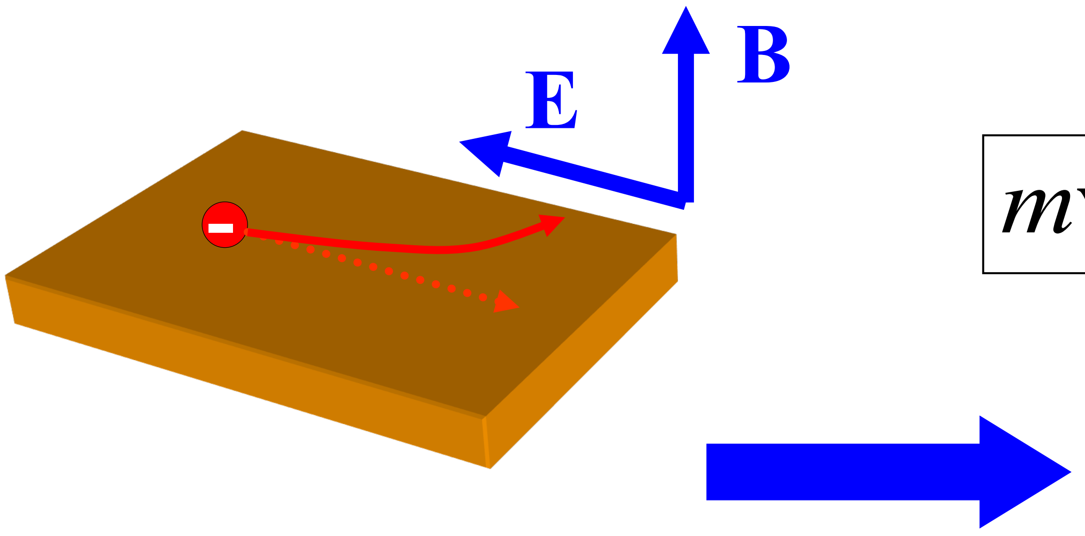

$$m\mathbf{v}/\tau = e(\mathbf{E} + \mathbf{v} \wedge \mathbf{B})$$

$$\mathbf{J} \cong \frac{\sigma_0}{1+(\mu B)^2}(\mathbf{E} + \mu\mathbf{E}\wedge\mathbf{B} + \mu^2\mathbf{B}(\mathbf{E}\cdot\mathbf{B}))$$

$$\mathbf{J} \equiv ne\mathbf{v}$$

$$\sigma_0 \equiv \frac{e^2 n\tau}{m}$$

$$\mu \equiv \frac{e\tau}{m}$$

$$\mathbf{J} = \frac{\sigma_0}{1+(\mu B)^2}(\mathbf{E} + \mu\mathbf{E}\wedge\mathbf{B} + \mu^2\mathbf{B}(\mathbf{E}\cdot\mathbf{B}))$$

$$\nabla\cdot\mathbf{J} = 0$$

$$\nabla\wedge\mathbf{E} = 0$$

$E_t=0$, $J_n=0$

Solved by:

- Conformal mapping
- Equivalent electrical circuits
- ………

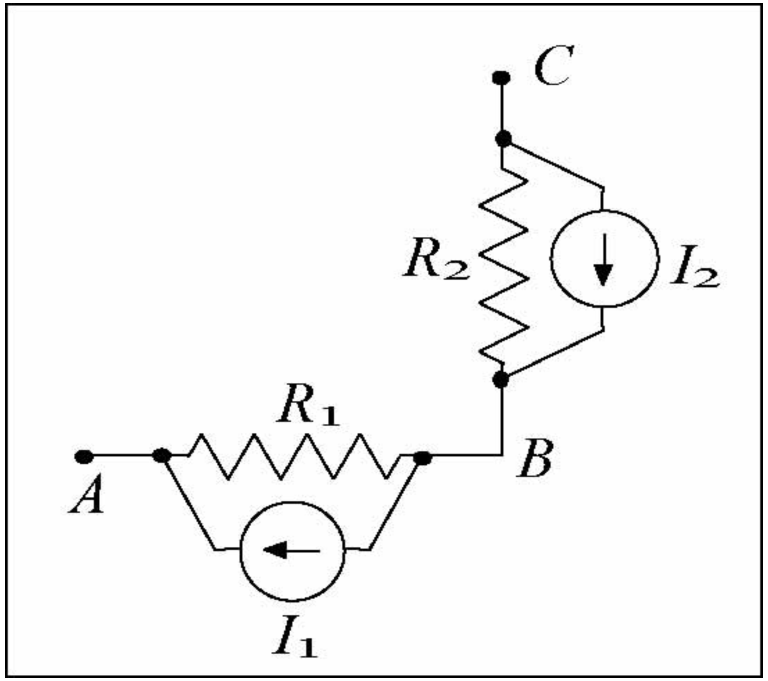

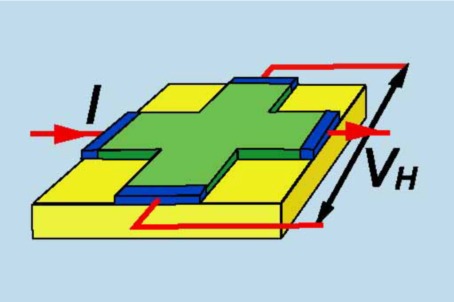

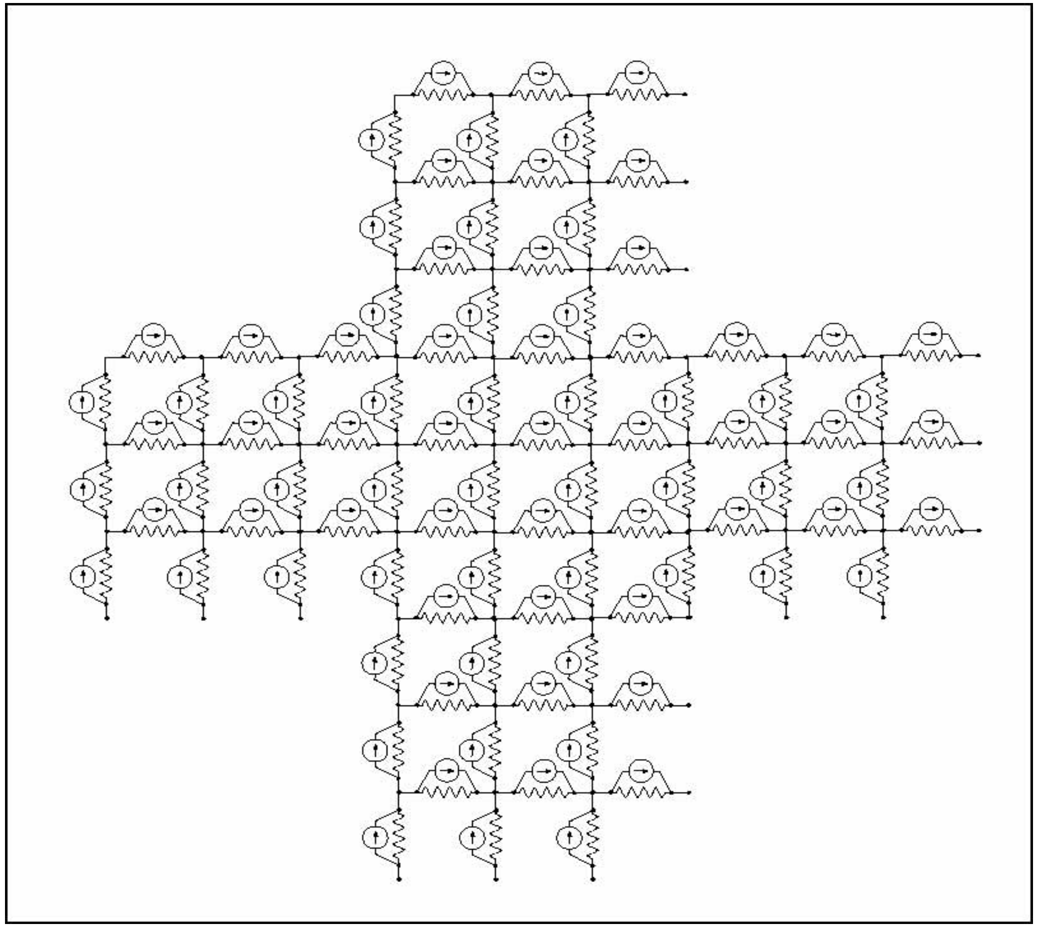

Hall cross equivalent circuit

$$R_1 = R_2 = R_0(1+\mu^2 B^2)$$

$$I_1 = (V_C - V_B)\mu B / R$$

$$I_2 = (V_B - V_A)\mu B / R$$

Hall devices: different configurations

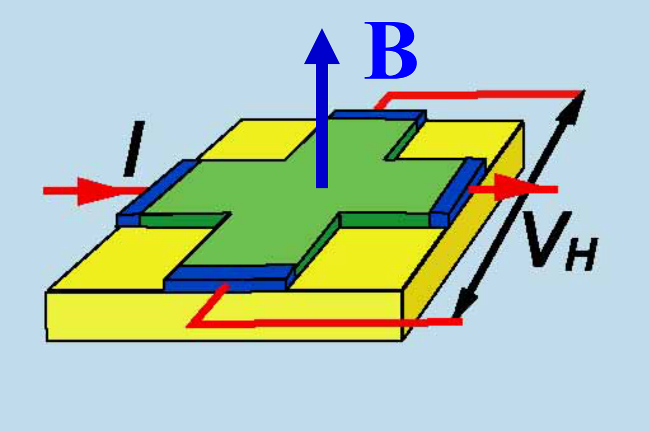

Hall cross

$$V_H = S_I \, I \, B$$

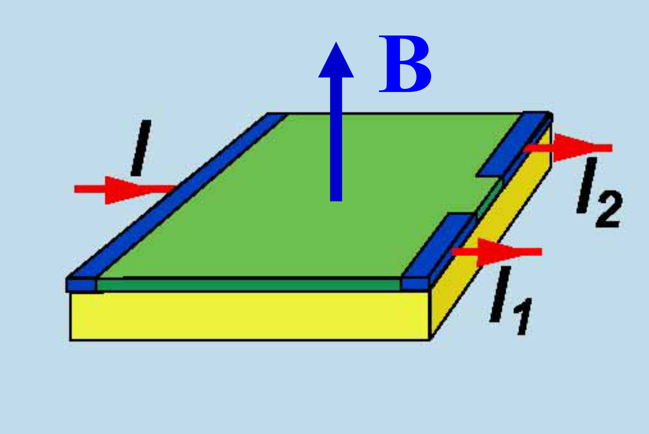

Split current

$$I_1 - I_2 = S_{Ic} \, I \, B$$

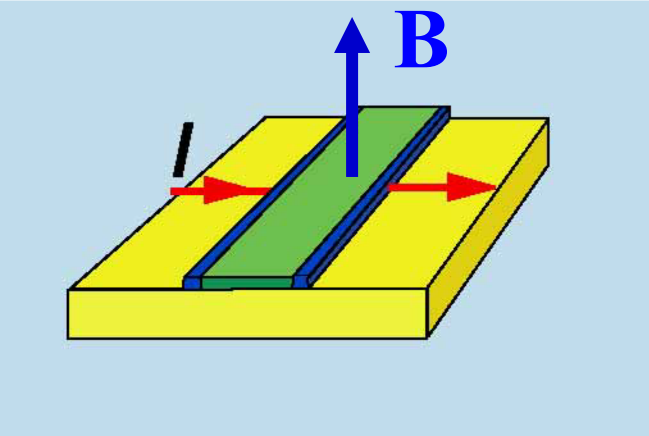

Magnetoresistance

$$R \cong R_0 (1 + \mu^2 B^2)$$

Hall devices: magnetoresistance

- Based on the Hall effect in non-magnetic conductors (do not confuse it with AMR).

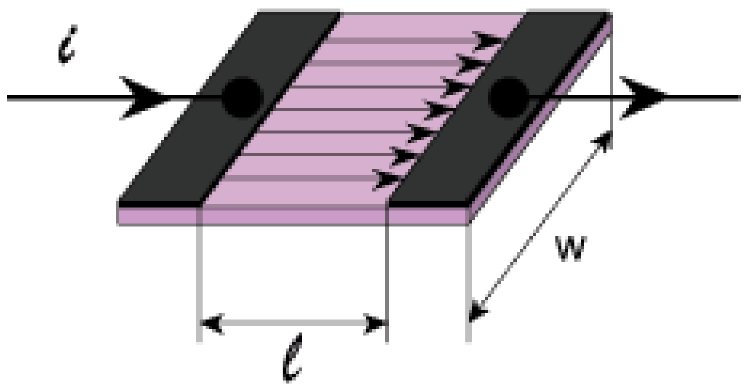

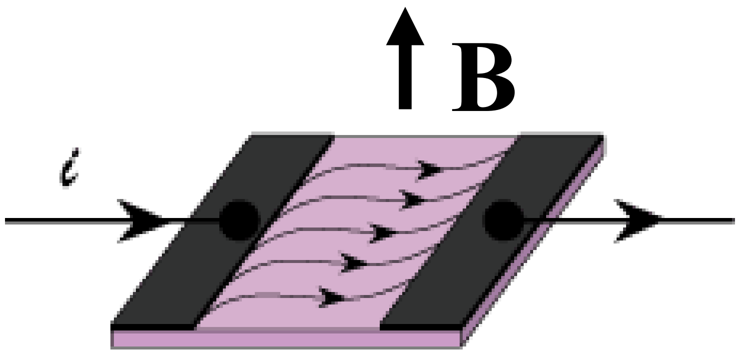

$$R_B = R_0 \frac{\rho_B}{\rho_0}\{1+m(\mu B)^2\}$$

R_B : Resistance under magnetic field (ohm)
R_0 : Resistance under non-magnetic field (ohm)
μ : Mobility ($cm^2/V \cdot s$)
ρ_B : Resistivity under magnetic field ($ohm \cdot cm$)
ρ_0 : Resistivity under non-magnetic field ($ohm \cdot cm$)
B : Magnetic flux density (T)
m : Geometric effect factor (ℓ / w)

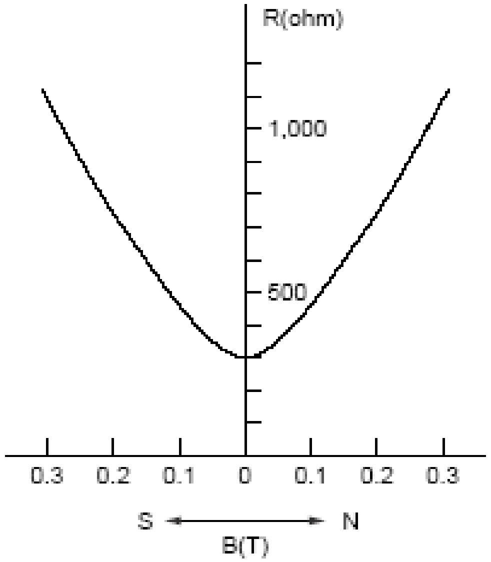

EPFL

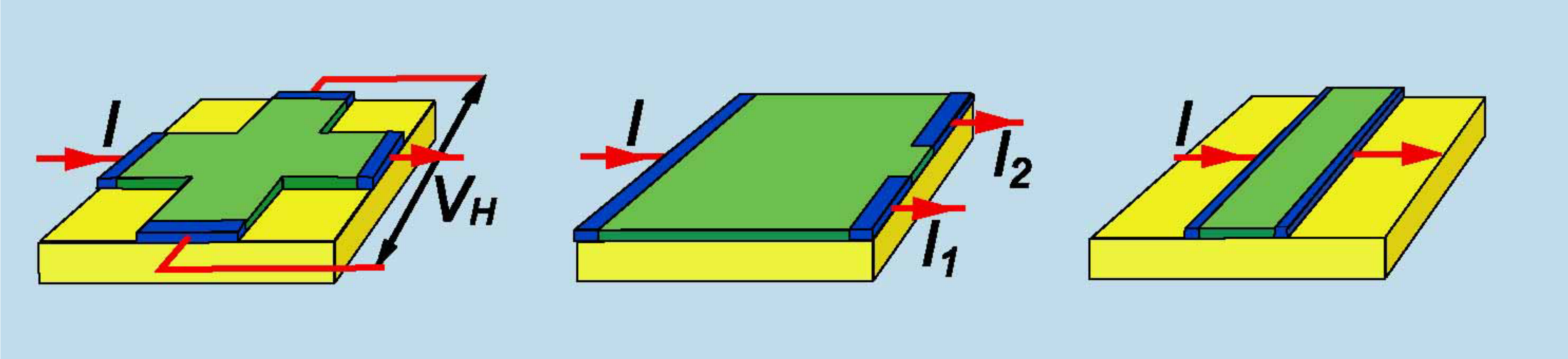

$$B_{\min} \equiv \frac{\sqrt{4\,k\,T\,R}}{V_H / B}$$

$$B_{\min} \equiv \frac{\sqrt{4\,k\,T\,/\,R}}{\Delta I / B}$$

$$B_{\min} \equiv \frac{\sqrt{4\,k\,T\,R}}{I(\partial R / \partial B)}$$

Similar magnetic field resolutions

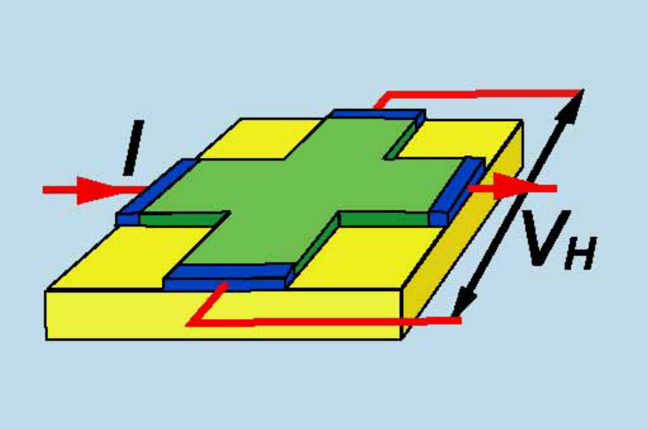

Linear
Better field resolution at low fields
1/f noise suppression possible

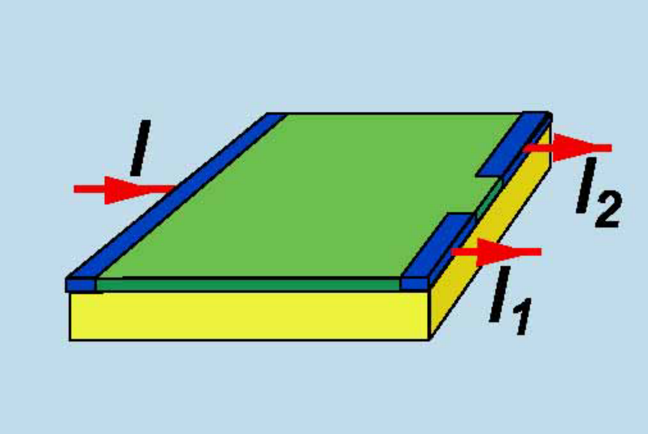

Linear
Better field resolution at low fields

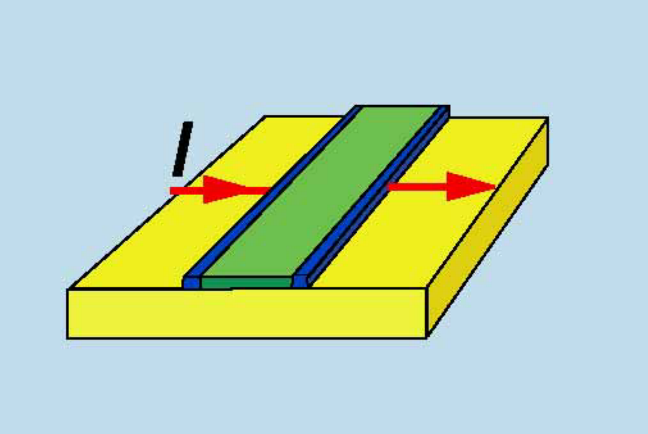

Non-linear
Better field resolution at high fields
Non-square sensing surface

Hall devices: Technologies and dimensions

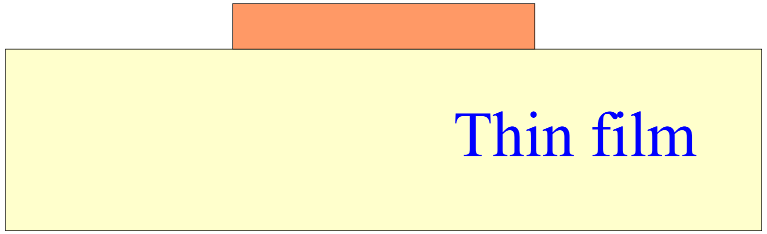

(Ex: InSb on GaAs)

Technologies

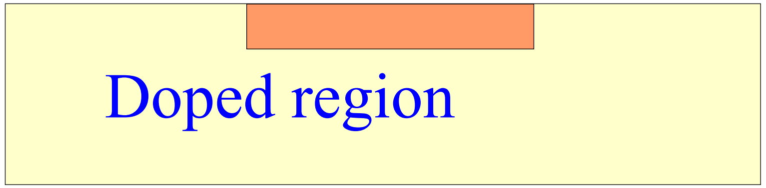

(Ex: p-doping in Si)

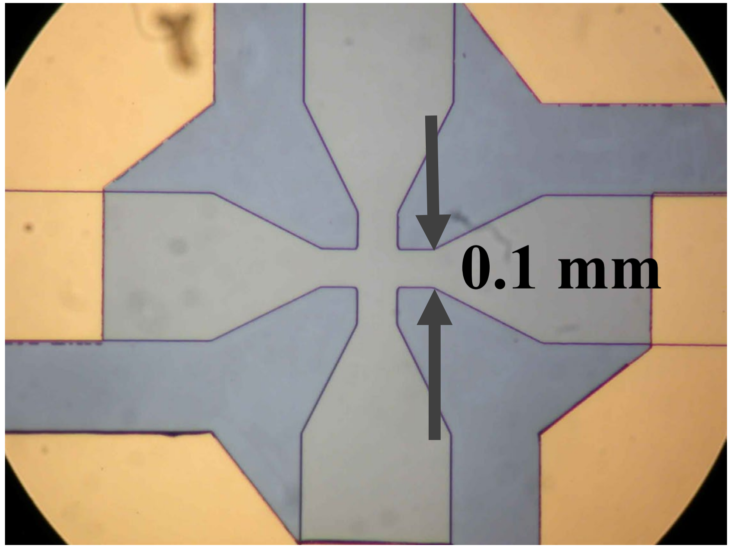

Commercial

Dimensions

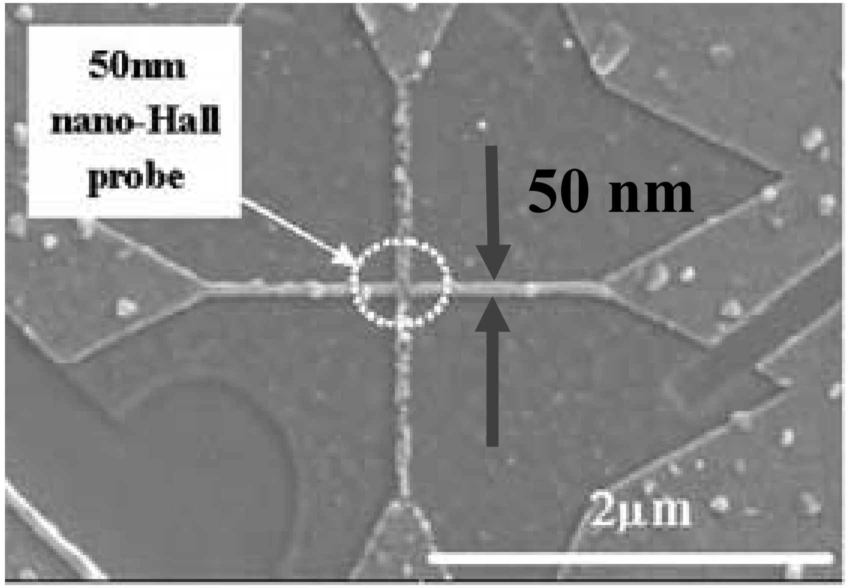

Research

Hall sensors in silicon CMOS technologies

« Standard » structure

Characteristics: h ~1 a 20 µm
Typical sensitivity : S_H ~ 300 V/AT

Major technology used in commercial devices

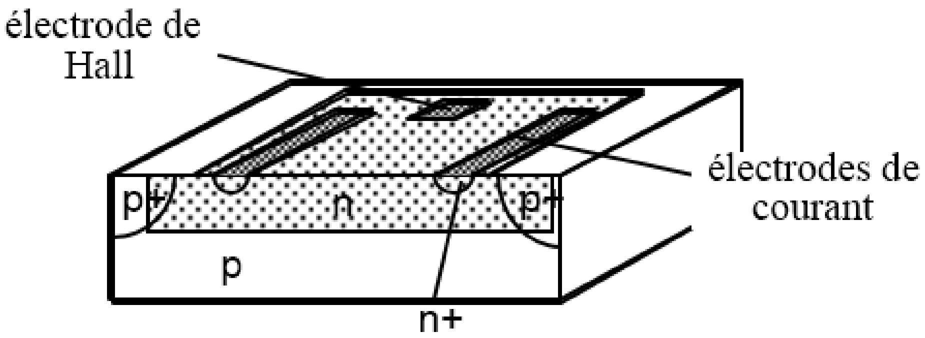

« MOS » structure

Characteristics: h~0.01 µm
large 1/f noise
Typical sensitivity : S_H ~ 1000 V/AT

Allows to “tune” the sensitivity
Only rarely used in commercial devices

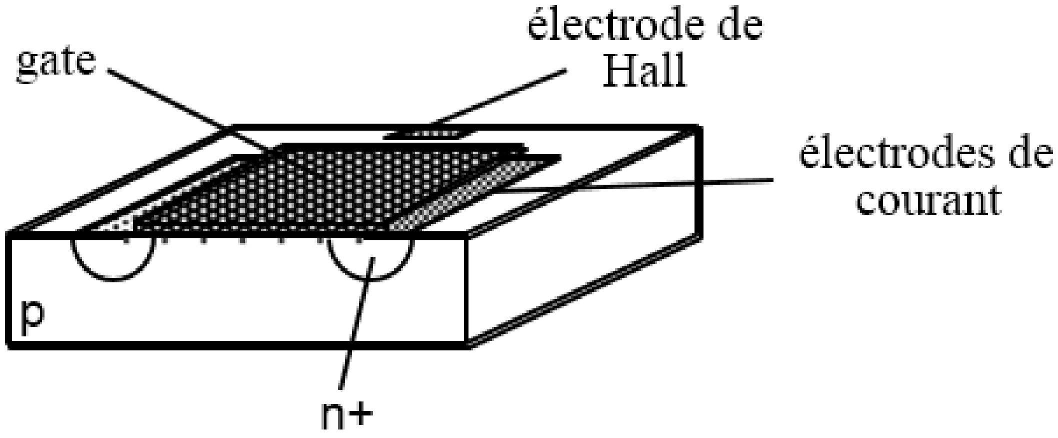

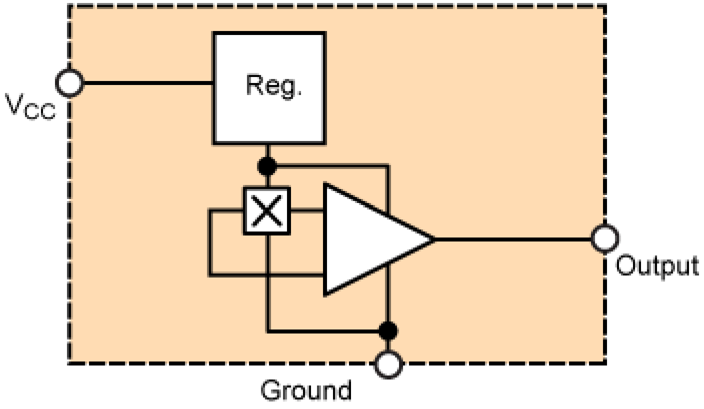
Reg.
VCC
Output
Ground

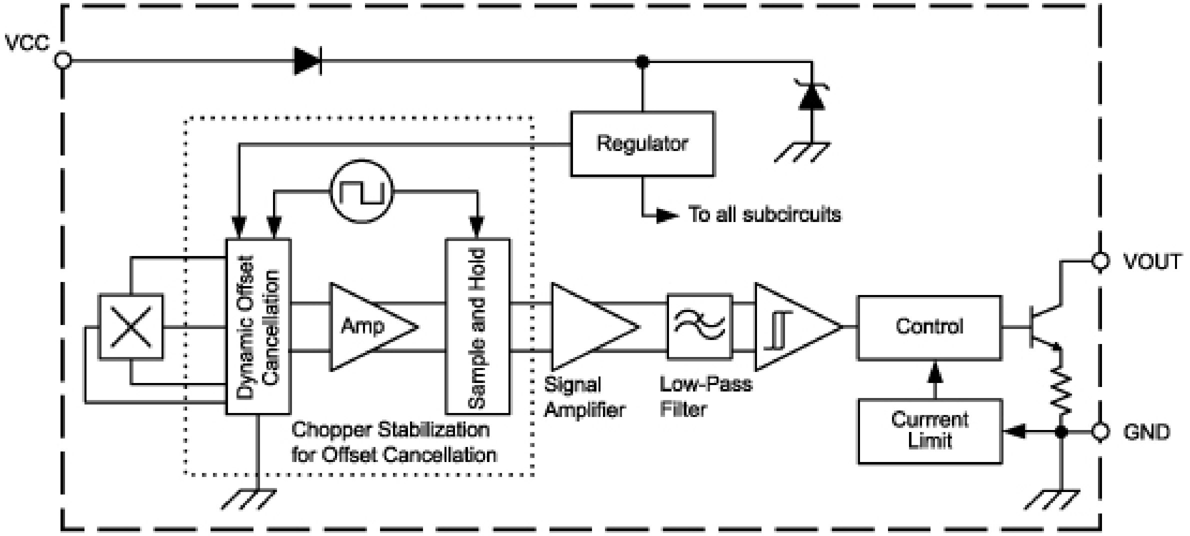
VCC
Regulator
To all subcircuits
Dynamic Offset Cancellation
Amp
Sample and Hold
Chopper Stabilization for Offset Cancellation
Signal Amplifier
Low-Pass Filter
Control
Current Limit
VOUT
GND

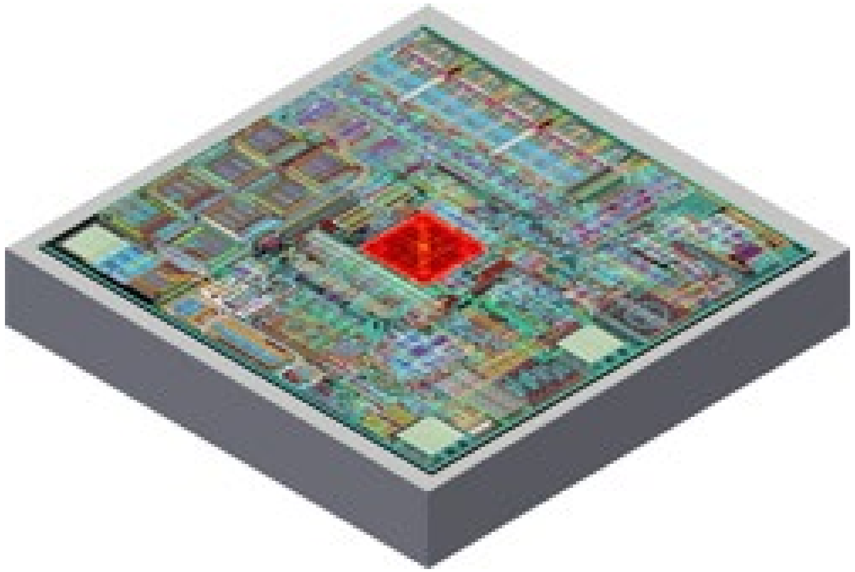

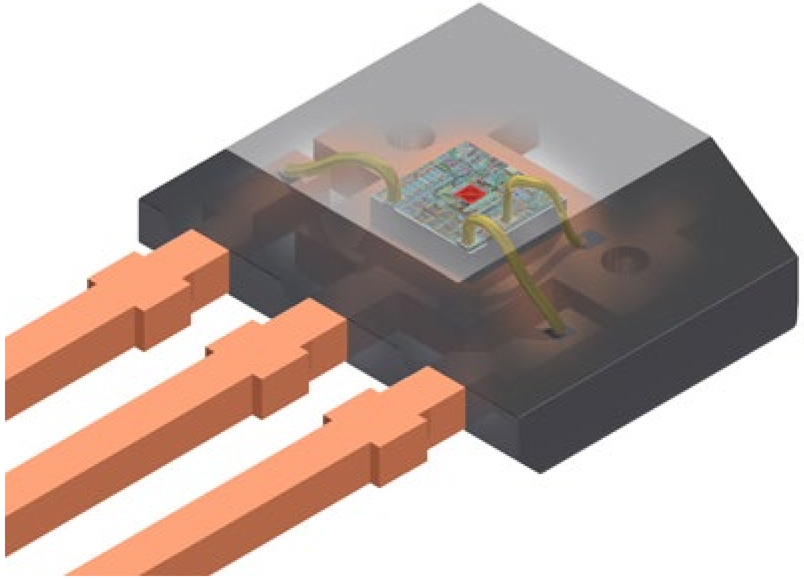

Hall devices: applications

Current sensing
(with feedback
to linearize the response)

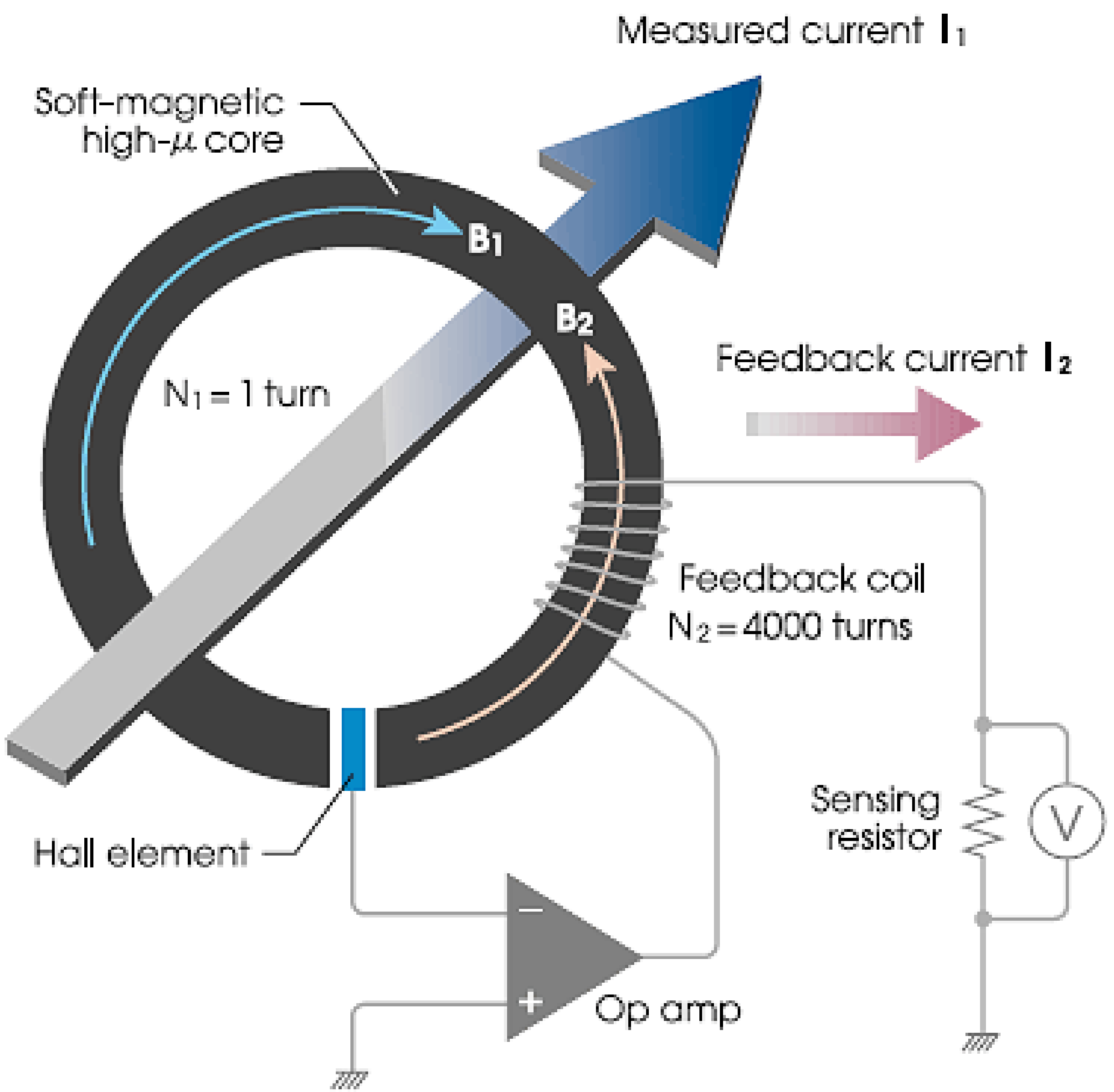

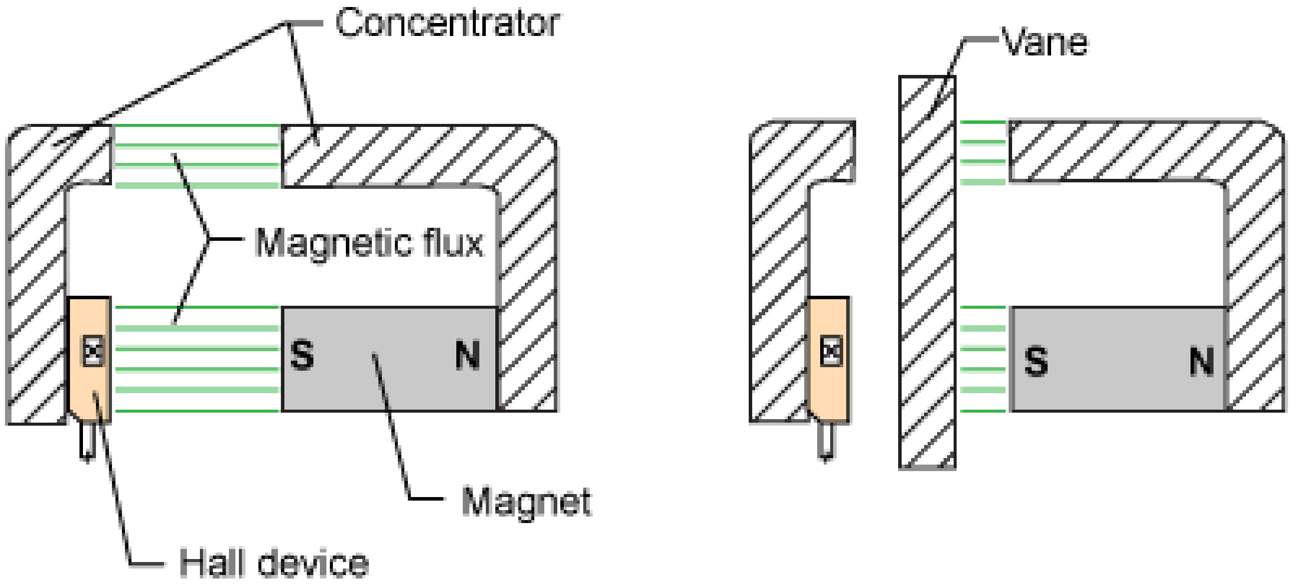

Demonstration of vane interruptor operation: (left) normal magnetic flux path without vane interruption, (right) vane shunting magnetic flux

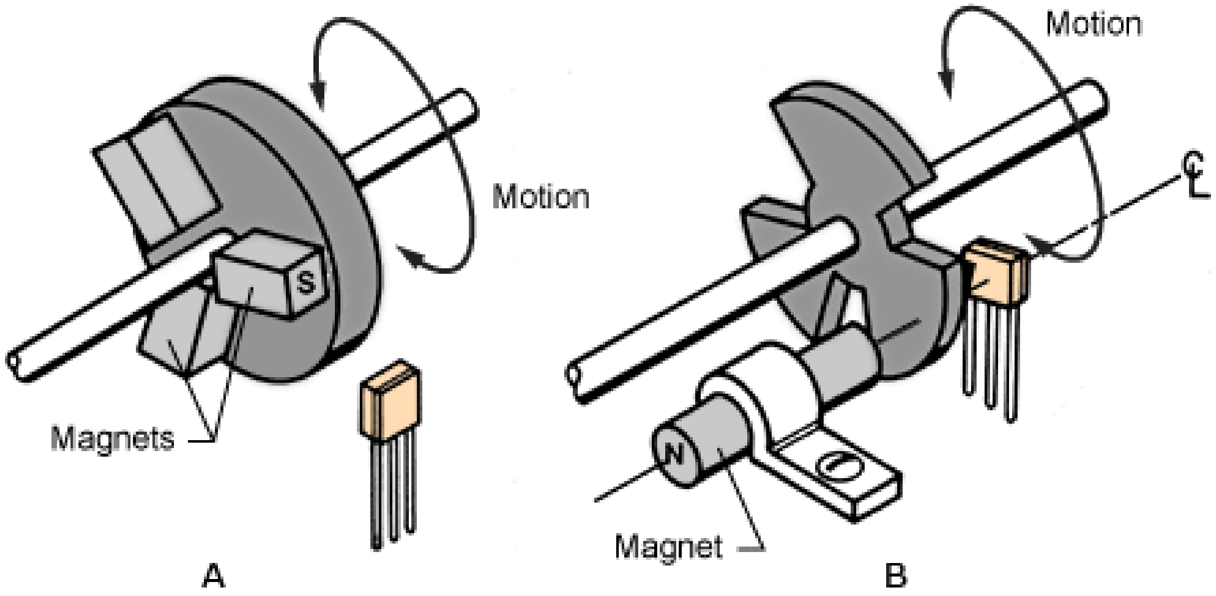

Typical configurations for rotors: (A) magnetic, and (B) ferrous vane

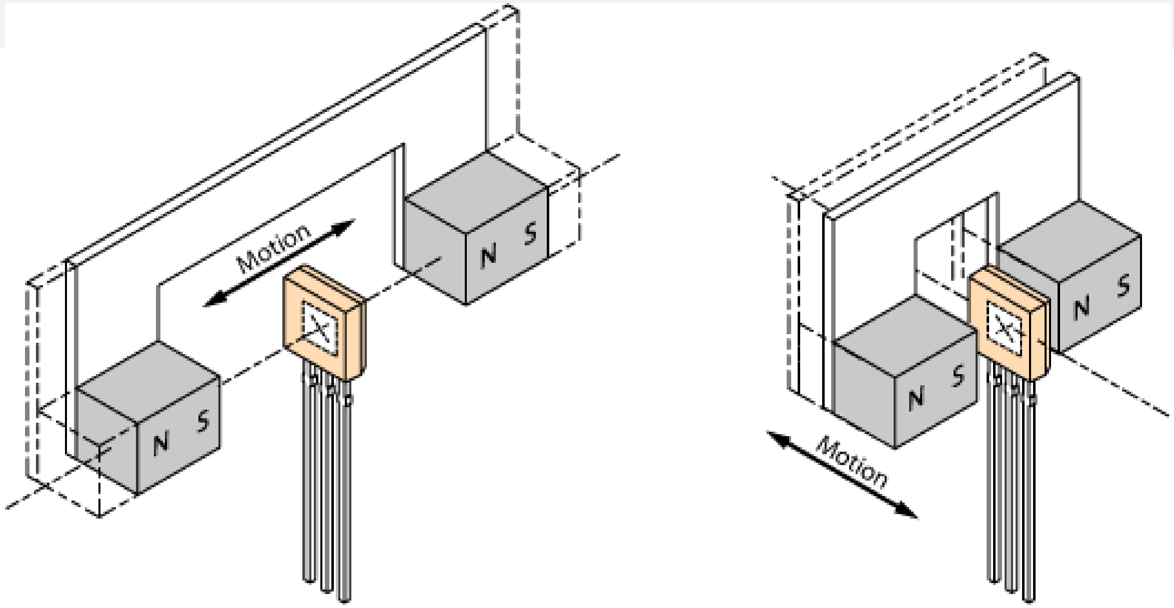

Examples of compound magnet configurations (either the Hall device or the magnet assembly can be stationary), with a south pole toward the branded face and a north pole toward the back side: (left) push-pull head-on and (right) push-pull slide-by

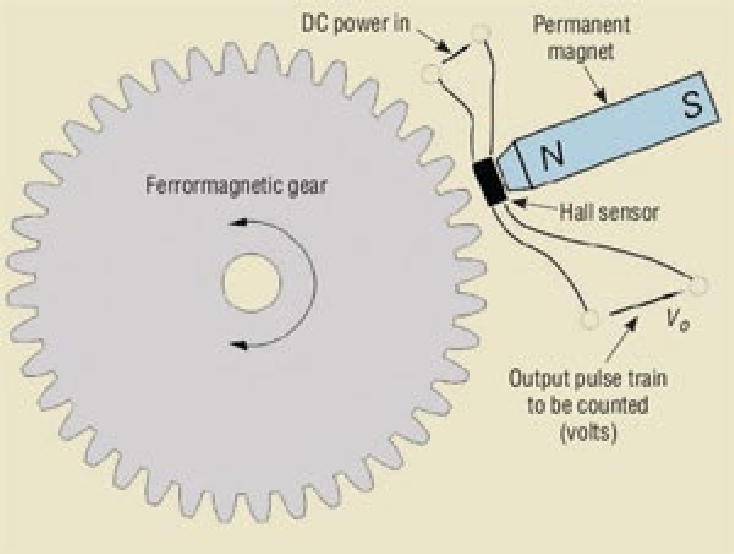

Speed sensing

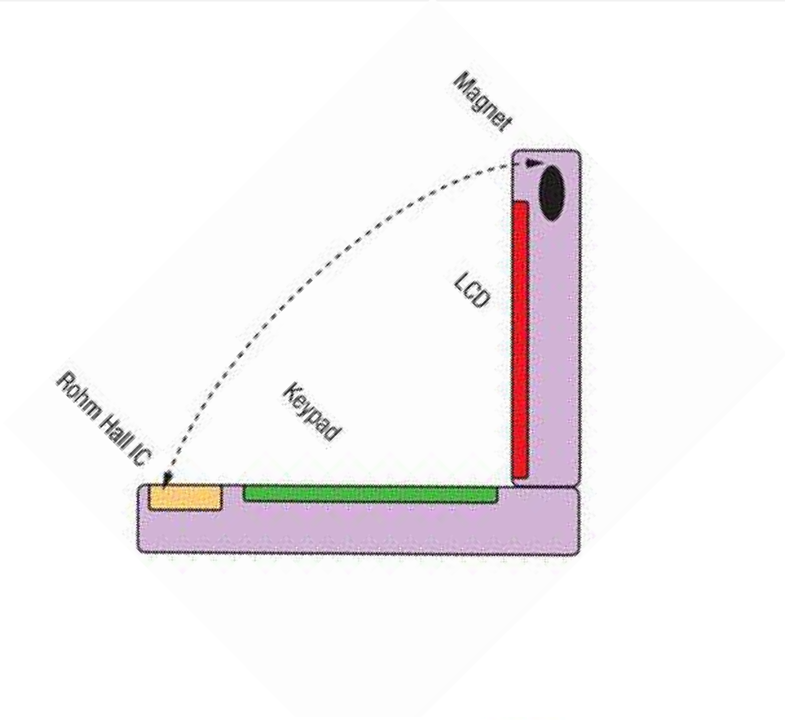
Magnet
LCD
Keypad
Rohm Hall IC

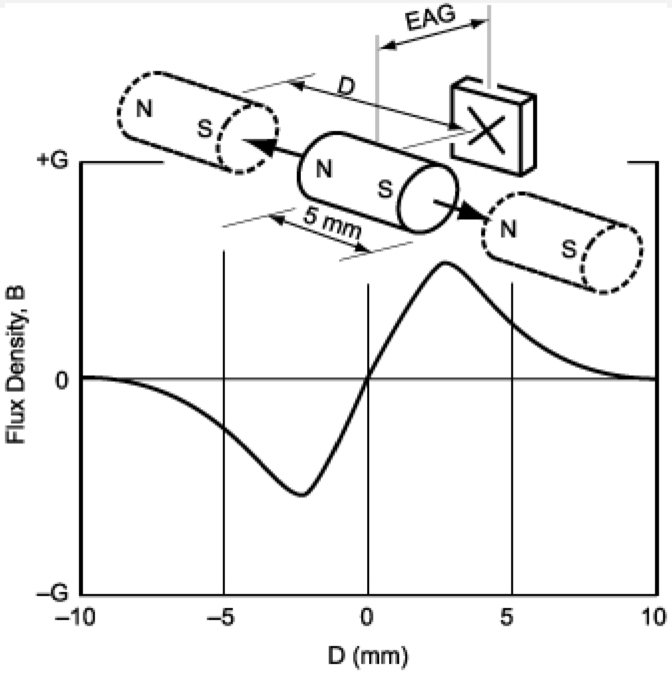
EAG
D
N
S
5 mm
+G
0
–G
Flux Density, B
–10
–5
0
5
10
D (mm)

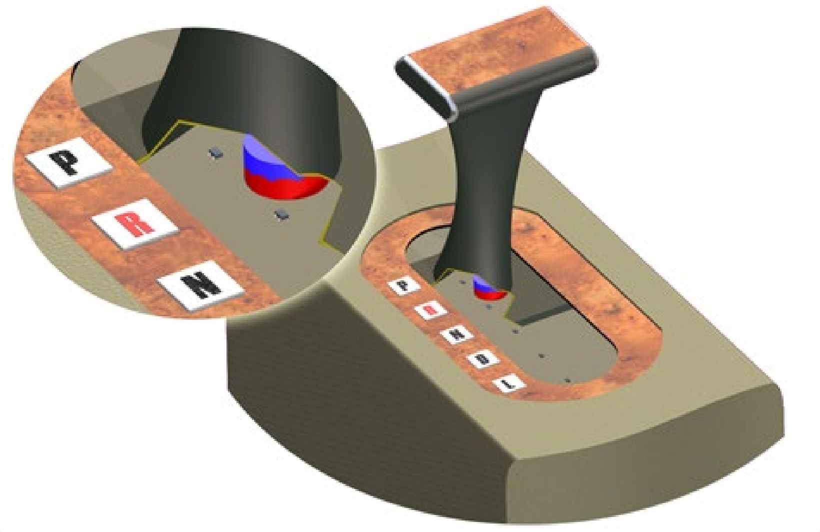
P
R
N

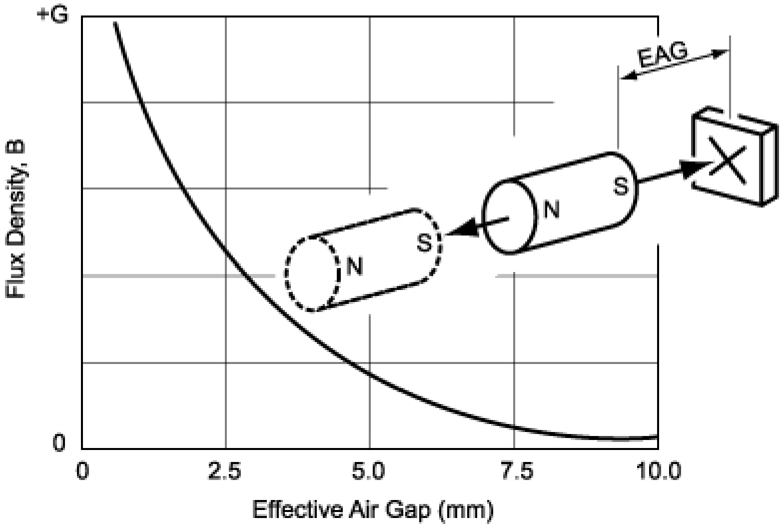
+G
0
EAG
N
S
Flux Density, B
0
2.5
5.0
7.5
10.0
Effective Air Gap (mm)

Quantum Hall effect in a 2D electron gas

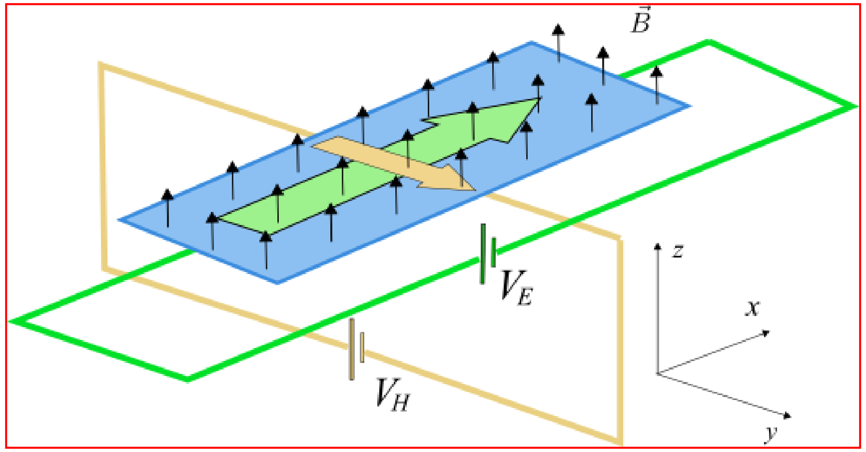

$$\rho_{xy} = \frac{V_H}{I}\frac{1}{N_y} \qquad \rho_{xx} = \frac{V_E}{I}\frac{1}{N_x}$$

N_i : No. of squares in i-direction

$$\rho_{xy} = \frac{1}{\nu}\frac{h}{e^2}$$

$$\frac{h}{e^2} = 25812.807557(18)\Omega$$

(Resistance standard !!)

ν=1,2,3,4,5,....1/3, 2/5, 3/7, ...

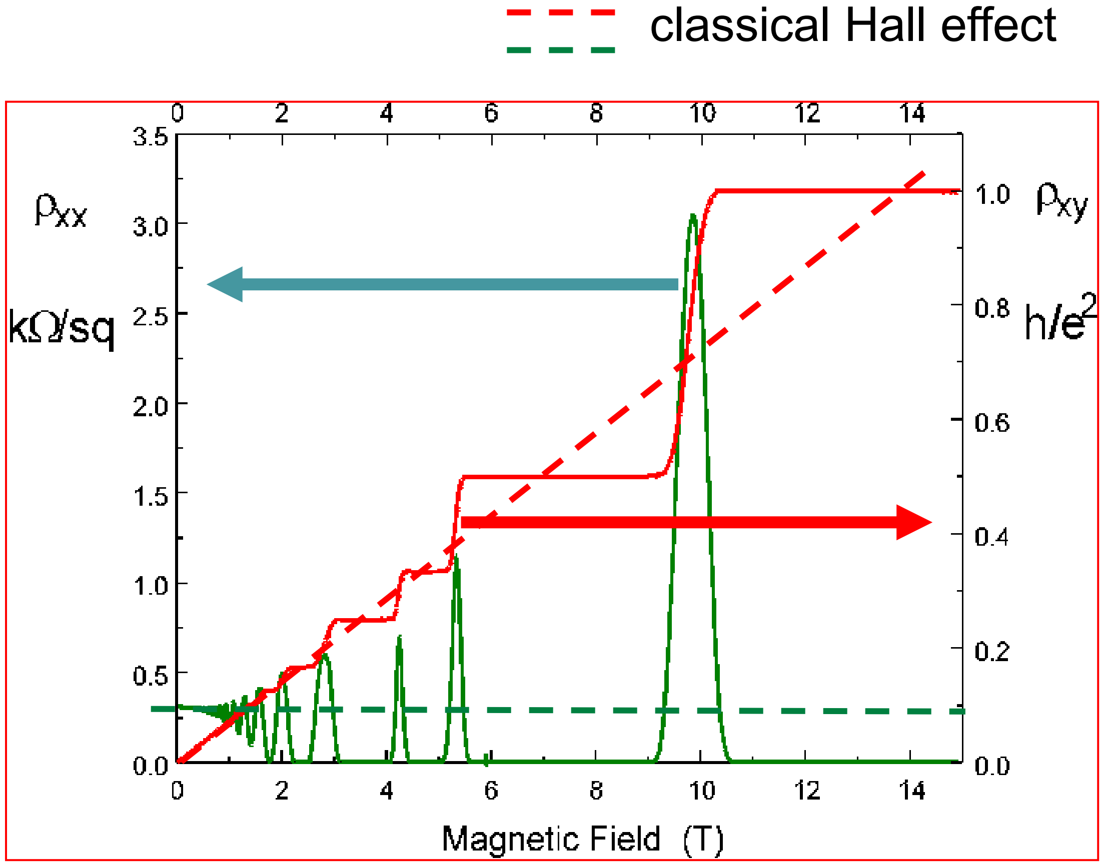

http://www.warwick.ac.uk/~phsbm/iqhe.gif

In **two dimensions**, electrons in a magnetic field follow circular cyclotron orbits.

These orbits are quantized. The energy levels (called Landau levels) of these orbits are:

$$E_n = \hbar\omega_c\left(n+1/2\right) = \hbar\frac{eB}{m}\left(n+1/2\right)$$

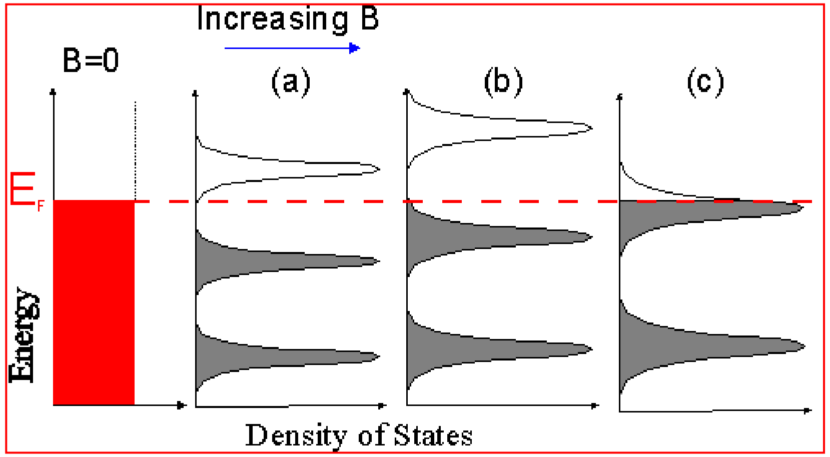

$\omega_c = \dfrac{eB}{m}$ is the "classical" cyclotron frequency.

For strong magnetic fields, many single particle states have the same energy E_n.

For a sample of area A, in magnetic field B, the degeneracy of each Landau level is:

$N = 2BA/\Phi_0$ Φ_0: is the quantum of flux.

For sufficiently strong B, each Landau level may have so many statesthat all of the free electrons in the system, at low T, sit in only a few Landau levels it is in this regime where one observes the quantum Hall effect.

Note: As for the Coulomb blockade in a 0D object, also for the quantum Hall effect in 2D object the energy levels discretization due to the "nanoscale size" is not the dominant phenomenon.

Anisotropic Magneto-Resistances (AMR)

Principle: The resistance depend on the angle between the current and the magnetization

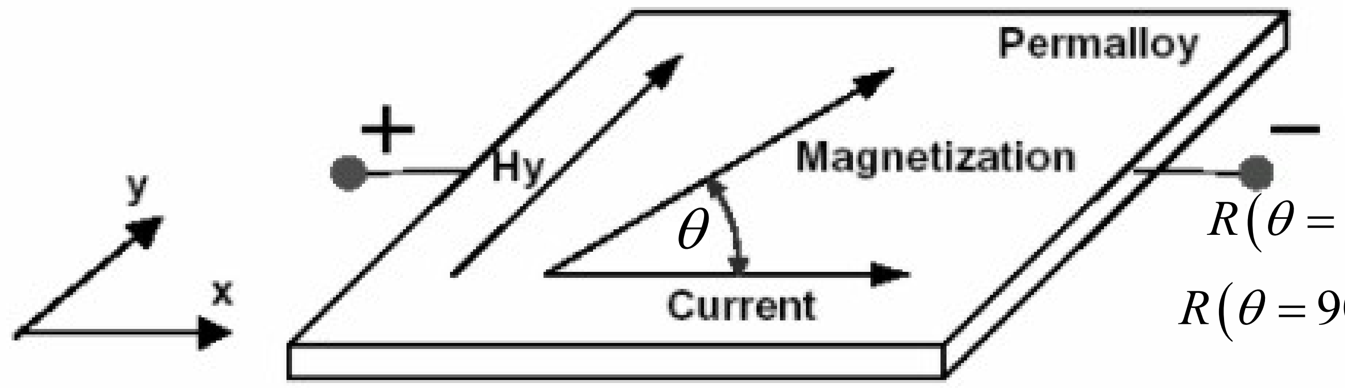

$$R(\theta = 0°) = R_{//} = \max R$$

$$R(\theta = 90°) = R_{\perp} = \min R$$

$$R(\theta) = R_{//} - \Delta R_{MR} \cdot \sin^2 \theta$$

$$R(\theta) = R_{\perp} + \Delta R_{MR} \cdot \cos^2 \theta$$

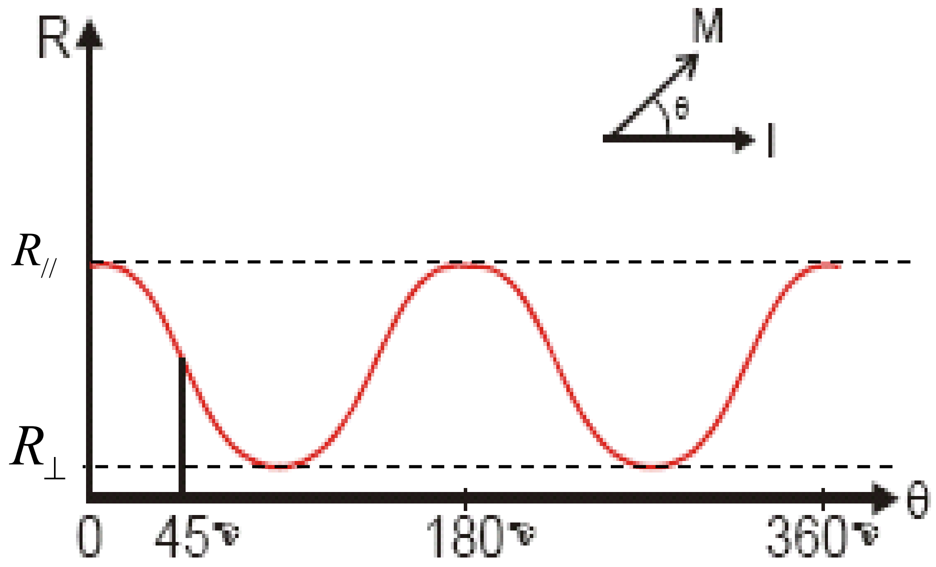

Matériau	r [10-8 Ωm]	Δr/r [%]	Ho [A/m]	Hc [A/m]	$\mu_0 M_s$ (T)
$Ni_{81}Fe_{19}$ (permalloy)	22	2.2	250	80	1.1
$Ni_{86}Fe_{14}$	15	3.0	200	100	0.95
$Ni_{50}Co_{50}$	24	2.2	2500	1000	1.25
CoFeB amorphe	86	0.07	2000	15	1.3

Orientation of the magnetization due to the shape anisotropy

The demagnetizing field (shape anisotropy) tends to allign the magnetization vector.

$$\text{For} \quad |H_y| < |H_0|, \quad \sin\theta \cong (H_y/H_0) \rightarrow$$
$$\rightarrow R(H_y) \cong R_{//} - \Delta R_{MR} \cdot (H_y/H_0)^2$$

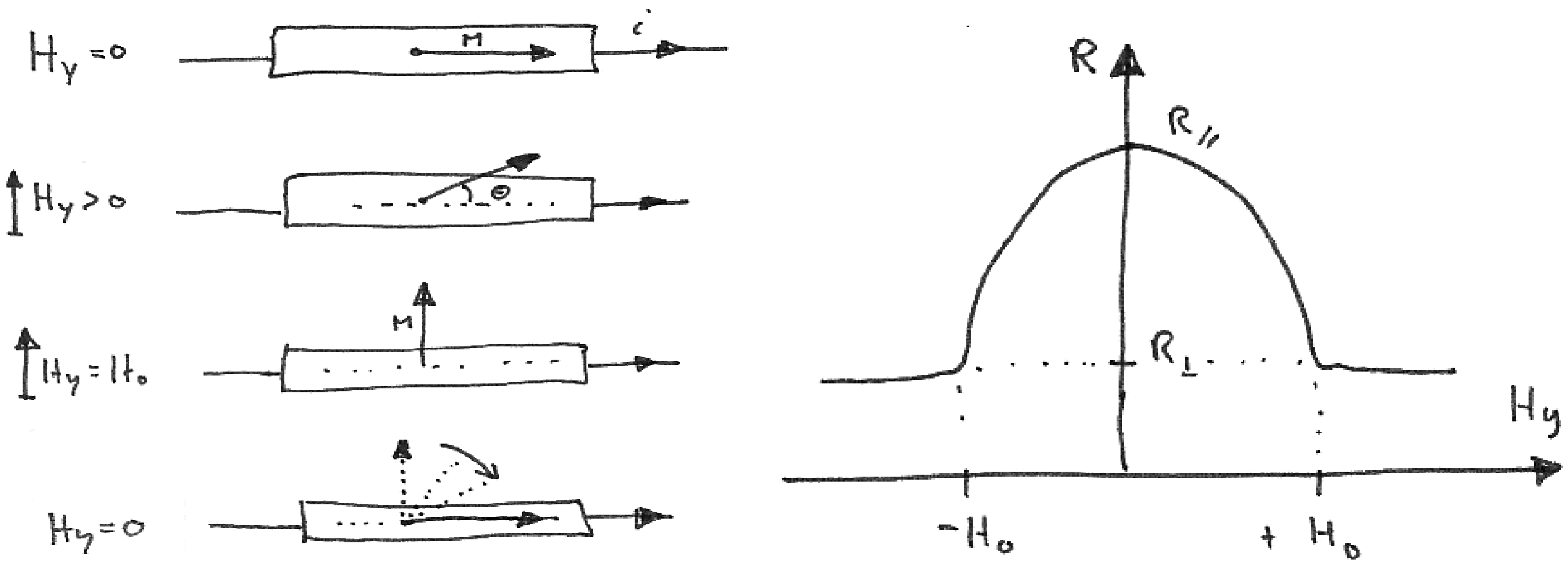

- Problem : zero sensitivity for small H_y
  Solution : « barber poles » geometry

« Barber poles» geometry

Principle: thin film AMR covered with a barber-poles structured metal

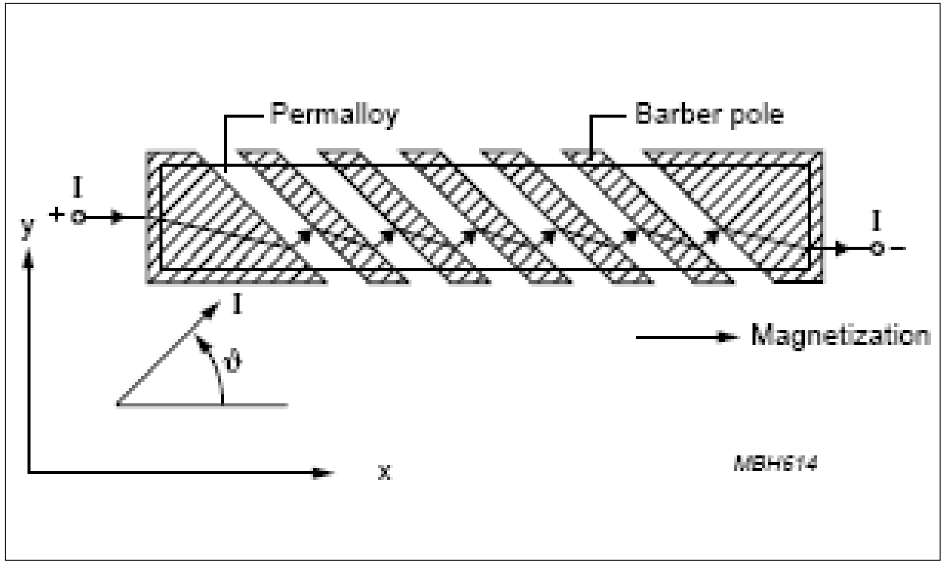

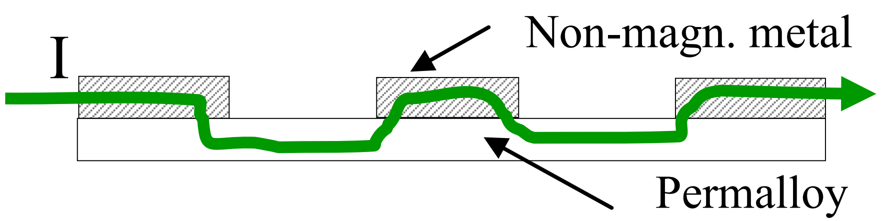

$$\rho_{permalloy} >> \rho_{non-magnetic\ metal}$$

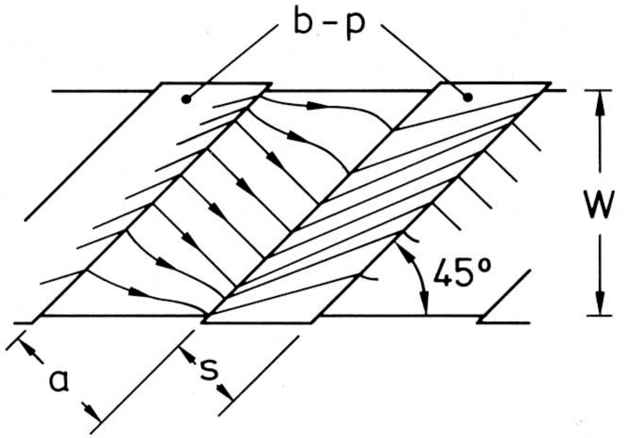

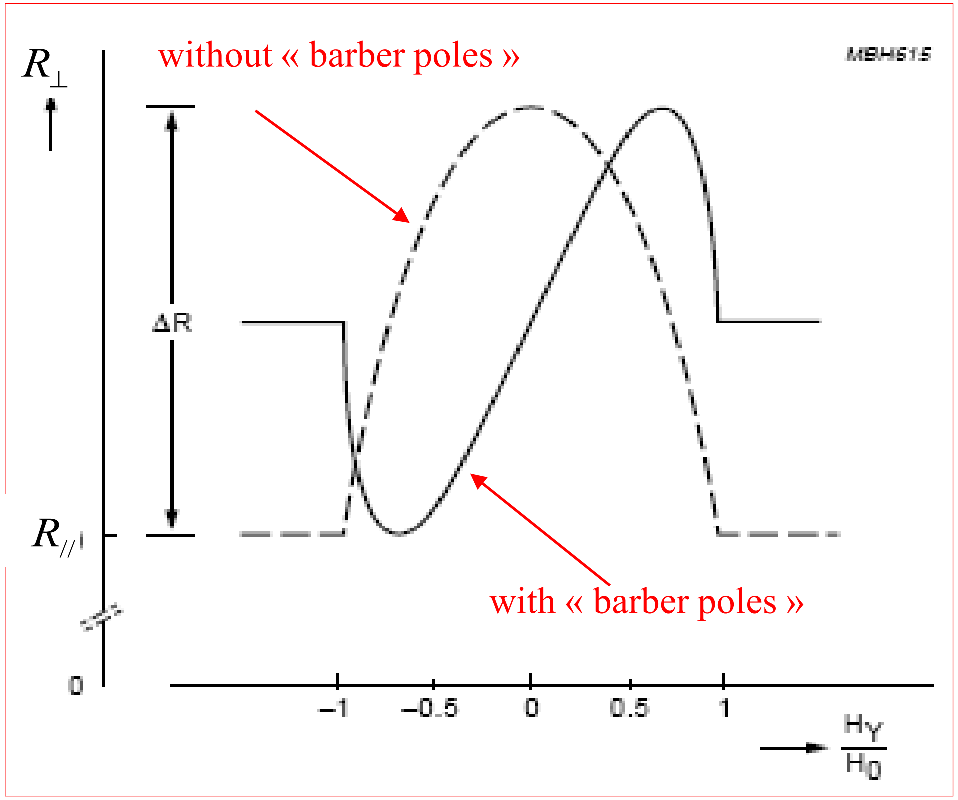

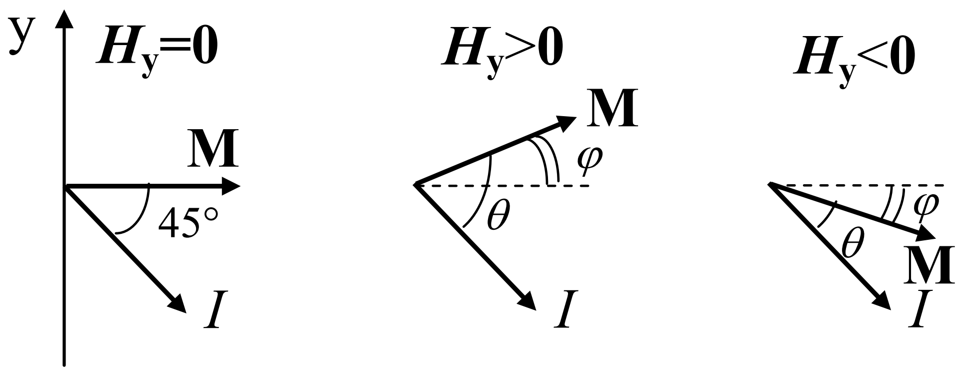

At low fields ($H_y/H_0 < 0.3$)

$$R \cong R_{//} - \frac{1}{2}\Delta R_{MR} + \Delta R_{MR}\frac{H_y}{H_0}$$

→ Highly Sensitive (and linear !!) at low fields H_y.

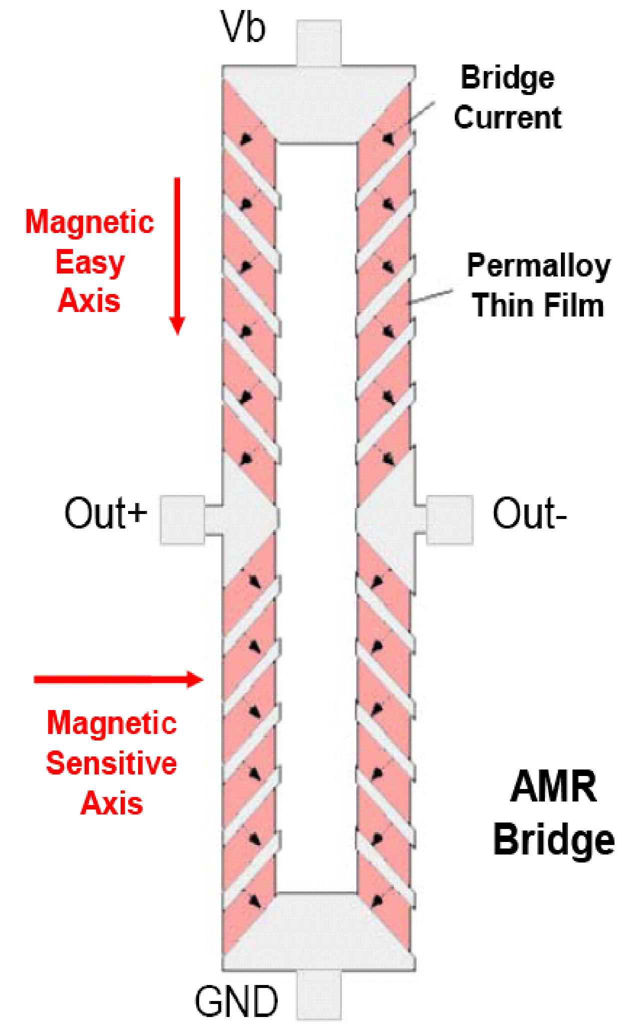

Figure 2 - AMR Sensor Bridge

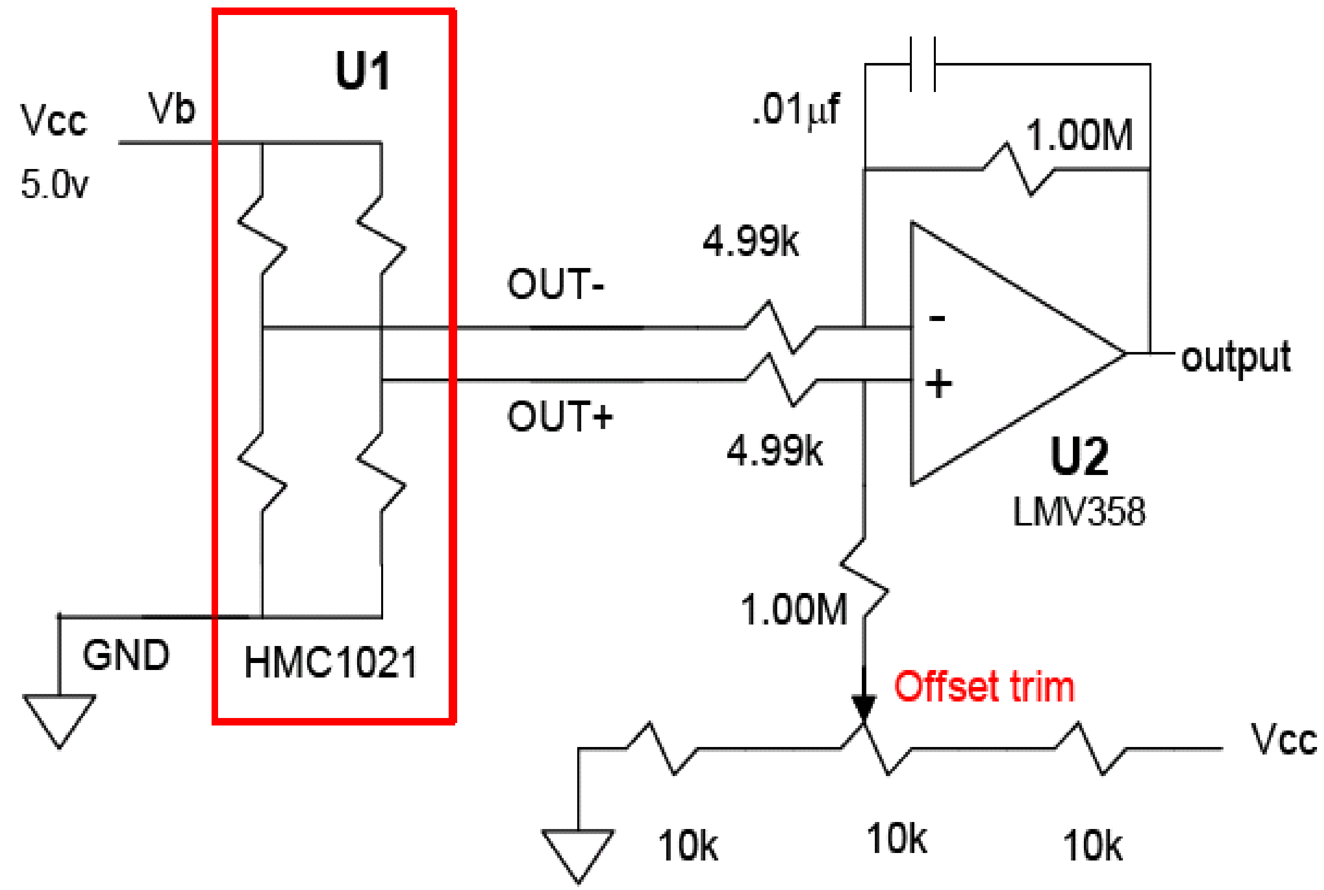

Figure 4 - AMR Sensor Amplification

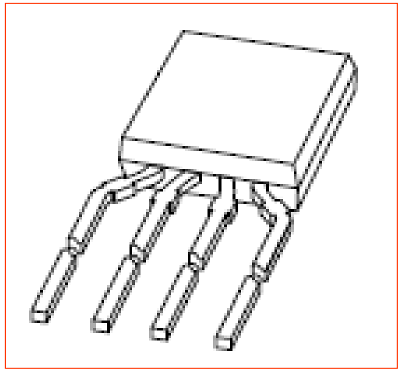

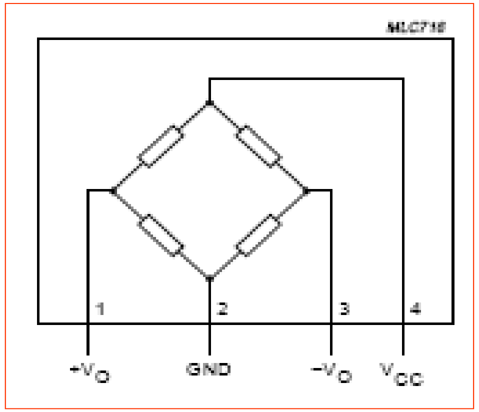

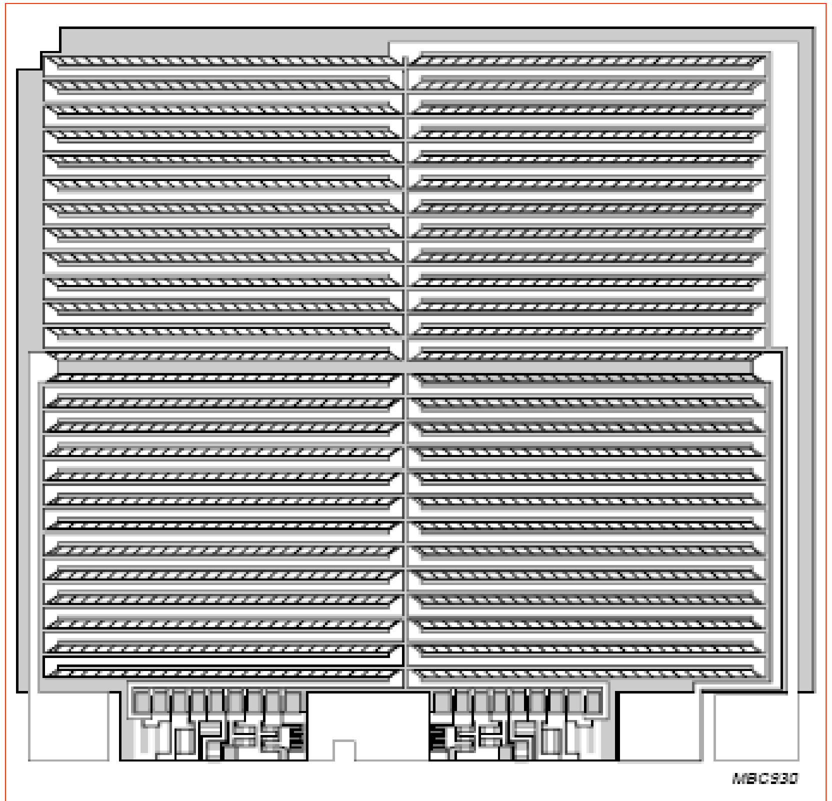

Fig.25 KMZ10 chip structure.

Key-features KMZ 10B:

Chip size	1.6 x 1.6	mm^2
Layer thickness	50	nm
Stipe width	10	µm
H_o	3.8	kA/m
Range	± 2	kA/m
Sensitivity	4.0	(mV/V)/(kA/m)
TC of S	-0.4	%/K
Resistance	1.7	kΩ
TC of R_o	+0.35	%/K

Applications of AMR sensors

Compass
Current sensing
Tracking systems for virtual reality
Angular and linear position sensing
Detection of ferrous objects (cars, planes, trains,…)
Underground drilling navigation , …

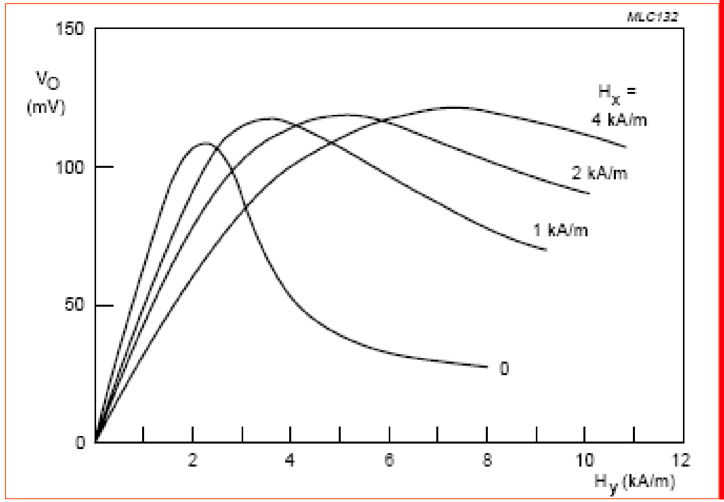

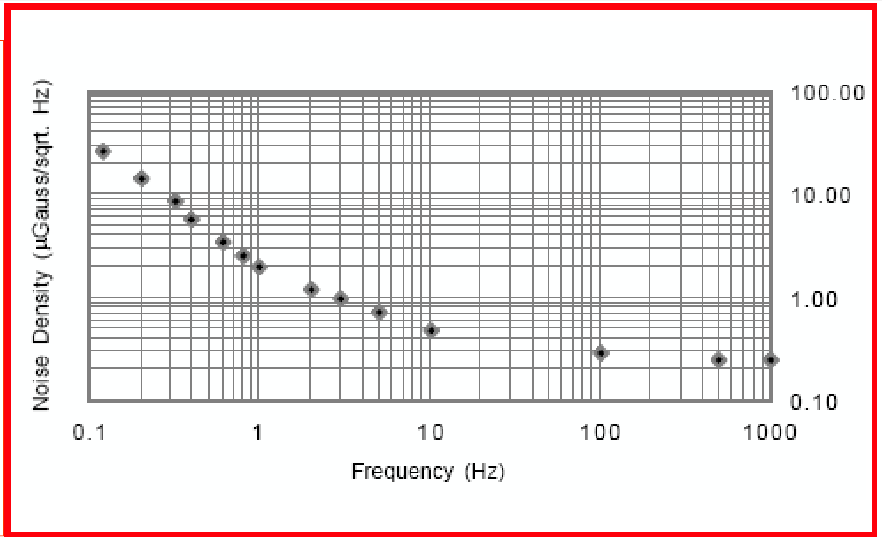

(a) *(b)*

(a) Increase range by adding a field along x. (b) Typical noise in AMR sensors.

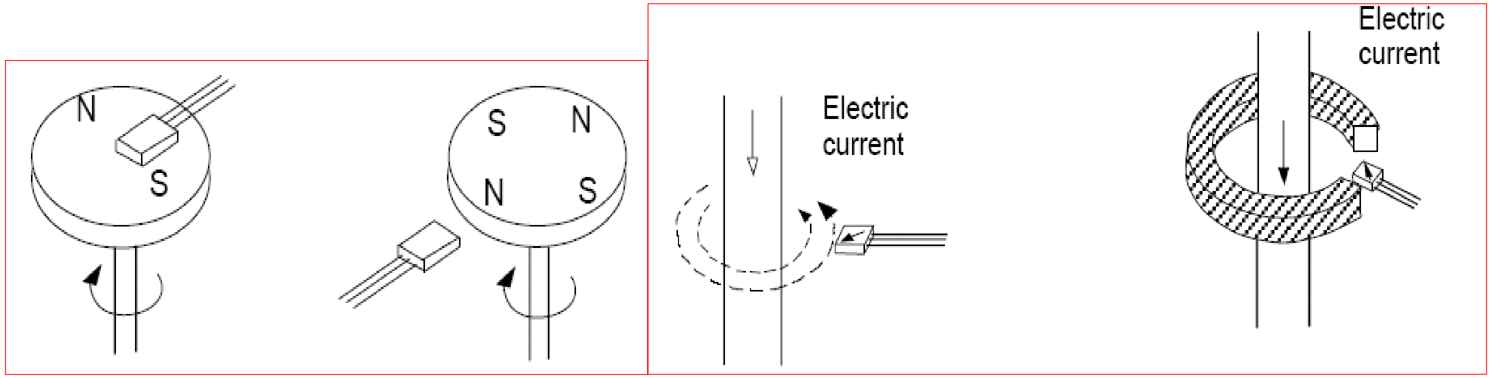

Applications of AMR sensors

Application of AMR array: Gastrointestinal motility

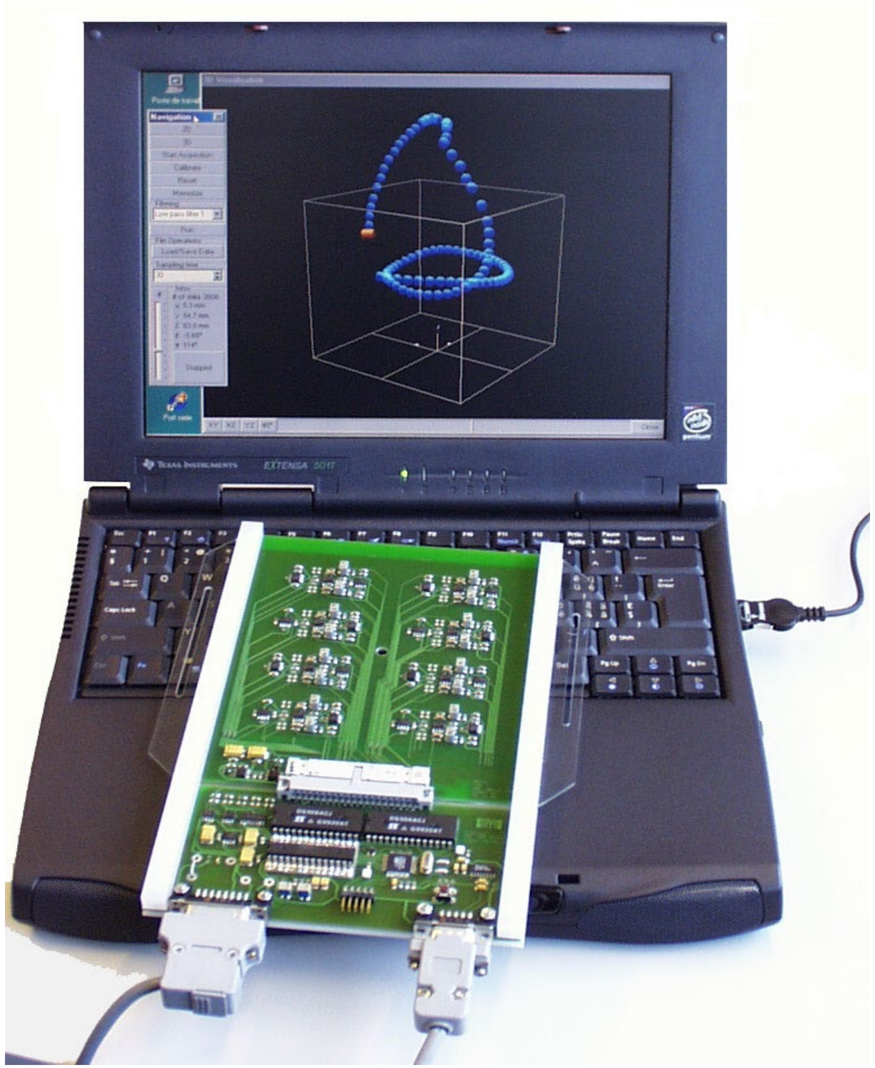

Giant Magneto-Resisitance (GMR)

Discovery:	1988 (Baibich et al.)
Basic effect:	Spin dependent scattering (charge carrier spin-scattering site spin)
On the market:	1994 (Nonvolatile Electronics)

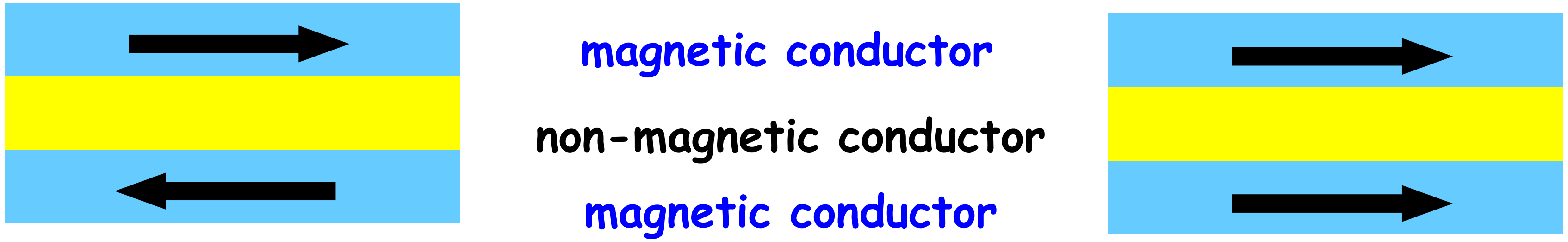

High resistance   Low resistance

Non-magnetic conductor layer thickness (<10nm)
< mean electrons free path

GMR: Basic configurations

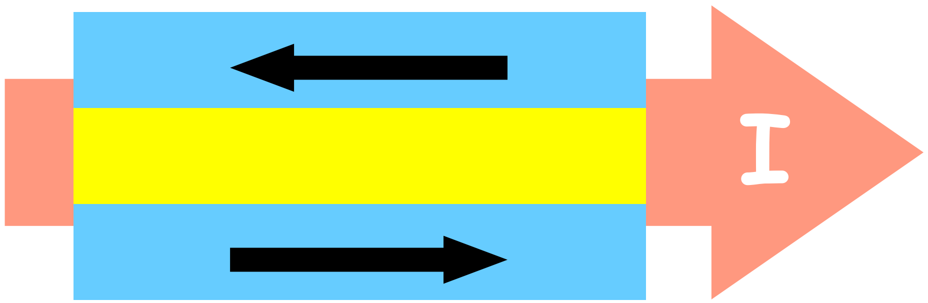

a) Current in the plane

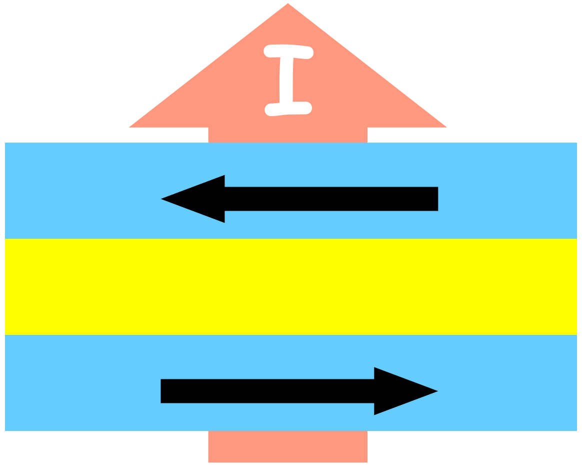

b) Current ⊥ to the plane

GMR sensors **H_{ext} → change in the angle between M_1 and M_2 → ΔR**

(GMR=Giant MagnetoResistance)

Principle: The resistance depends on the angle between the two magnetization vectors.

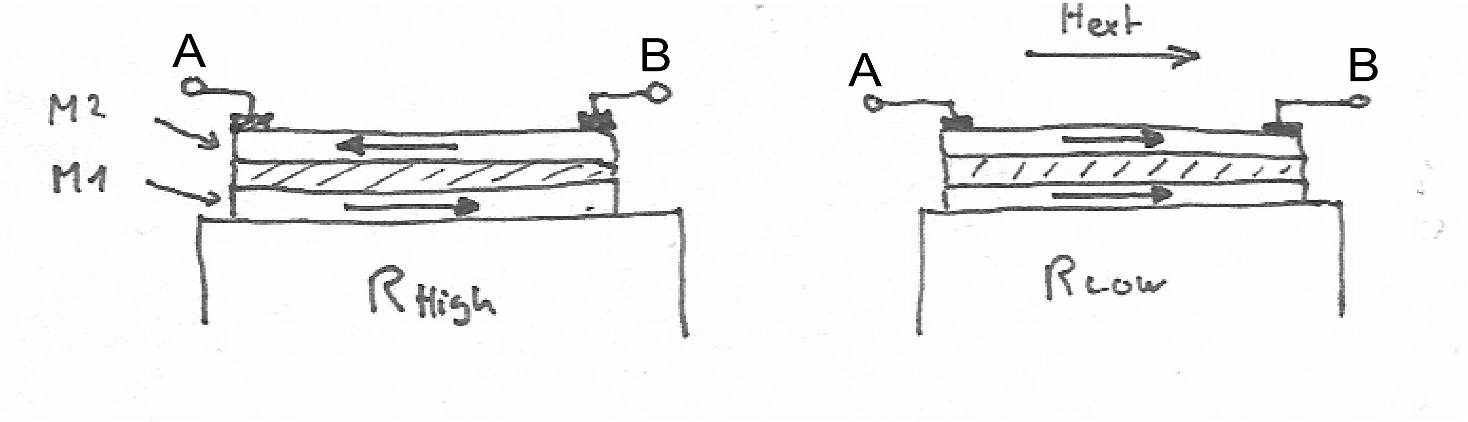

- Thin Multilayer (ex : Fe 3nm/Cr 0.9 nm) < electrons mean free path
- Characteristics :

  R~ few kΩ
  $\Delta R/R$=-5 to -20% (Sensitivity : 10 - 50 µV/V / A/m)
  Range : 0 to 10 mT
  Resolution : 0.1 nT/Hz$^{1/2}$

$$R = R_{\varphi=180^\circ} - \Delta R_{GMR}\left(1+\cos\varphi\right)/2$$

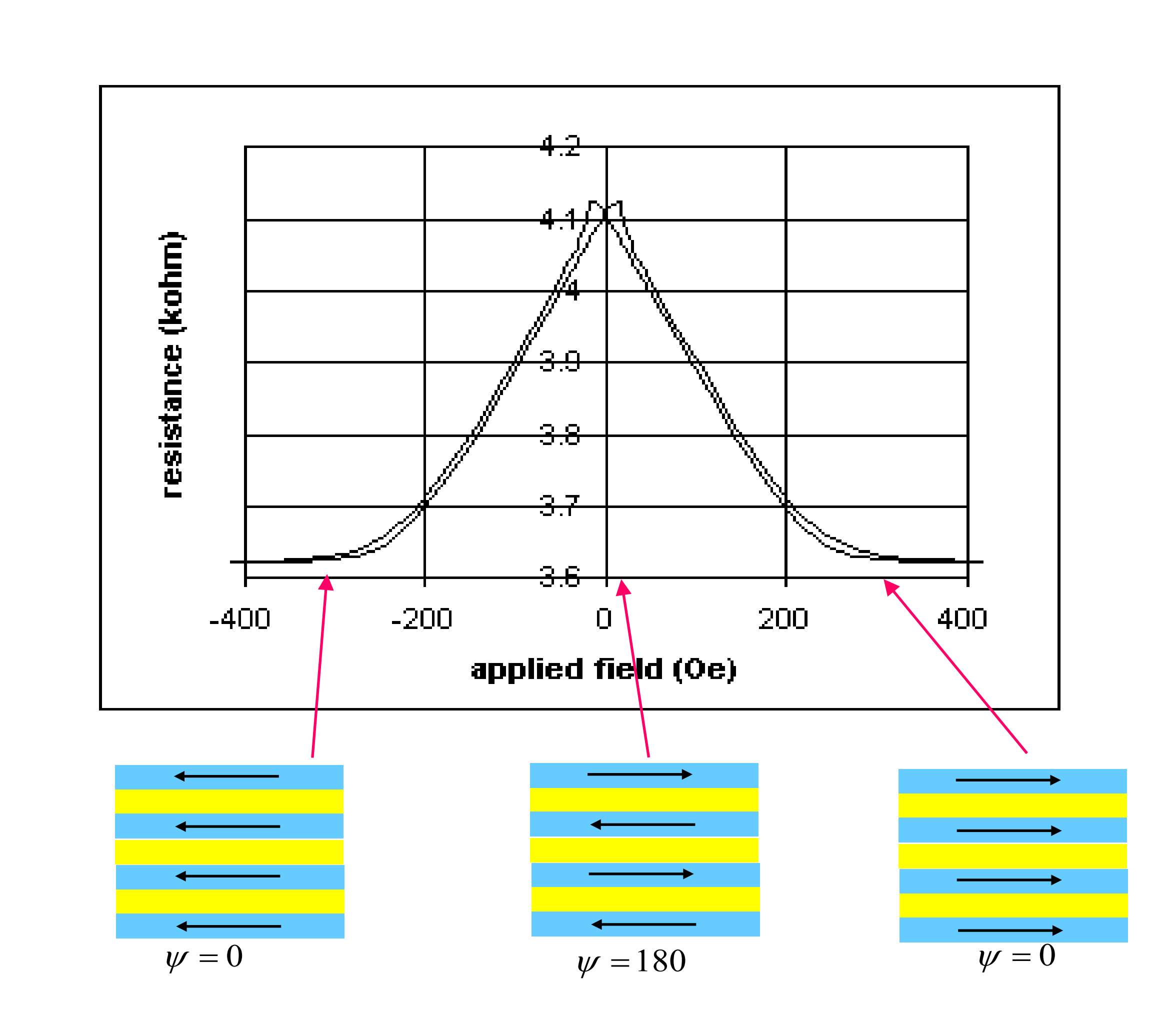

Problem: Non linear about H=0.
Solution: M_1 fixed ("pinned layer"), M_2 with "easy axis" at 90° with respect to M_2

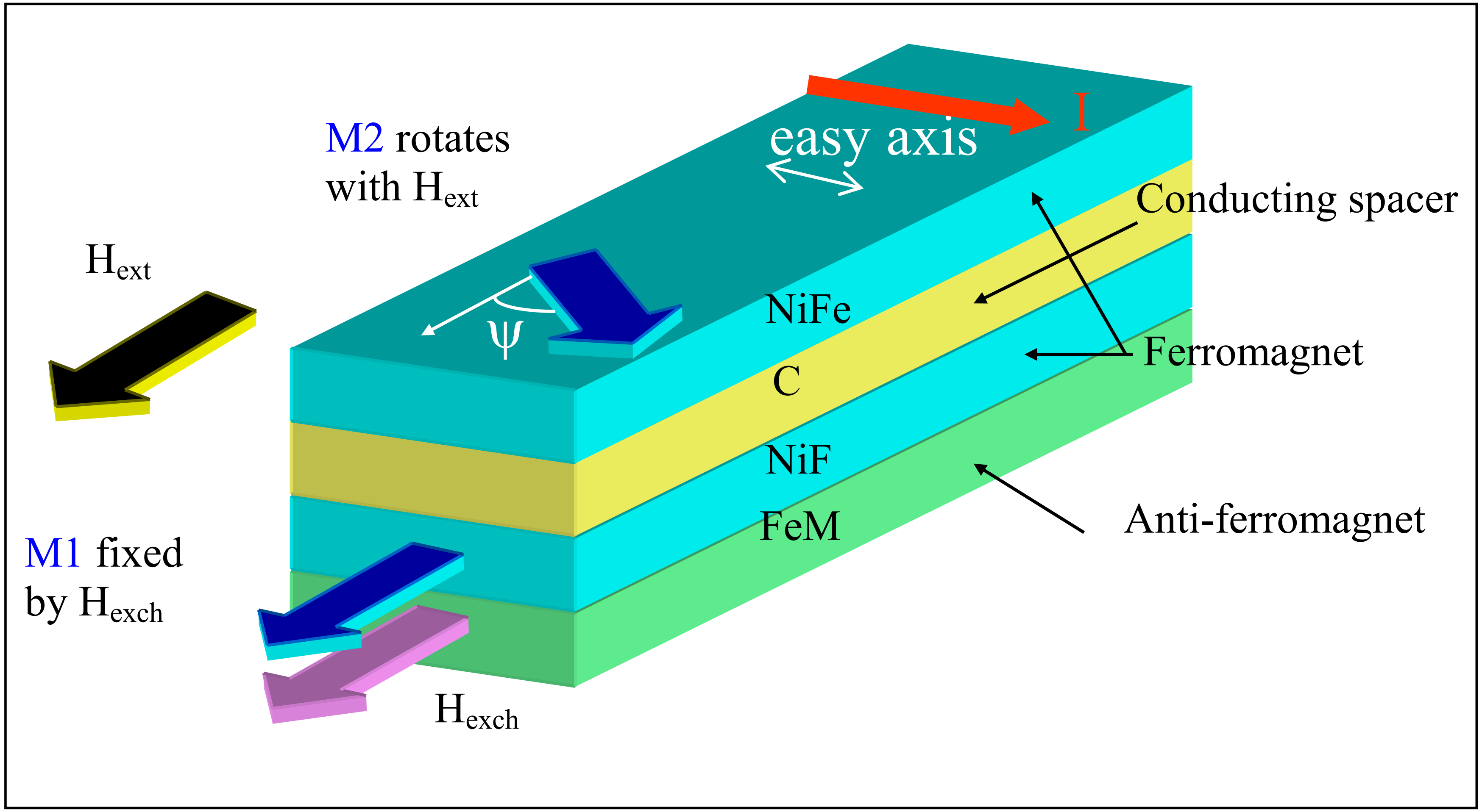

The M1 layer is strongly coupled to the anti-ferromagnetic layer. The M2 layer is weakly coupled to the M1 layer and can rotate with the external field.

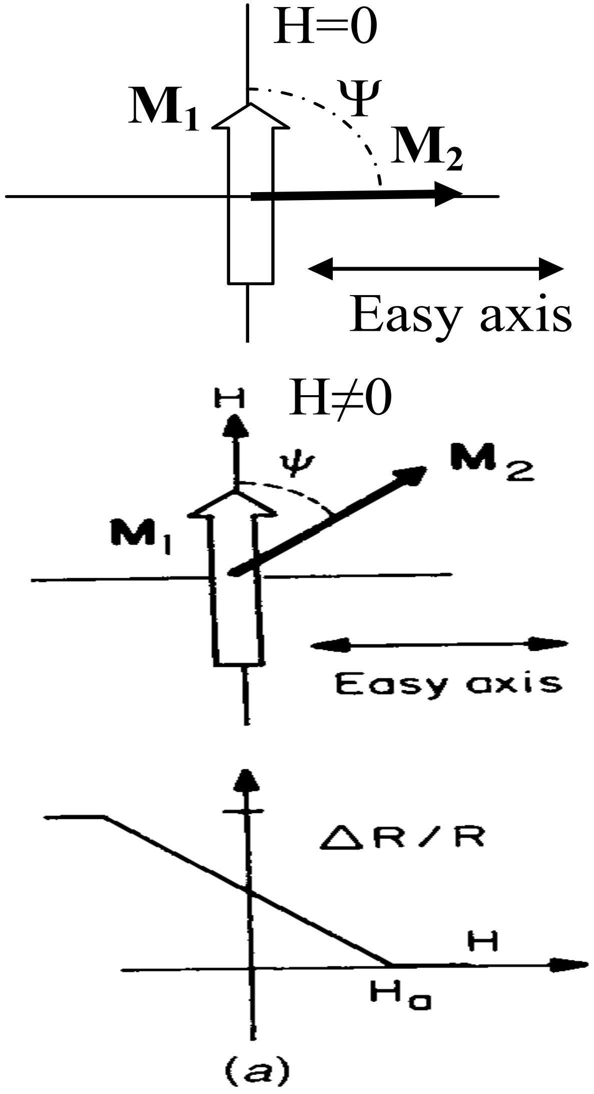

$\mathbf{M}_1 \perp (easy\ axis) \Rightarrow R(H)\ linear$

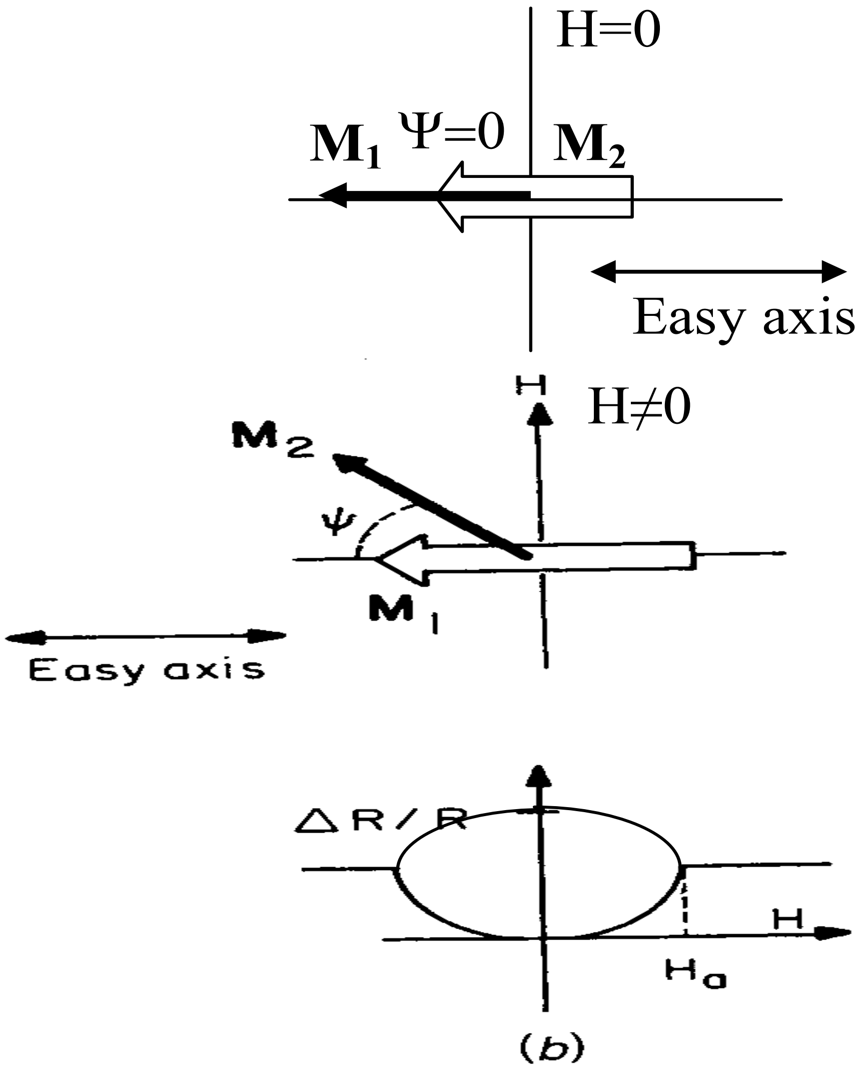

$\mathbf{M}_1 // (easy\ axis) \Rightarrow R(H)\ quadratic$

GMR: «Equivalent model»

- Spin-spin coupling → scattering between free electron and fixed site.
  Spin up / spin down → more scattering.
- $\rho\uparrow\downarrow > \rho\uparrow\uparrow = \rho\downarrow\downarrow$
- Independent of current direction
- Periodicity: 360^0

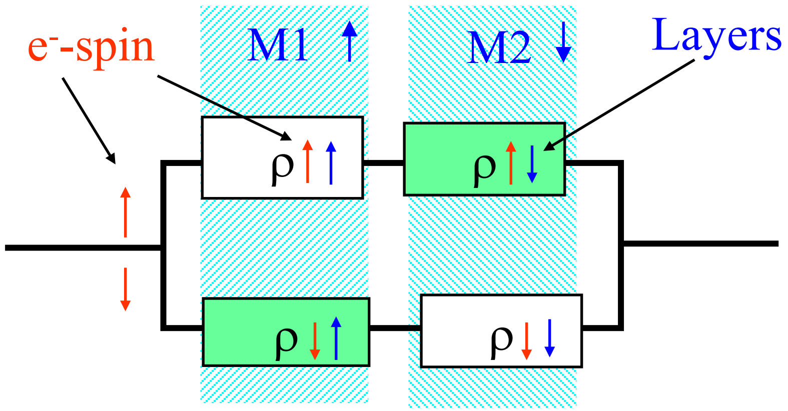

M1 anti-// M2 → ρ large

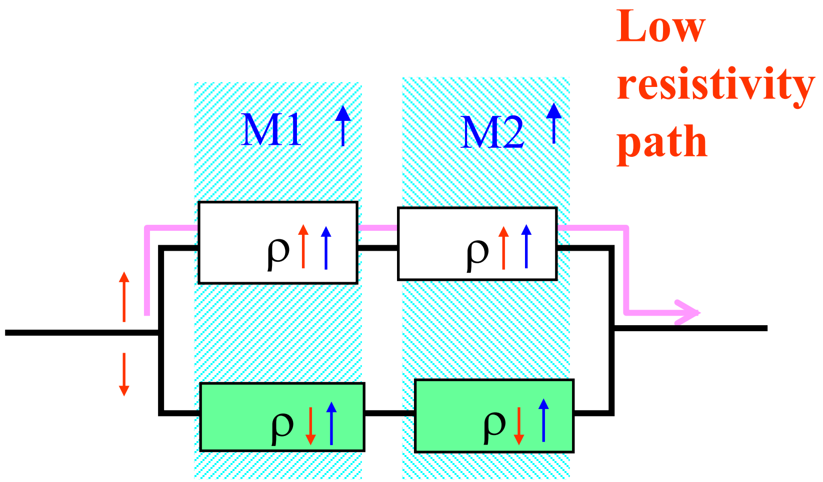

M1 // M2 → ρ small

GMR: Applications

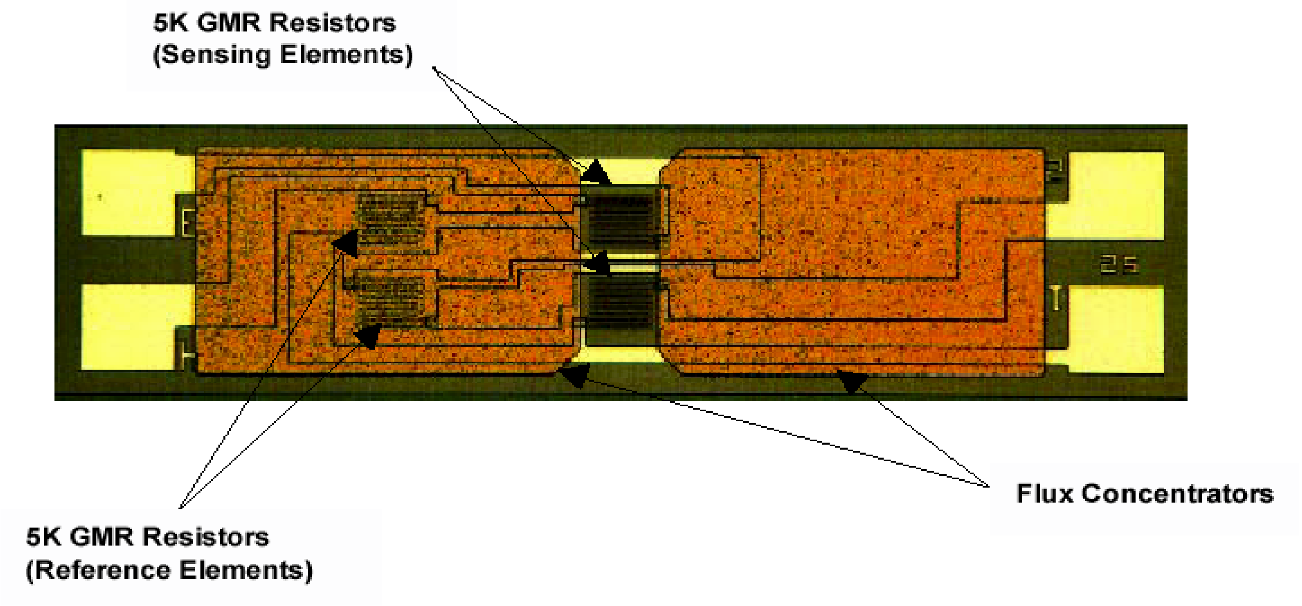

GMR Applications:

- Read heads for hard disks
- Position & velocity sensors
- Magnetic memories (MRAM)

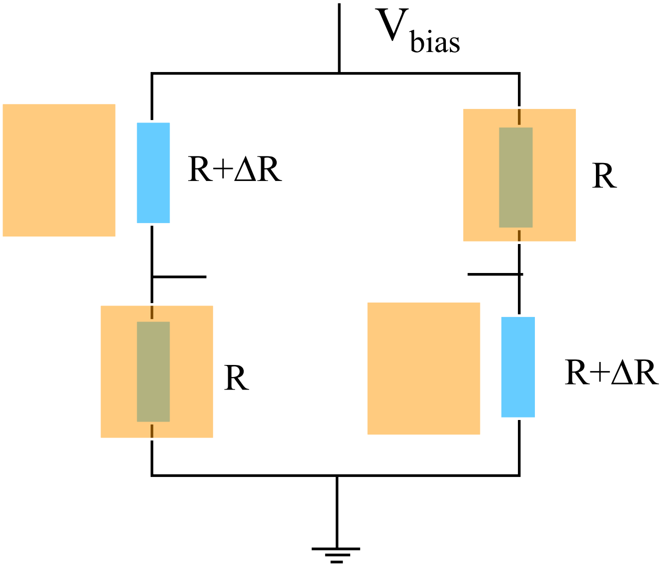

$$V_{out} = \frac{V_{bias}}{2} \frac{\Delta\rho}{\rho} \frac{1}{H_a} G_{mag} \; H$$

G_{mag} = gain of concentrators ~10

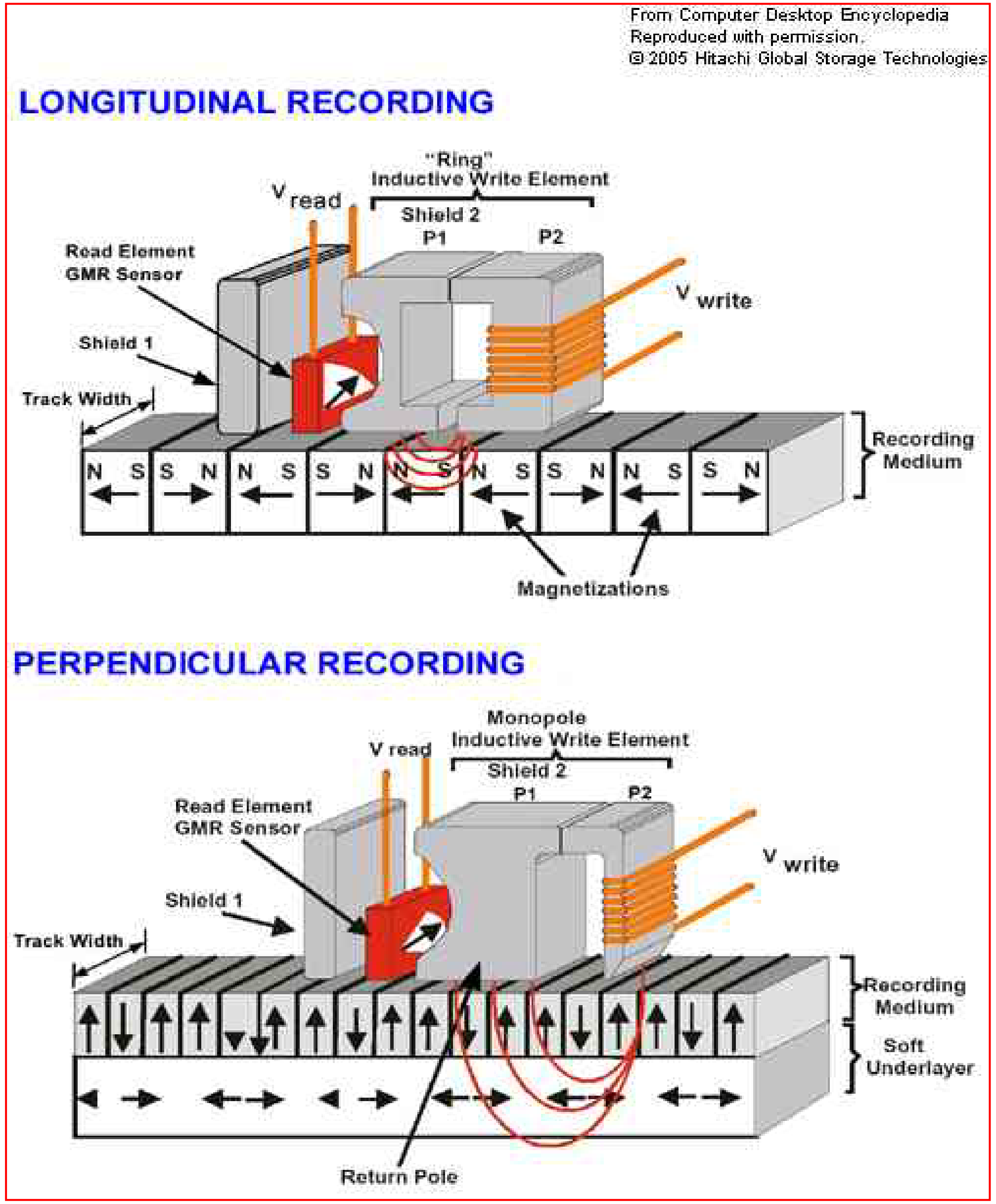
From Computer Desktop Encyclopedia
Reproduced with permission.
© 2005 Hitachi Global Storage Technologies
LONGITUDINAL RECORDING
"Ring"
Inductive Write Element
V read
Shield 2
P1
P2
Read Element
GMR Sensor
V write
Shield 1
Track Width
Recording Medium
N S S N N S S N N S N S S N N S S N
Magnetizations
PERPENDICULAR RECORDING
Monopole
Inductive Write Element
V read
Shield 2
P1
P2
Read Element
GMR Sensor
V write
Shield 1
Track Width
Recording Medium
Soft Underlayer
Return Pole

Hard disk read-write-head

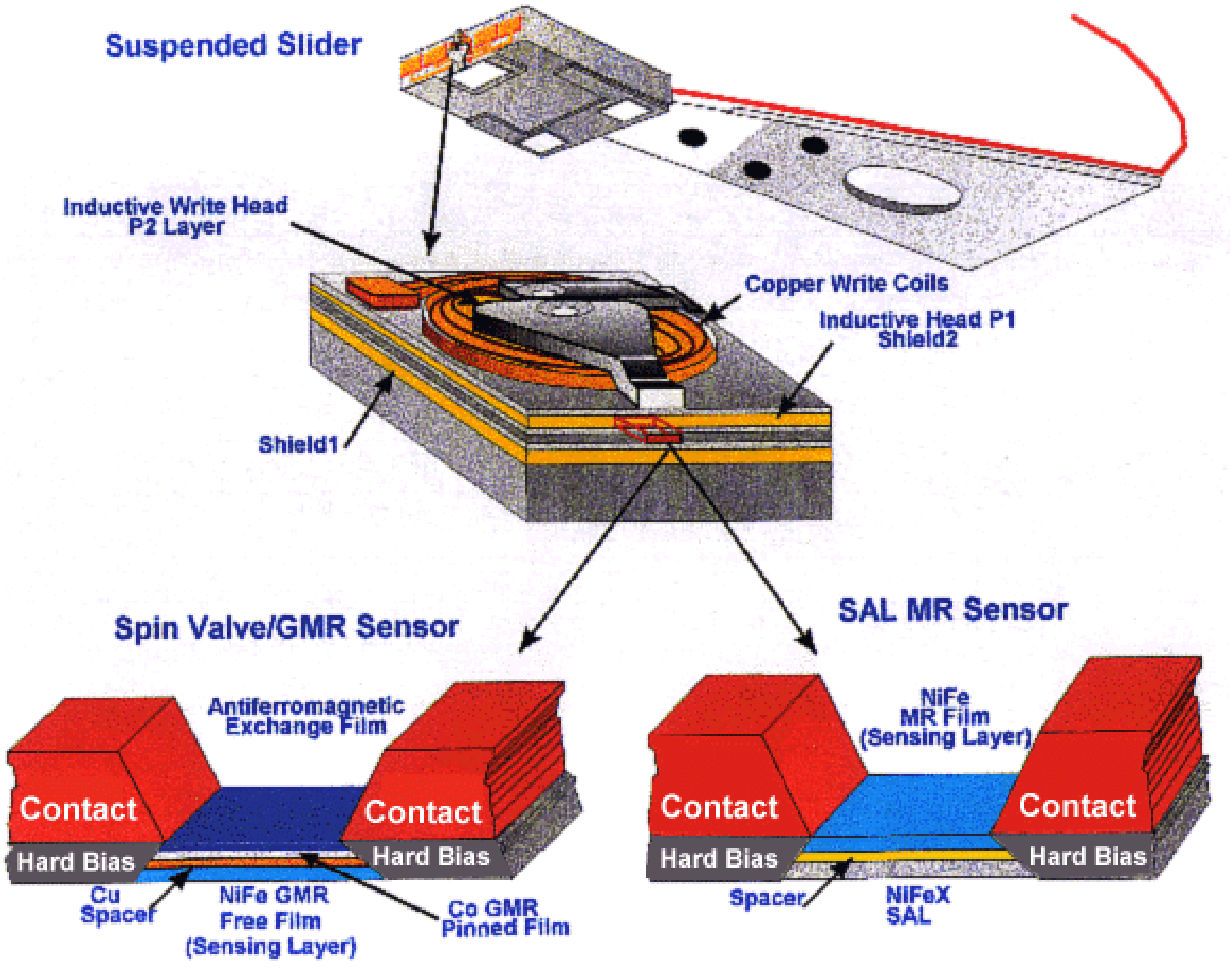

Figure 2. MR and GMR head structures.

Writing *by a coil.*

Reading *by AMR or GMR sensors.*

«Hall» flow sensor

Force on ions :

$$\mathbf{F} = q(\mathbf{E} + \mathbf{v} \times \mathbf{B})$$

$$V_S = kDvB\cos\omega t$$

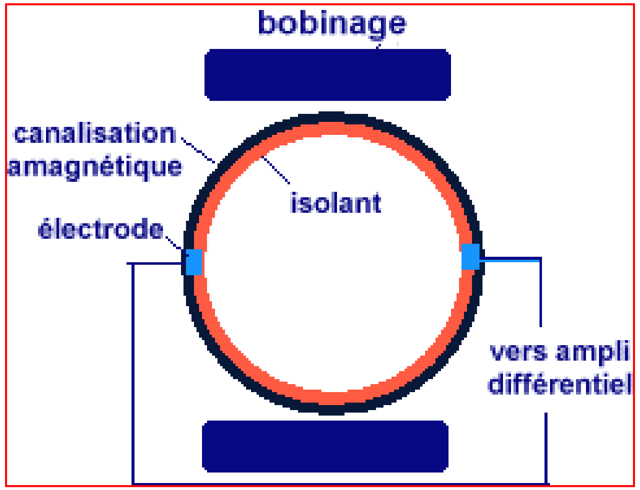

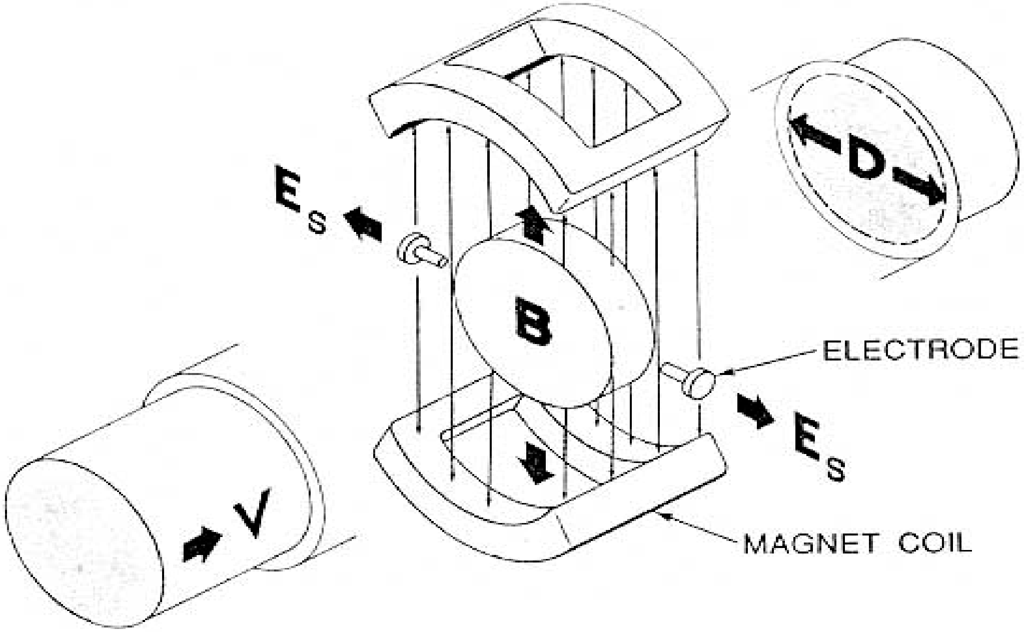

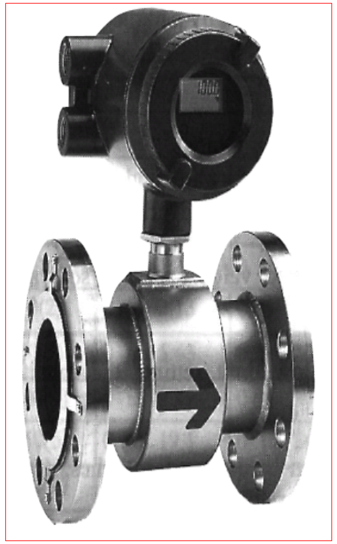

Relais (Switch) REED

- Sensor ON/OFF, made of two pieces of soft ferromagnets (exemple: NiFe).

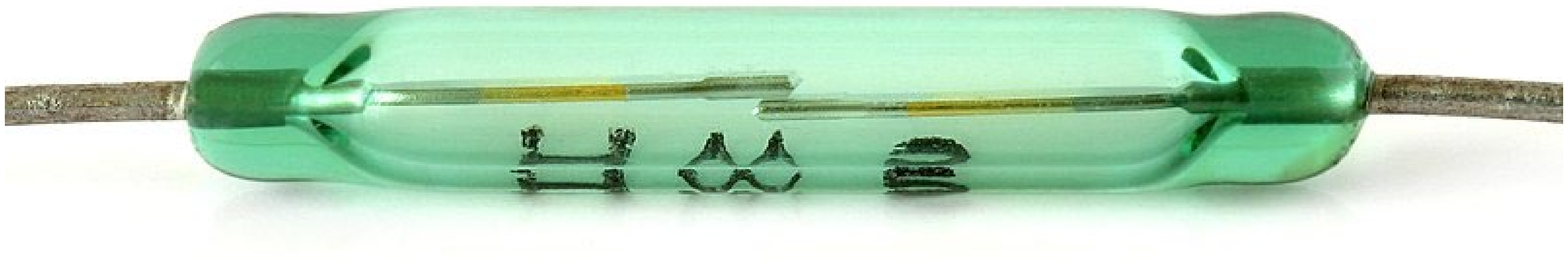

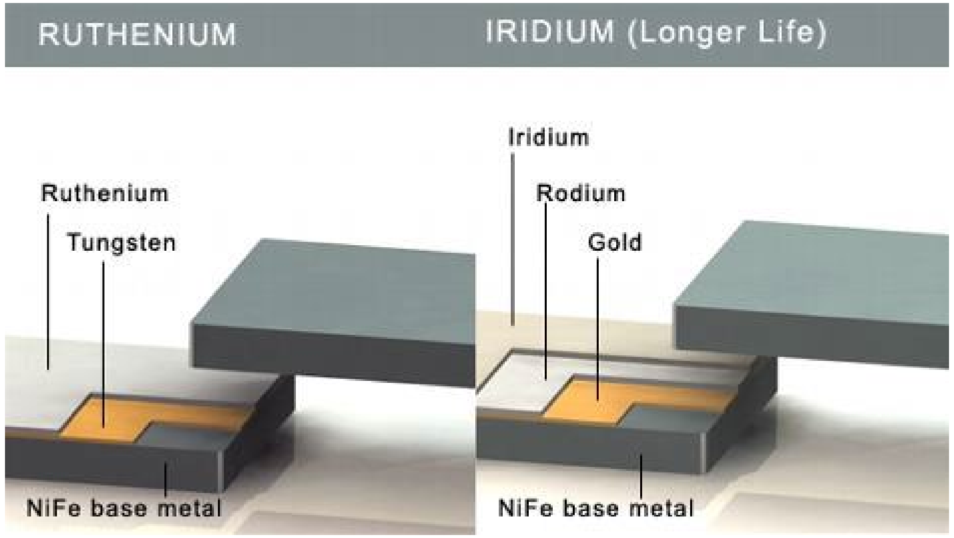

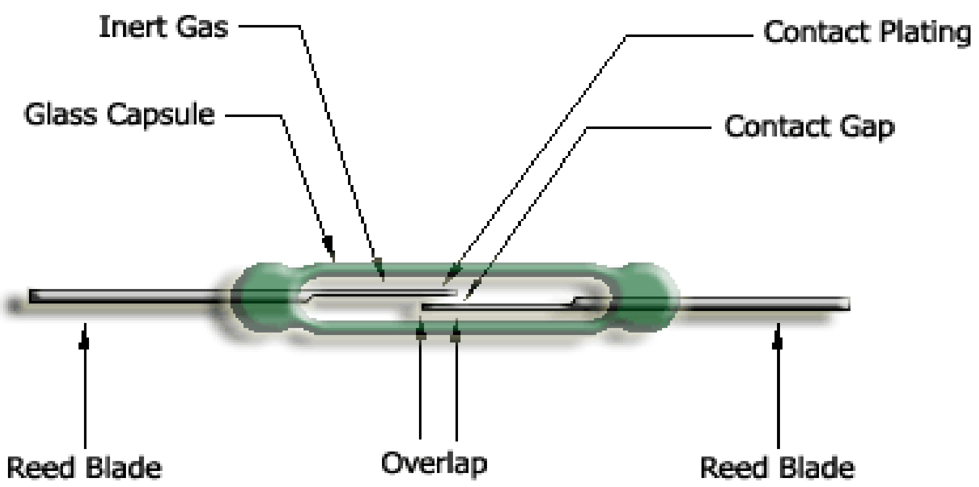

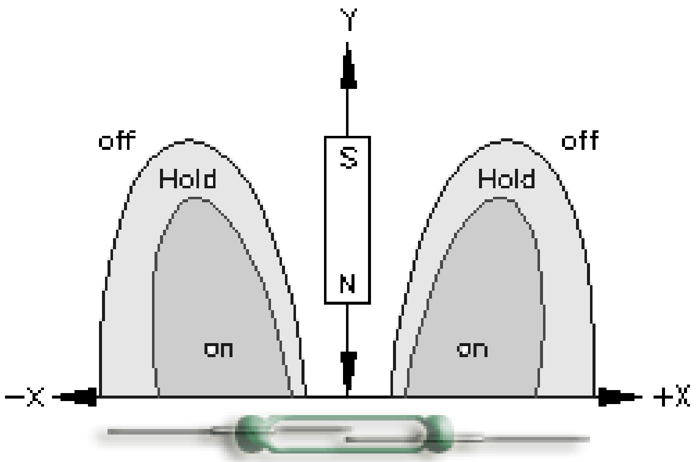
Y
off
Hold
S
N
off
Hold
on
on
−X
+X

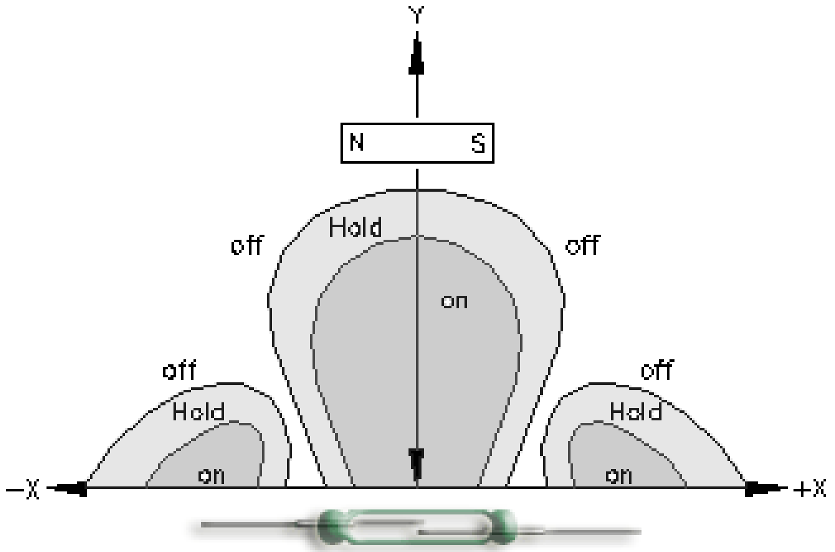
Y
N
S
off
Hold
off
on
off
Hold
on
off
Hold
on
−X
+X

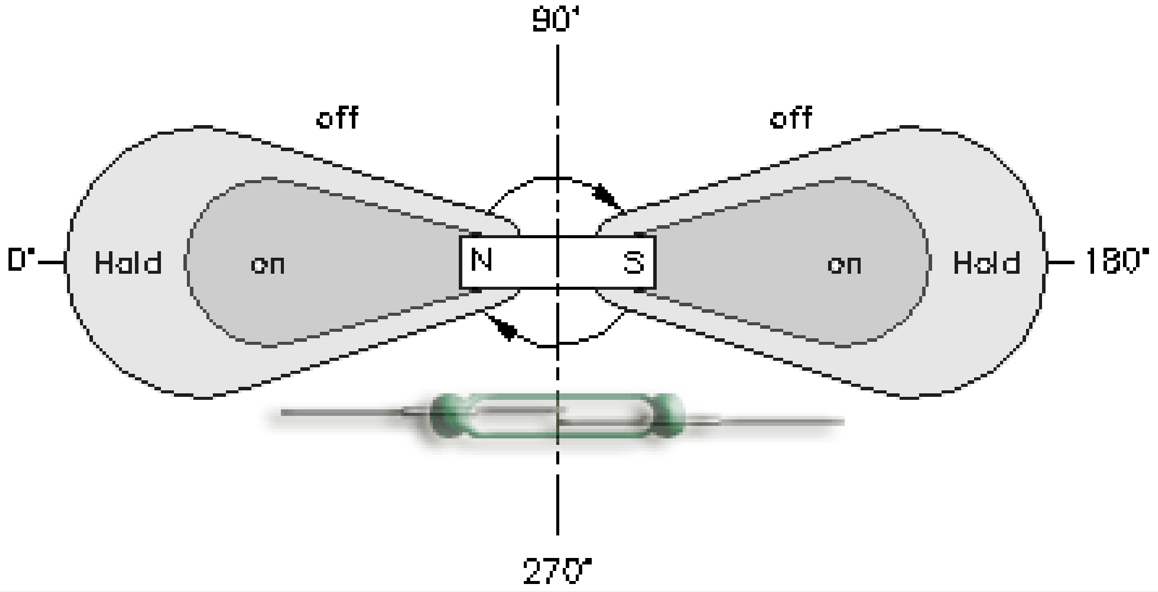
90°
off
off
0°
Hold
on
N
S
on
Hold
180°
270°

Magnetic shielding

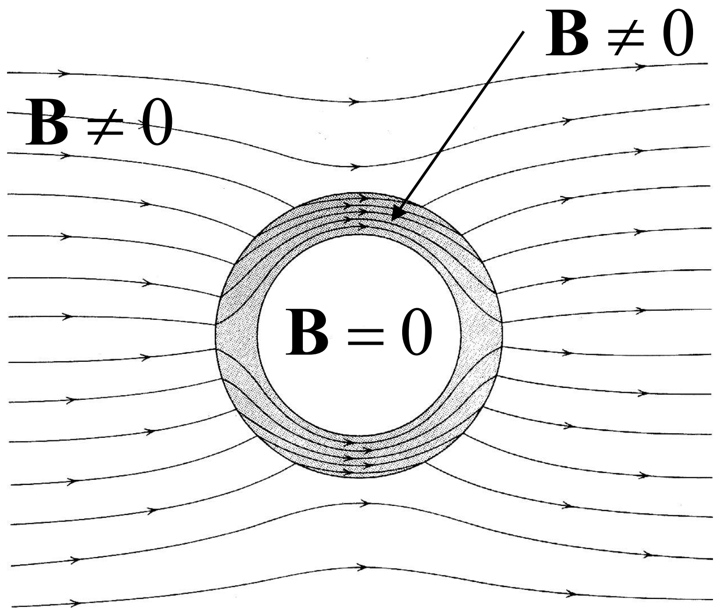

Screening (B=0 inside the "box"):
The magnetic dipoles in the material are oriented in such a way that they produce a field of equal magnitude but in the opposite direction to the external field.
The total magnetic field inside the box is zero.

A possible material: "mu-metal" (alloys with ~80% Ni): $\mu_r \sim 100000$

Magnetic chopper

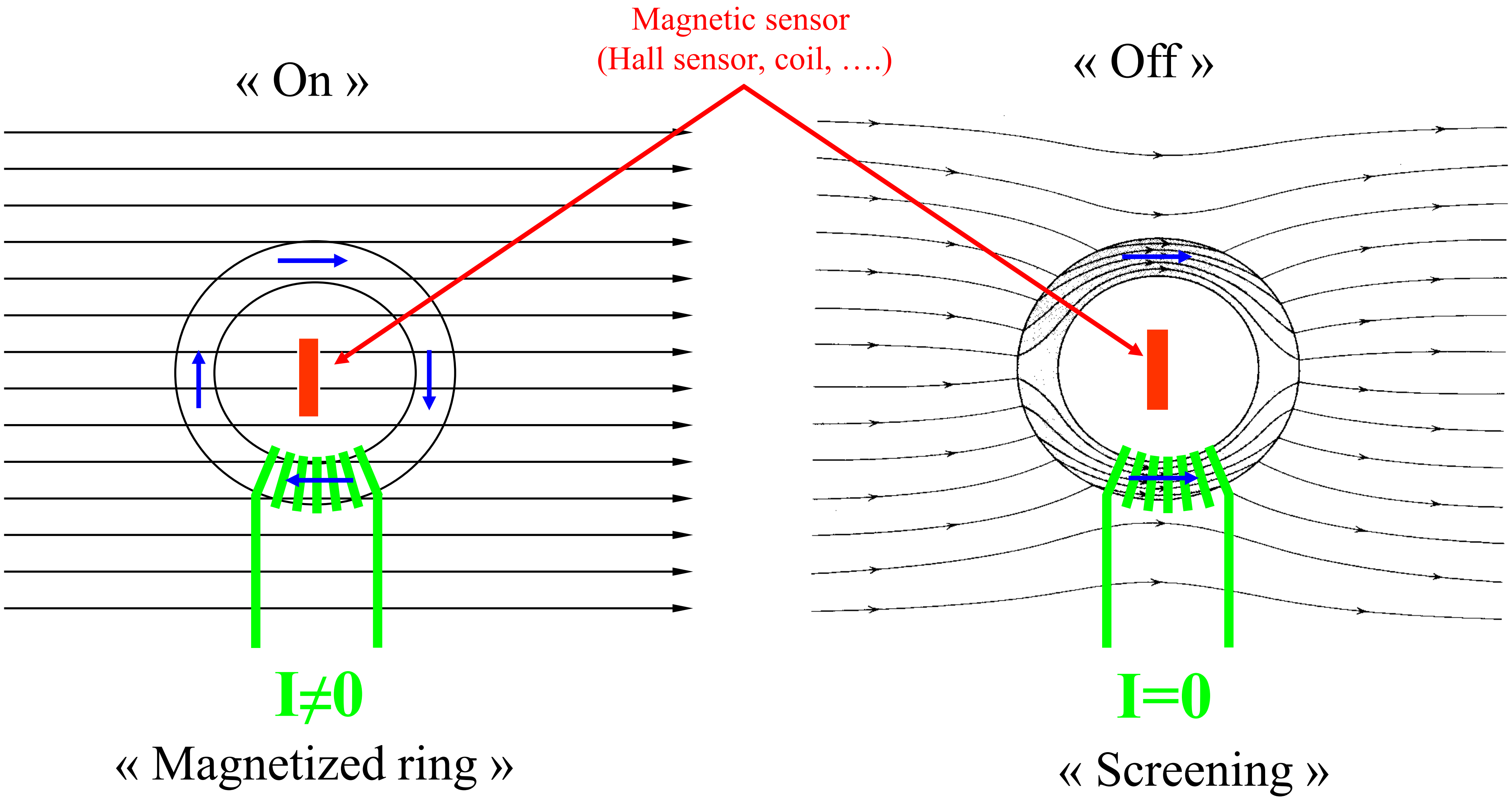

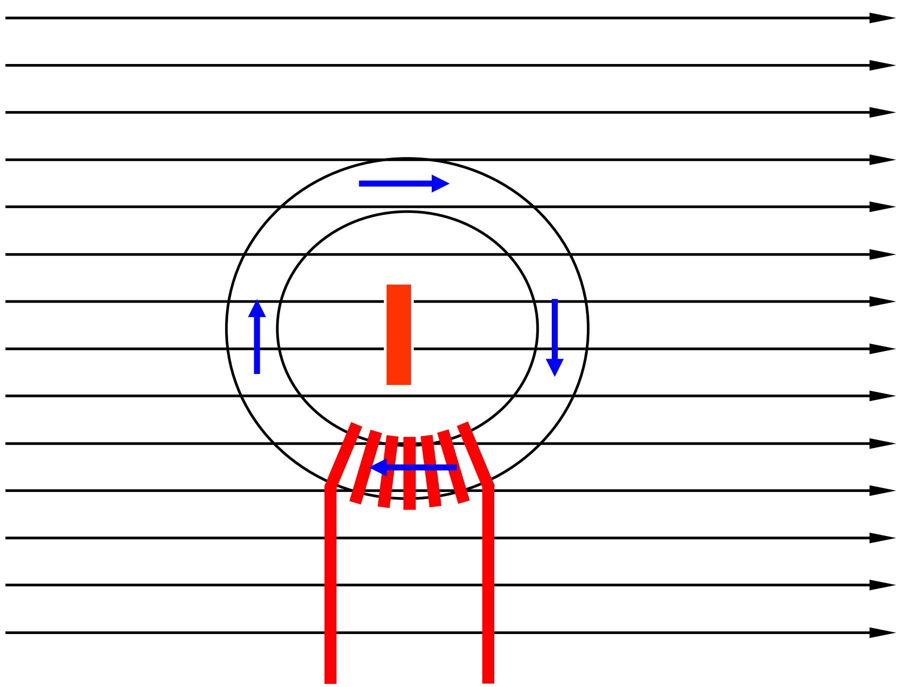

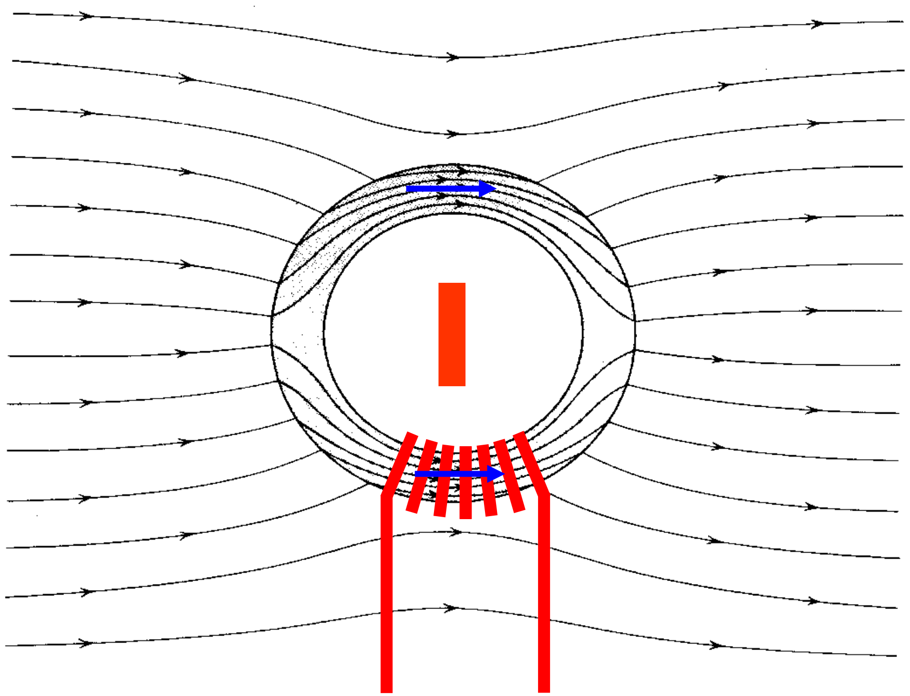

$I \neq 0$ $\quad$ $I = I_0 \cos(\omega_m t)$ $\quad$ $I = 0$

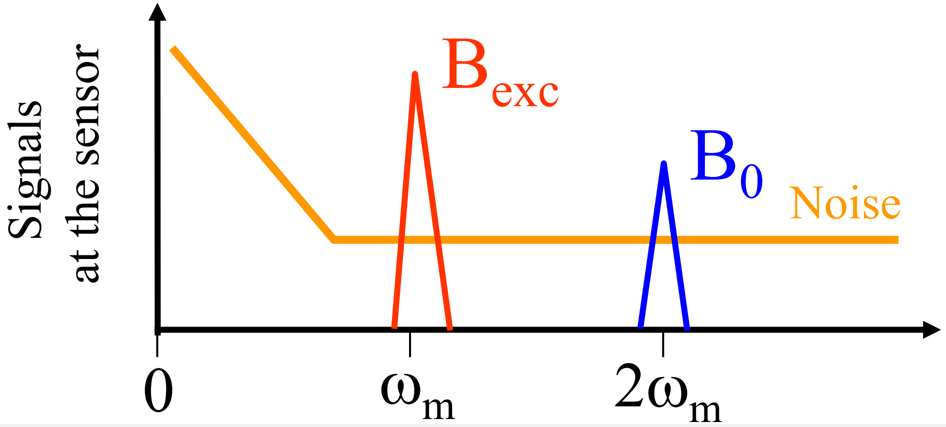

Magnetic chopper: example

Hall sensor

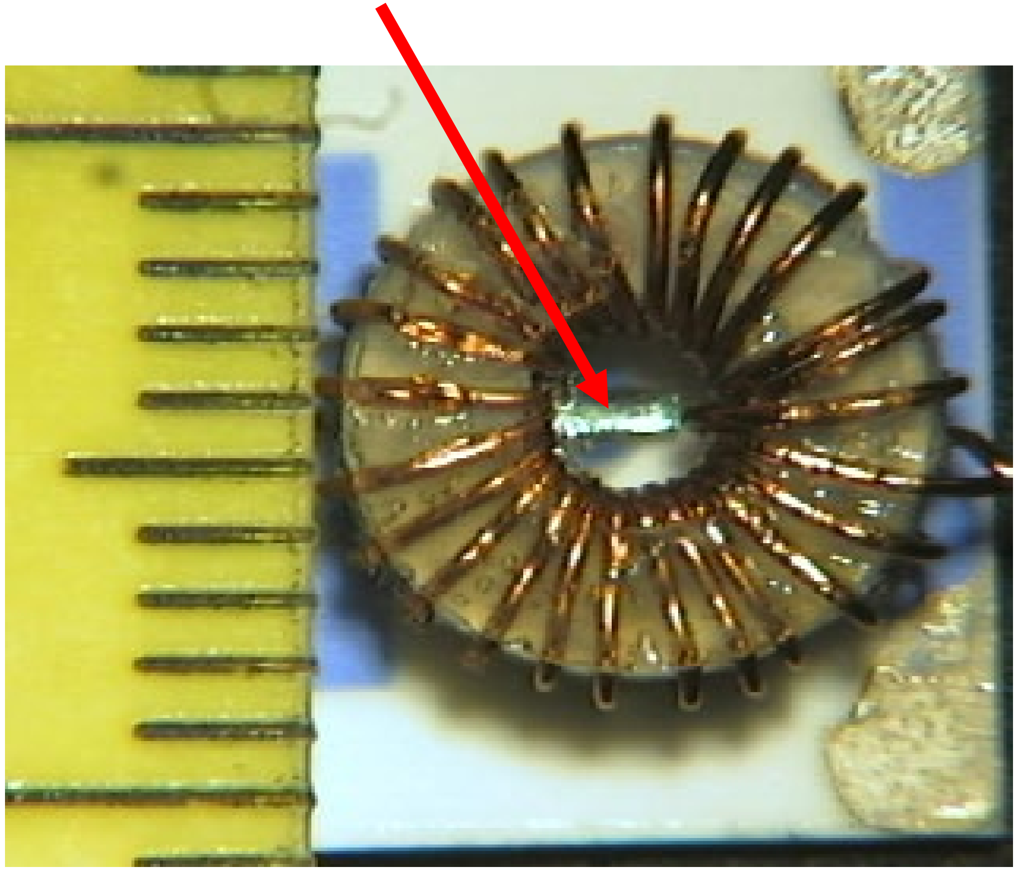

Fluxgate magnetic sensor: possible realizations

Excitation: Coil
Detection: Hall sensor

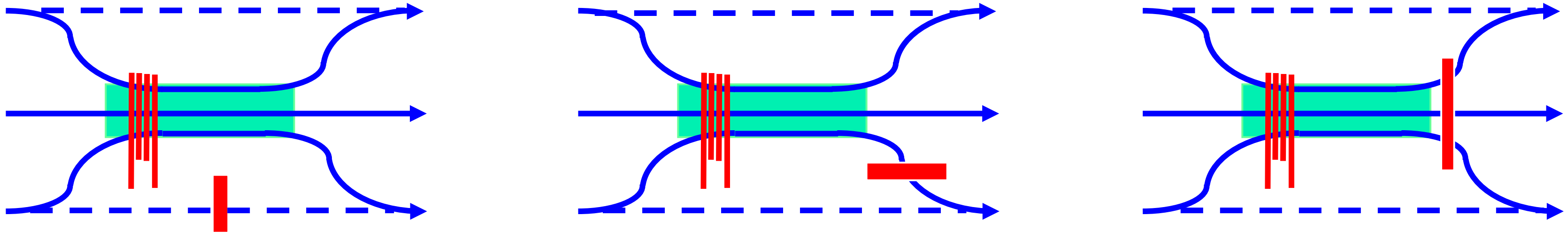

Excitation: Coil
Detection: Coil

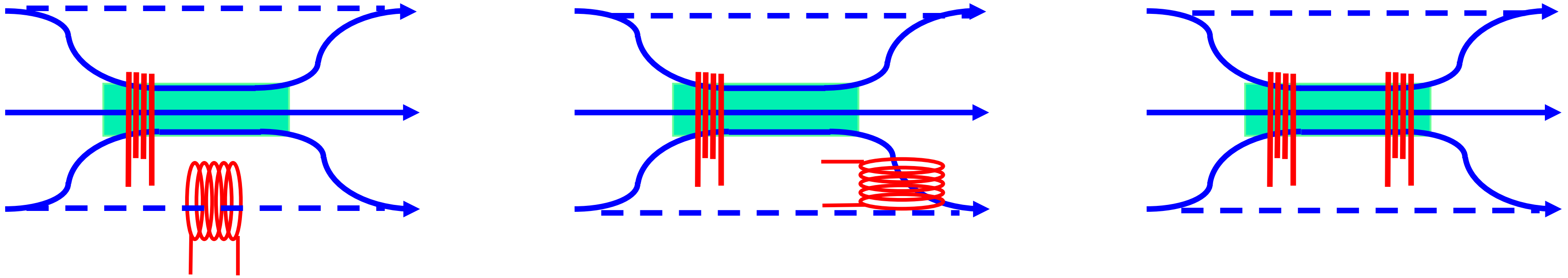

Fluxgate magnetic sensor

Excitation: Coil
Detection: Coil

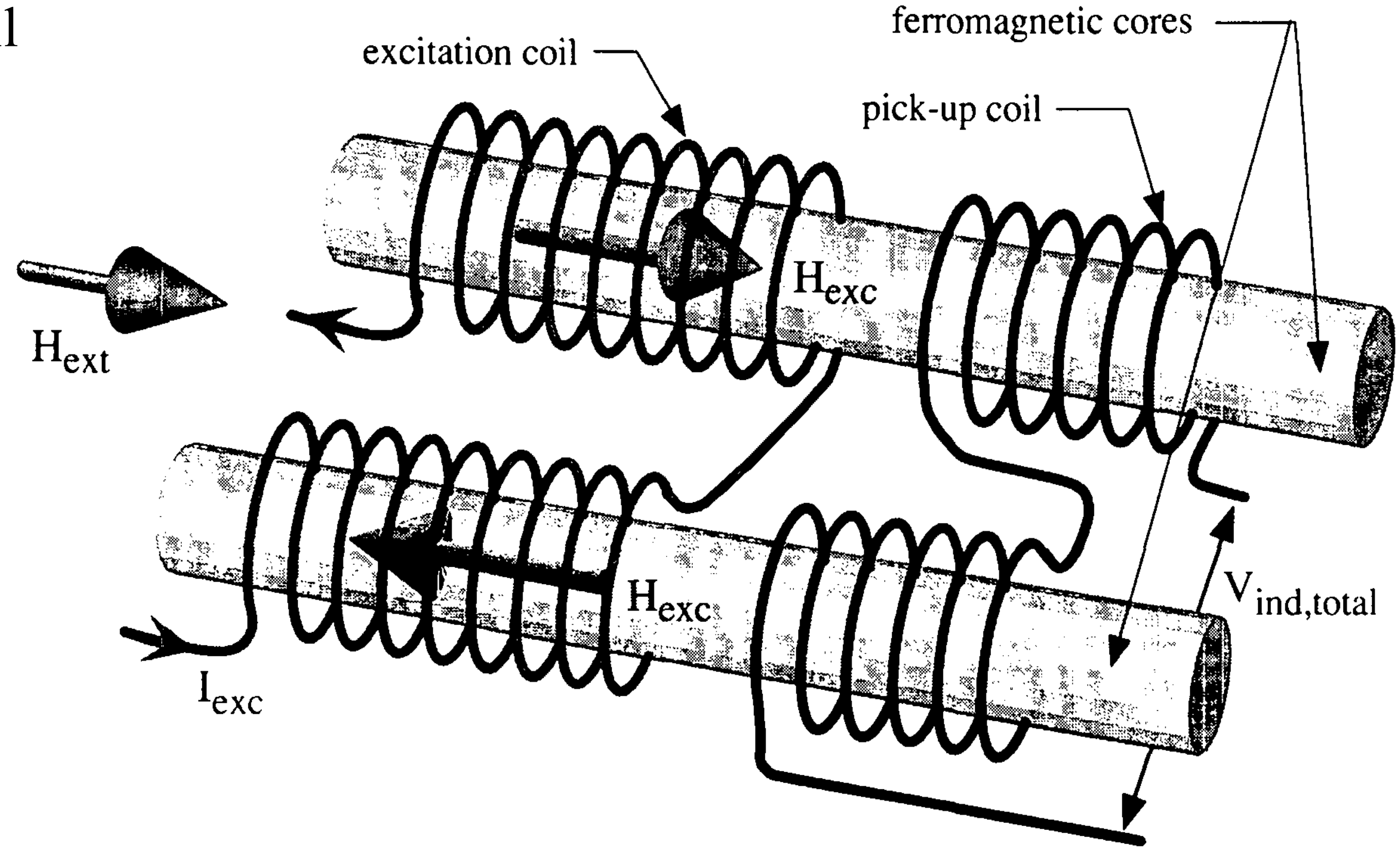

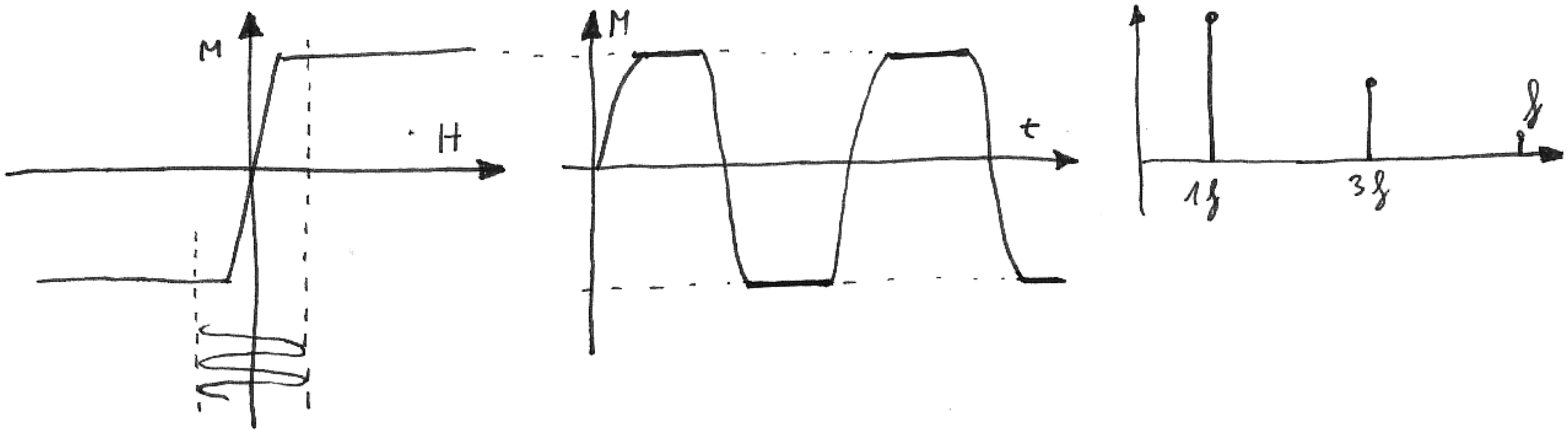

For an symmetric oscillating H with no offset with respect to zero) → odd harmonics only.

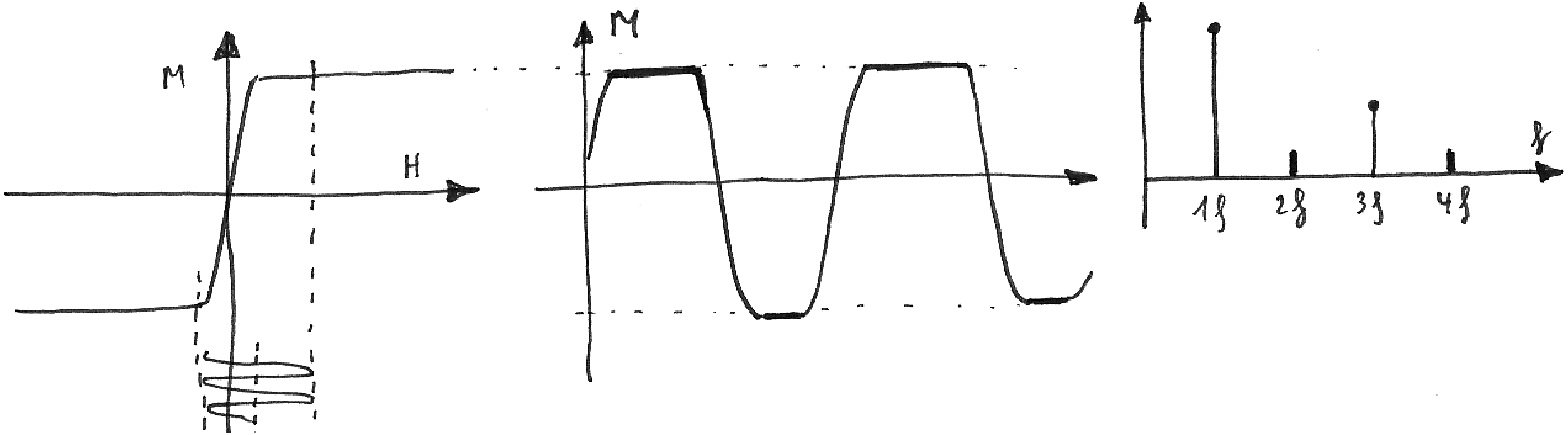

*For an symmetric oscillating H with offset with respect to zero → odd and **even** harmonics.*

EPFL

Field to be measured: component of H_{ext} parallel to the detection coil axis

1. non-saturated core (I_{exc}=0, H_{exc}=0) : $\mu = \mu_{in}$ $B = \mu_{in} H_{ext}$

2. saturated core ($I_{exc} \neq 0$, $H_{exc} \neq 0$) : $\mu_{sat} << \mu_{in}$ $B \cong \mu_{sat}\left(H_{exc} + H_{ext}\right)$

$$\rightarrow \quad \Delta B \cong \left(\mu_{in} - \mu_{sat}\right) H_{ext} \cong \mu_{in} H_{ext}$$

Non-linear μ: $B = \mu_{in} H - \alpha H^3$ (simple approximation)

Field to be measured: H_{ext}

Modulation field : $H_{exc} \sin \omega t$

Total field: $H = H_{ext} + H_{exc} \sin \omega t$

Modulation of the total magnetic induction :

$$B = \underbrace{\mu_{in} H_{ext}}_{DC} + \underbrace{\mu_{in} H_{exc} \sin \omega t}_{f} - \underbrace{\alpha H_{ext}^{3}}_{DC} - \underbrace{3\alpha H_{exc}^{2} H_{exc} \sin \omega t}_{f} - \underbrace{3\alpha H_{ext} H_{exc}^{2} \sin^{2} \omega t}_{2f} - \underbrace{\alpha H_{exc}^{3} \sin^{3} \omega t}_{3f}$$

$$V_{ind} = -\frac{d\phi_B}{dt} \propto \frac{dB}{dt}$$

The component at 2ω is directly proportional to H_{ext}. To measure the field H_{ext} → detection of of the harmonic at 2ω

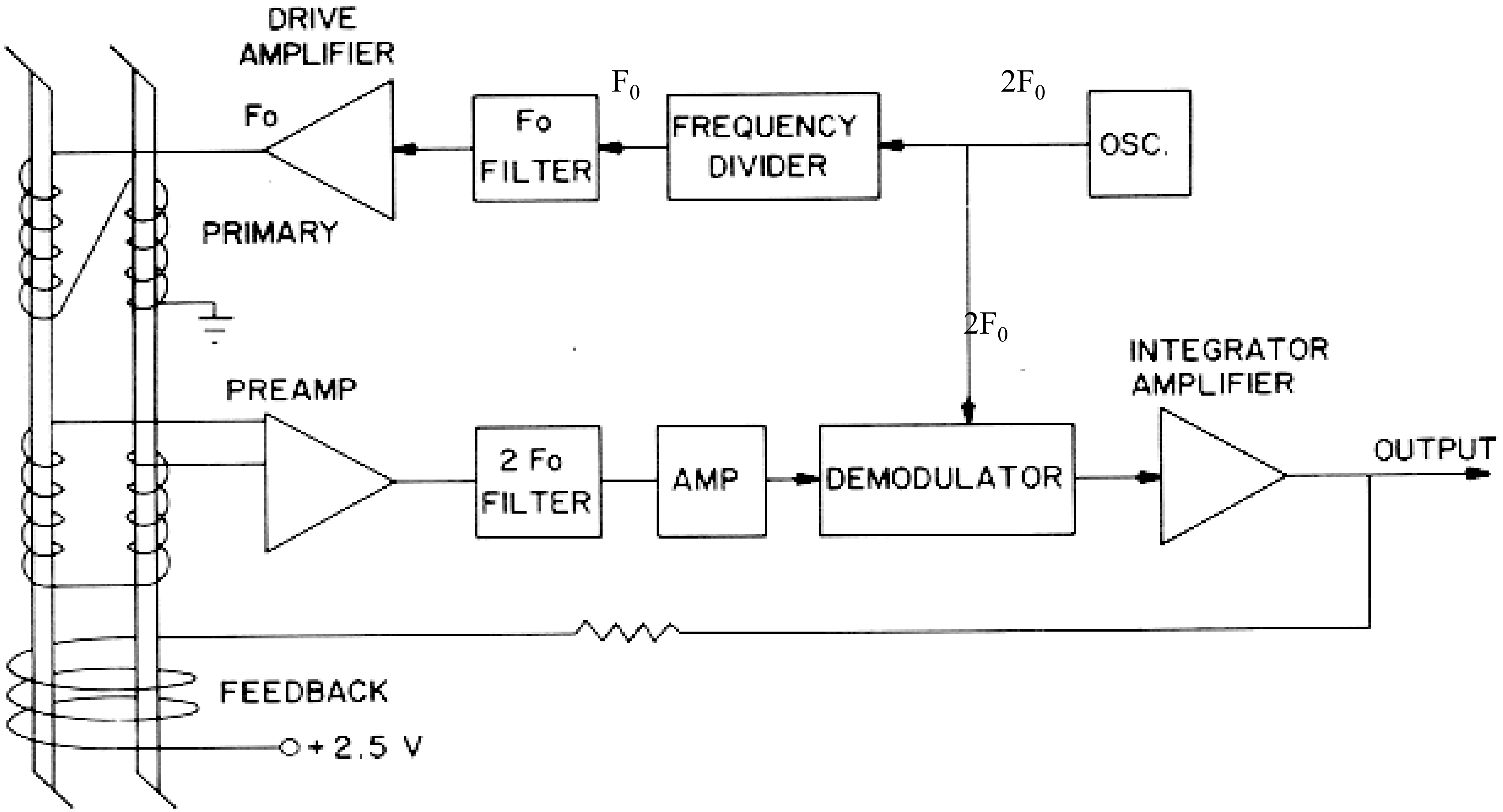
DRIVE
AMPLIFIER
Fo
Fo
FILTER
F0
FREQUENCY
DIVIDER
2F0
OSC.
PRIMARY
2F0
INTEGRATOR
AMPLIFIER
PREAMP
2 Fo
FILTER
AMP
DEMODULATOR
OUTPUT
FEEDBACK
+ 2.5 V

Fluxgate Sensor (Stefan Meyer Fluxmaster)

Applications

- Measurement of the Earth's field vector components
- Monitoring stray magnetic fields near power cables, transformers, etc.
- Palaeomagnetic investigations: Measurement of weak fields in rocks
- Calibration of Helmholtz coils
- Package inspection
- Residual field measurements (shielding effectiveness)
- Magnetic field control and compensation via analog output

Specifications

Range switch	±2 μT, ±20 μT, ±200 μT
Highest resolution	0.1 nT
Accuracy at 20 °C	0.5 % ± 5 nT ± 1 Digit
Temperature range	0 to 50 °C
Zero drift	<0.1 nT/K
Analog output	0.01 V/μT, 0.1 V/μT, 1 V/μT dep. on pos. of range switch, BNC-socket
Bandwidth	0 to 1 kHz (–3 dB)
Noise	<0.7 nT RMS (0.1 Hz < f < 200 Hz), typ. 20 pT/$\sqrt{\text{Hz}}$ at f = 1 Hz
Battery	9 V (PP3, Alkaline)
Continuous operation with one battery	~20 h
Automatic neutralization	±60 μT, selectable
Size of electronics unit	151 mm × 82 mm × 33 mm
Protection	IP65
Size of sensor	diam. 10 mm × 30 mm
Length of connecting cable	1.5 m
Weight of complete device	380 g

Low-Noise Fluxgate Sensor (Stefan Meyer FL1 100)

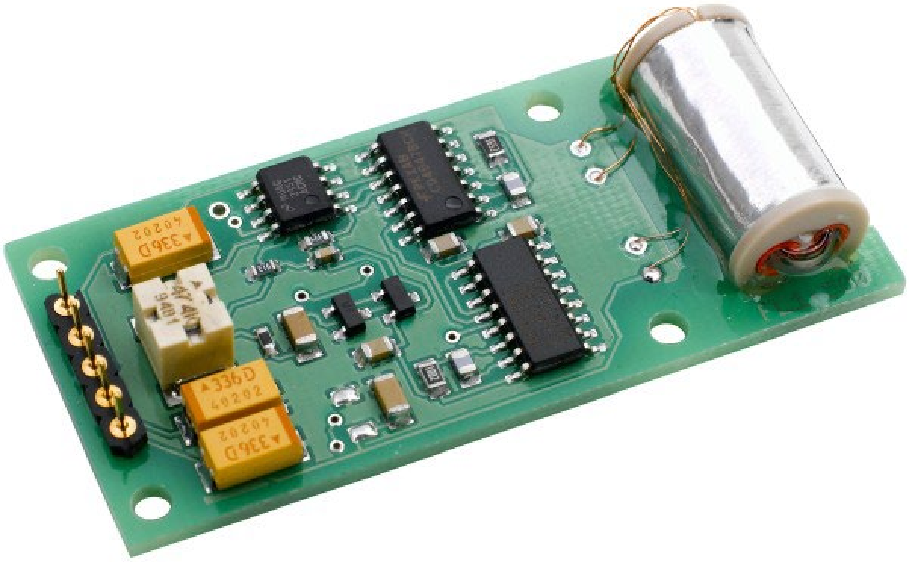

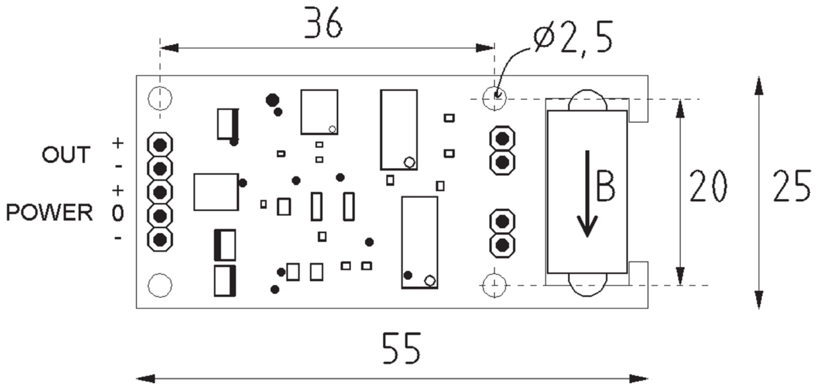

Specifications

Measurement range	$\pm 100\ \mu T$
Calibration accuracy	0.5%
Offset error	<200 nT
Operating temperature	0 to +70 °C
Zero drift	<0.1 nT/K
Supply voltages	±12 to 16 V
Current consumption @ ± 12 V	+30 mA, −15 mA
Analog output	$0.1\ V/\mu T$, max. ±10 V
Bandwidth	0 to 1 kHz (−3 dB)
Noise	$<20\ pT/Hz^{1/2}$ @ 1 Hz
Power supply rejection	>100 dB
DC output impedance	<1 Ω
Dimensions	55 mm × 25 mm × 11 mm
Weight	10 g
Connector	5 contacts

Fluxgate applications: Integrated compass

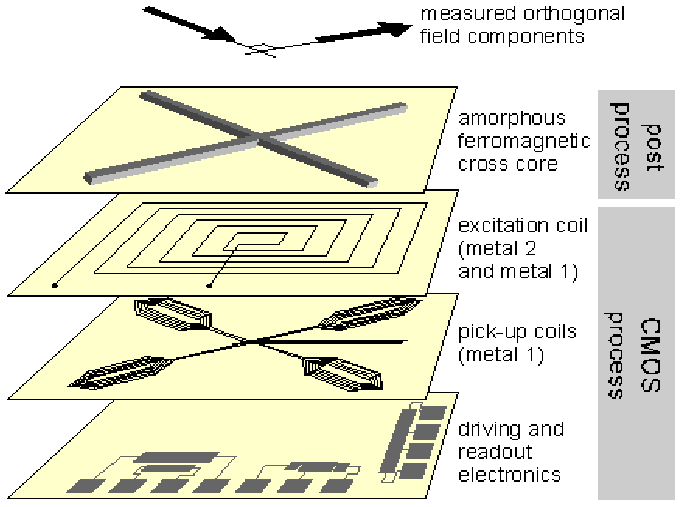

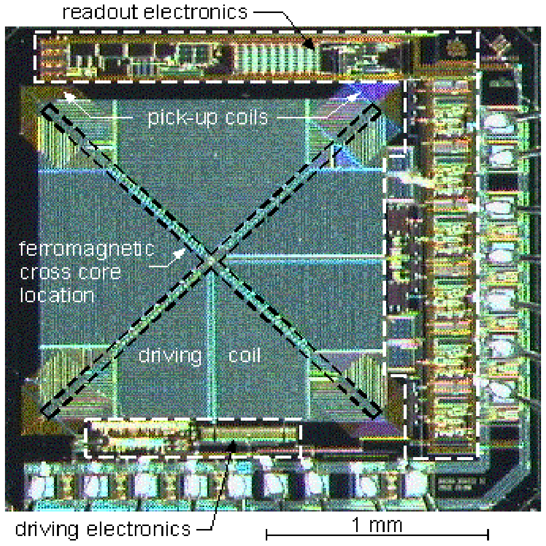

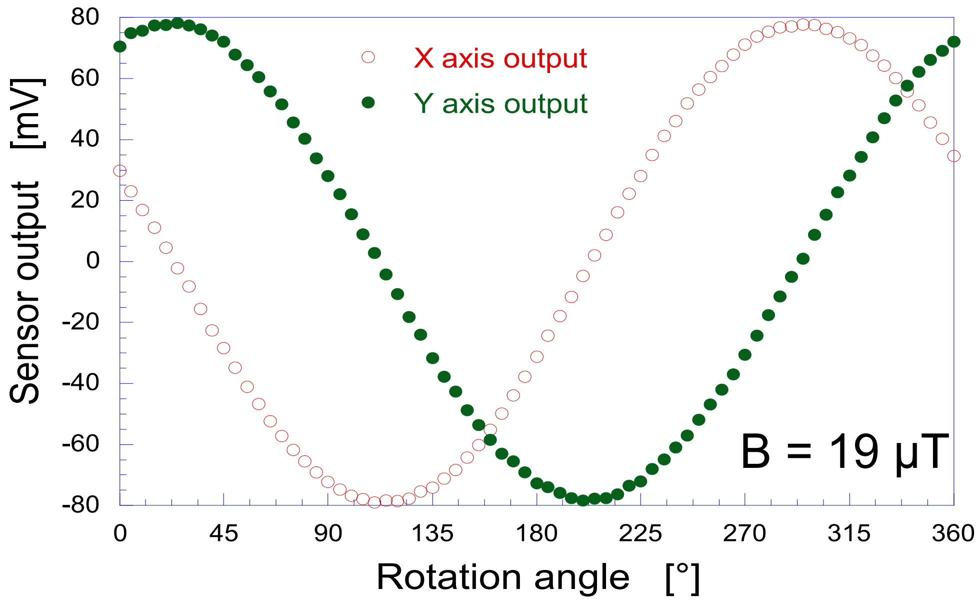

Angular accuracy: ± 1.5°
(at the Earth's magnetic field range)

Fluxgate applications: archeology and geomagnetism

Archéologie

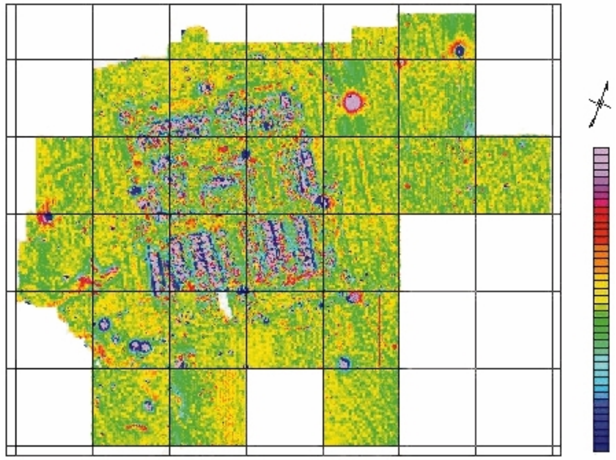

Two 1 m long gradiometer tubes, 1 m apart. Each contains two fluxgates, one at each end of the tube. Top detectors reject the large and time dependent earth field (about 40000 nT) and isolate the very slight readings caused by archaeological features (down to 0.1nT).

Géomagnétisme (Gakona, Alaska)

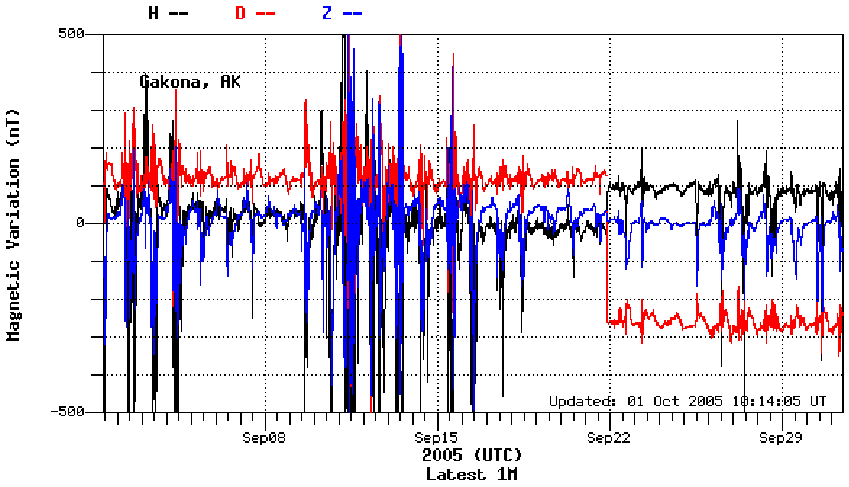

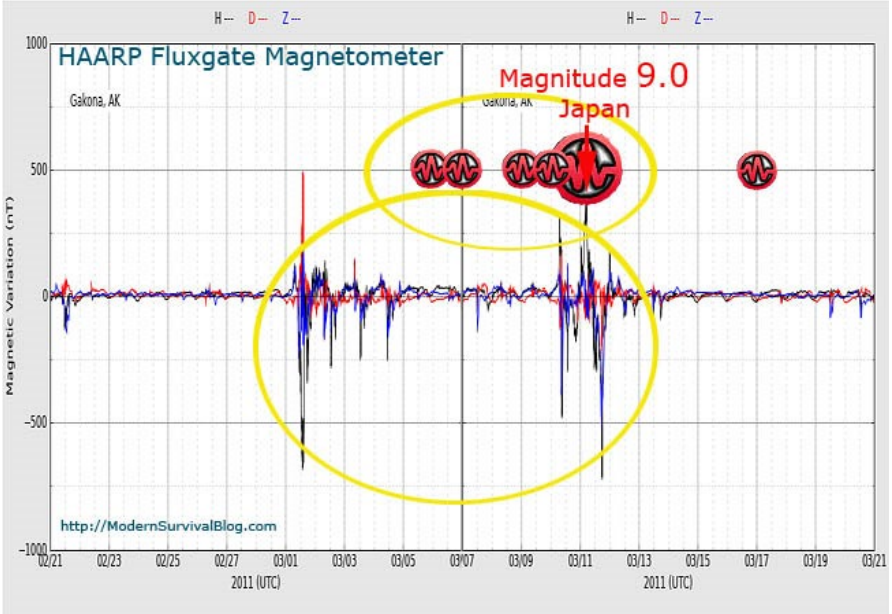

SQUID (Superconducting Quantum Interference Device)

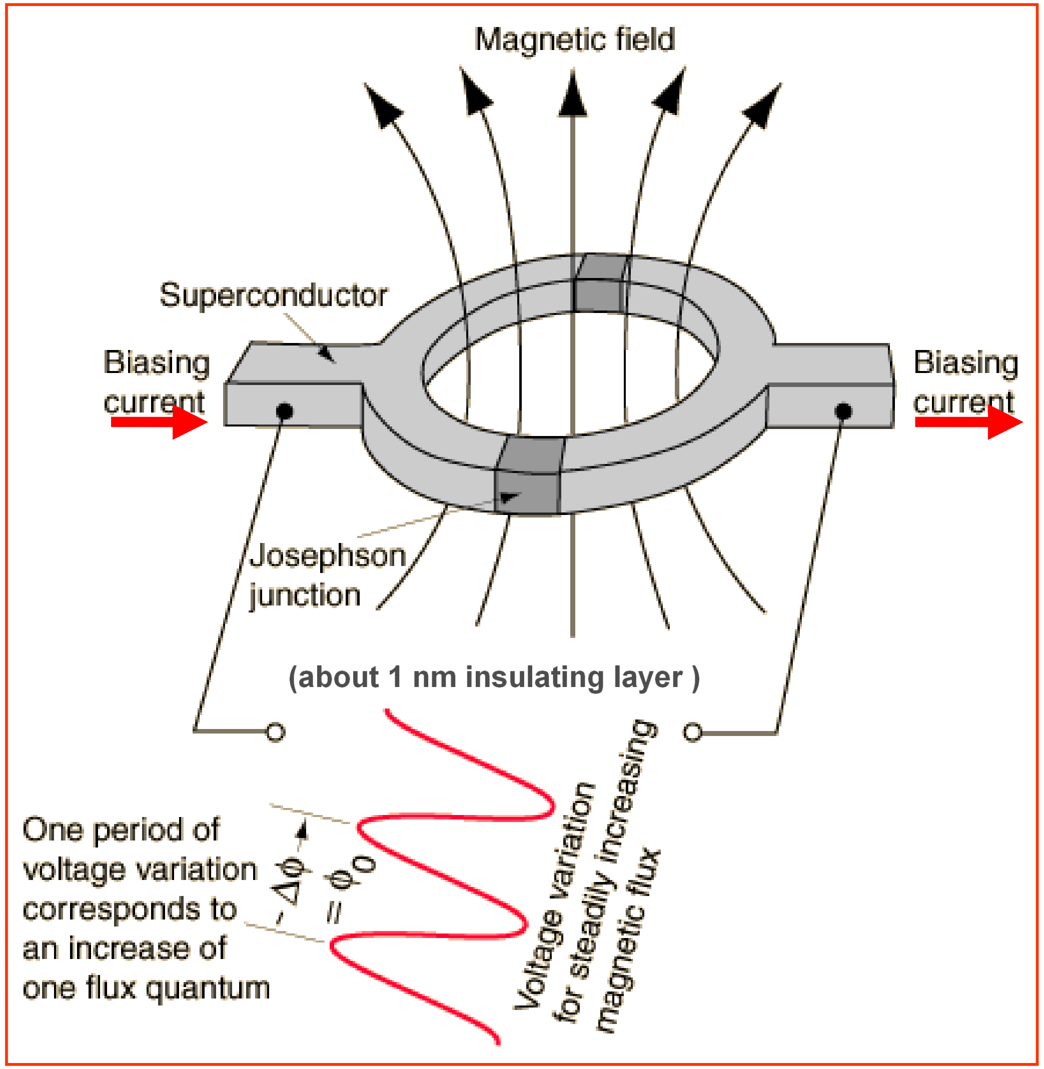

Condition de quantization:

$$\Phi_B = n\Phi_0 \quad n \in \mathbb{N}$$

$\Phi_0 = h/2e \cong 2\times 10^{-15}$ T m^2 :quantum de flux

Φ_B : flux total dans la boucle

$$\Phi_B = \Phi_{B_{ext}} + \Phi_{B_{int}}$$

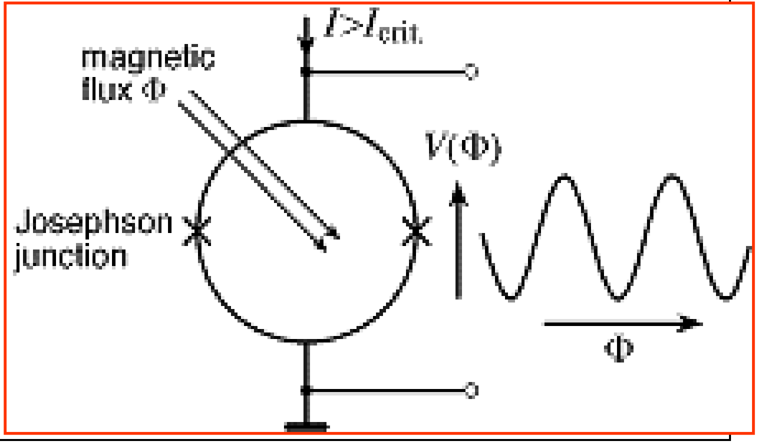

A SQUID is a ring of superconducting material with, usually, two junctions called Josephson junctions. Josephson predicted that a superconducting current can be sustained in the loop, even if its path is interrupted by thin insulating (or normal metal) barriers. In a superconducting loop the magnetic flux Φ_B passing through it, which is the product of the magnetic field and the area of the loop, is quantized in units of $\Phi_0 = h/2e \cong 2\times 10^{-15}$ T m^2 (i.e.. $\Phi_B = n\Phi_0$). A superconducting current will compensate for the presence of an externally applied magnetic field so that the total flux through the loop Φ_B (due to the external field plus the field generated by the current) is always a multiple of Φ_0. If a bias current less than the junction critical current is injected through the loop there will be no voltage across the loop. If the bias current is raised above this critical current, then a voltage develops across the loop. The critical current I_c is a function of the magnetic flux through the loop and may be expressed as

$$I_c = 2i_c \left| \cos(\pi \frac{\Phi_{B_{ext}}}{\Phi_0}) \right|$$

where i_c is the critical current in absence of an externally applied magnetic field. Note that this equation is identical in form to the equation describing quantum interference of light diffracted by two slits. By analogy, the behavior of this double Josephson junction loop displays interference in the current-voltage behavior as magnetic flux threads the loop, hence the name Superconducting QUantum Interference Device, SQUID. The critical current is so sensitive to the magnetic flux through the superconducting loop that very tiny variations of the magnetic field can be measured. The critical current is usually obtained by measuring the voltage drop across the junction as a function of the total current through the device.

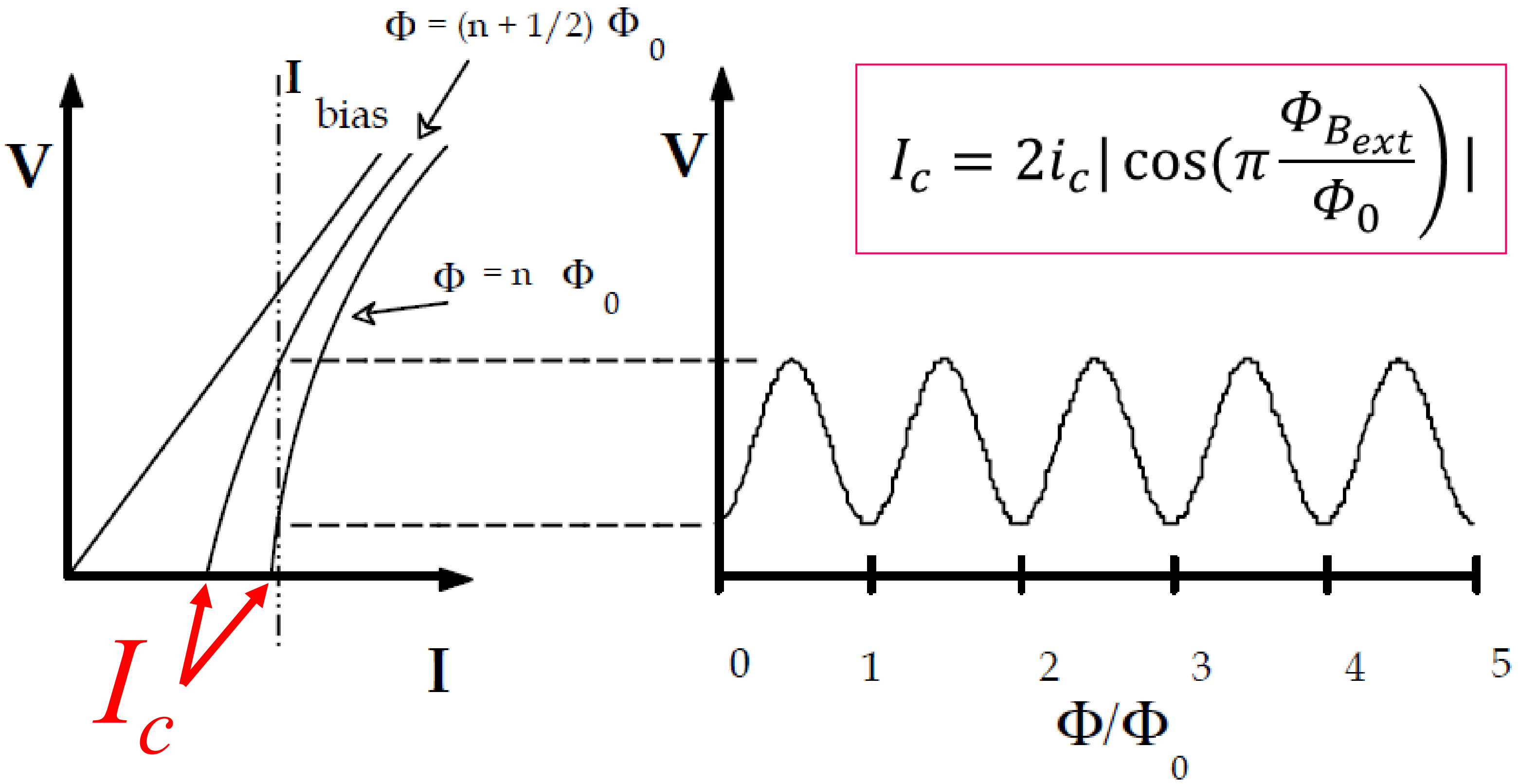

$$I_c = 2i_c|\cos(\pi\frac{\Phi_{B_{ext}}}{\Phi_0})|$$

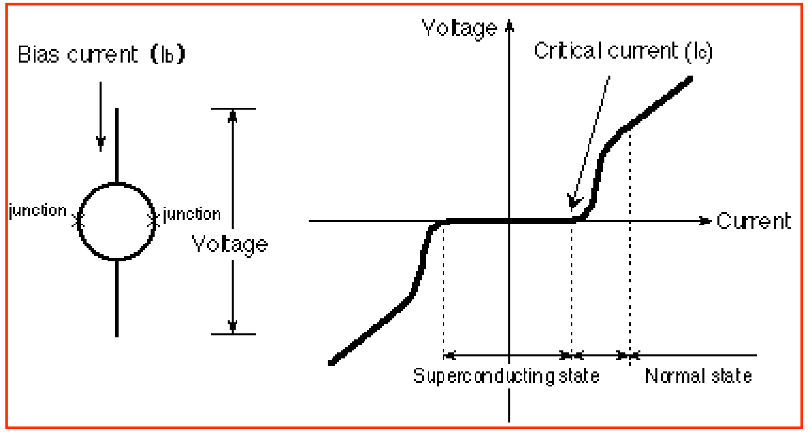

Bext = 0

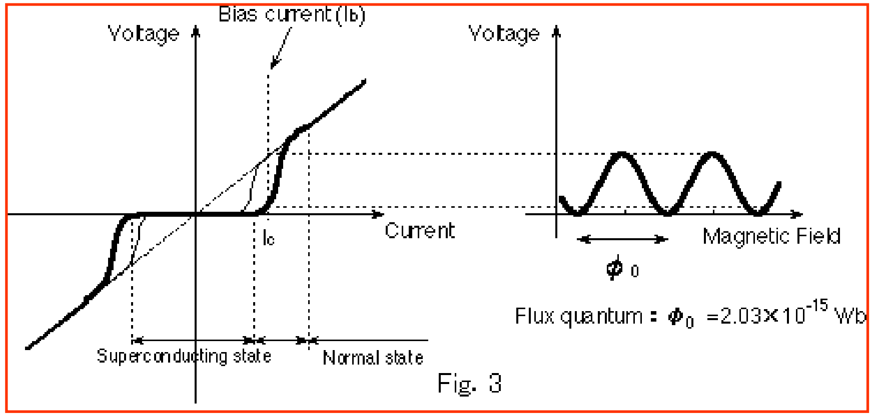

Bext > 0

- Needs superconducting materials (→ low temperatures)
- Measuring range: 10^{-6} à 10^{-14} T ! (Earth field $B=10^{-4}$ T)
- Resolution : 1 à 10 $fT/Hz^{1/2}$
- To measure B precisely the ring surface has to be estimated precisely (relatively low precision but very high resolution)

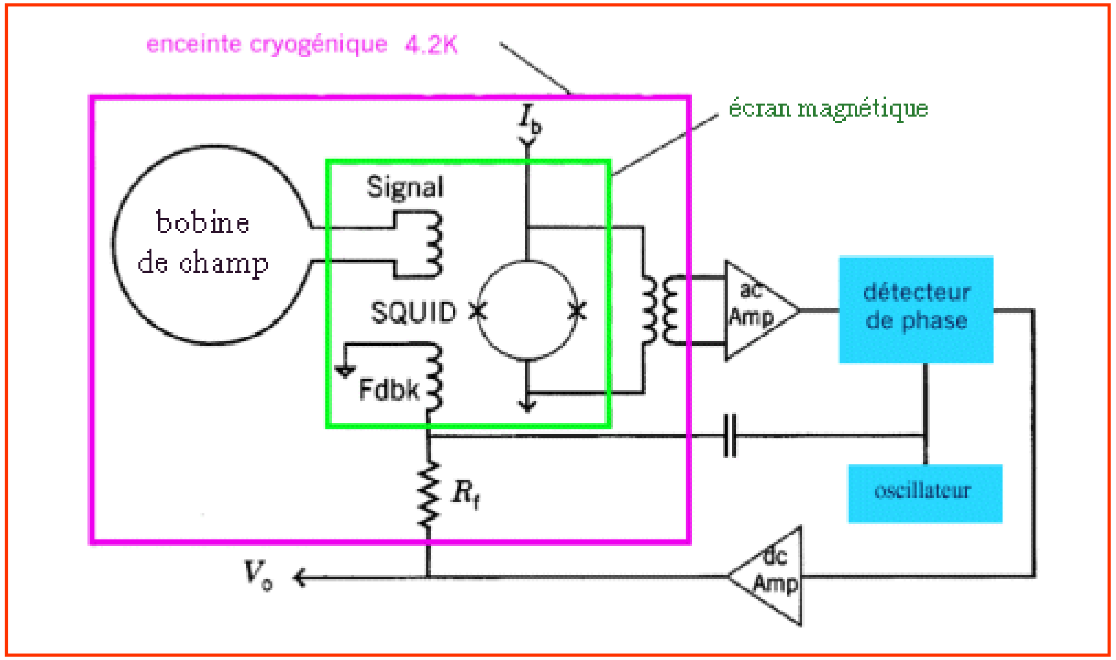

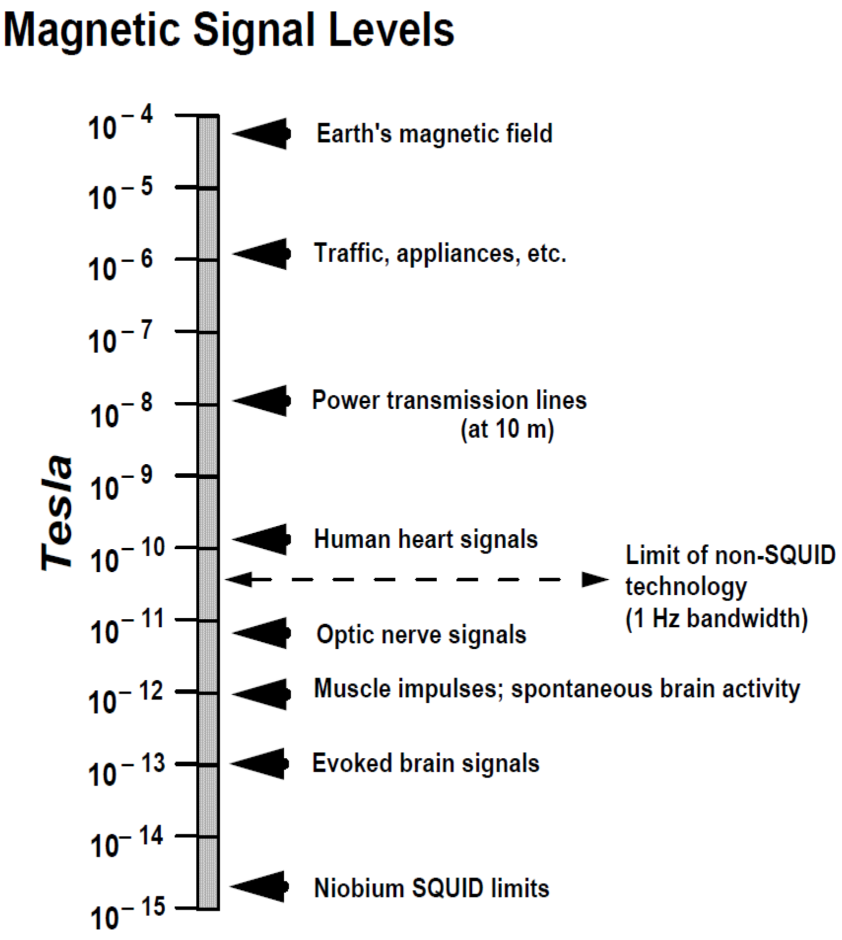

Sensor	Field Noise in fT/Hz$^{1/2}$ At 1 Hz	At 100 Hz
Flux Gate (room temperature)	30,000	30,000
77 K YBCO dc SQUID Magnetometer	<100	<40
4.2 K Nb dc SQUID Magnetometer	<5	<4

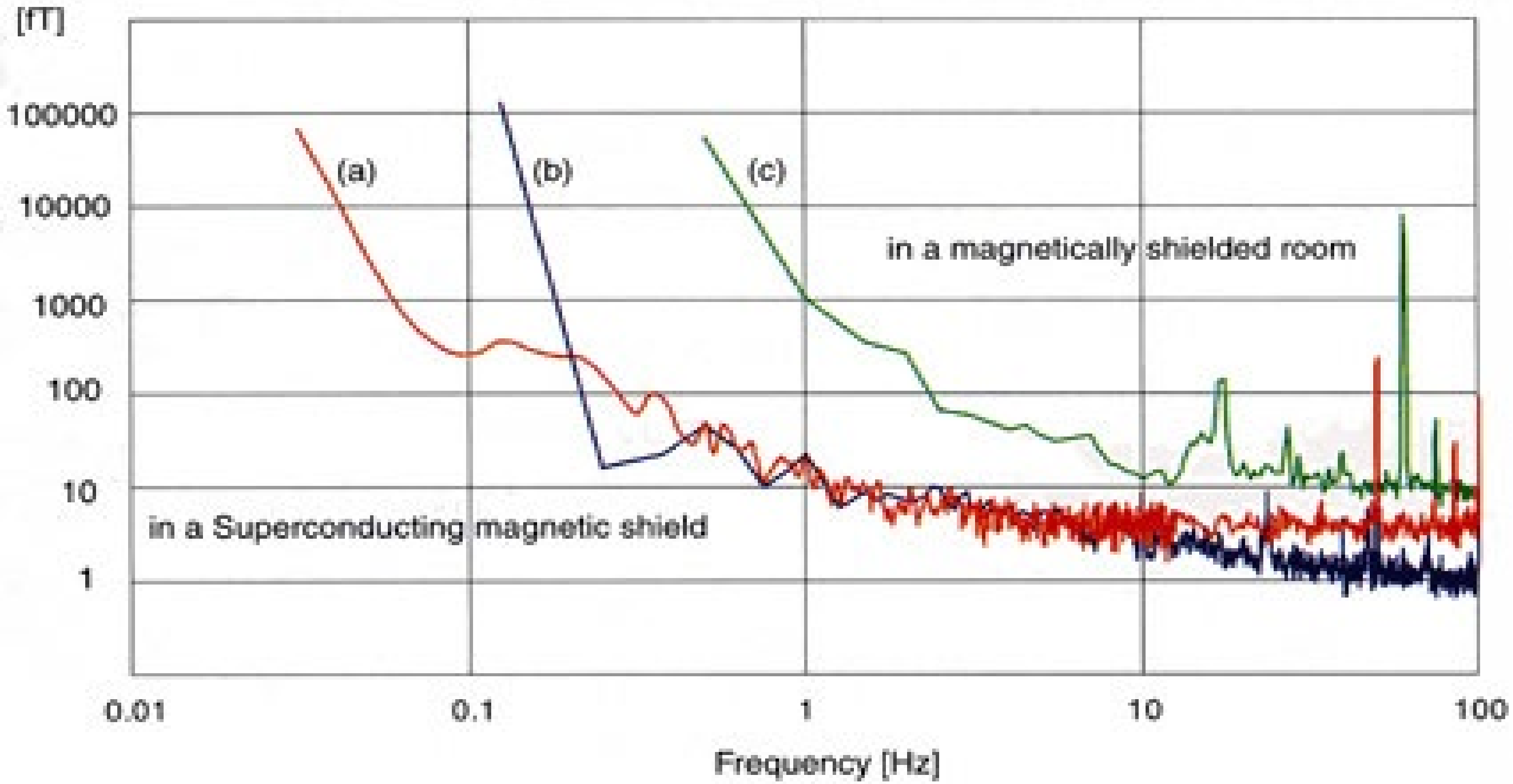

SQUIDs applications

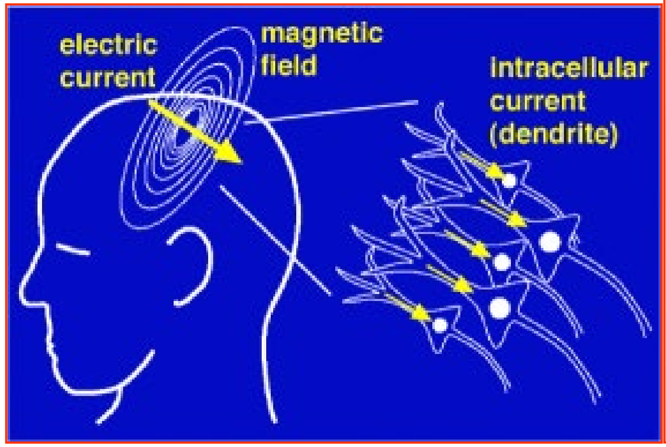

<u>SQUIDs applications:</u>
magnetoencephalogram (MEG)
magnetocardiogram (MCG)
biological testing using fine magnetic markers
geological surveying
food inspection
…..

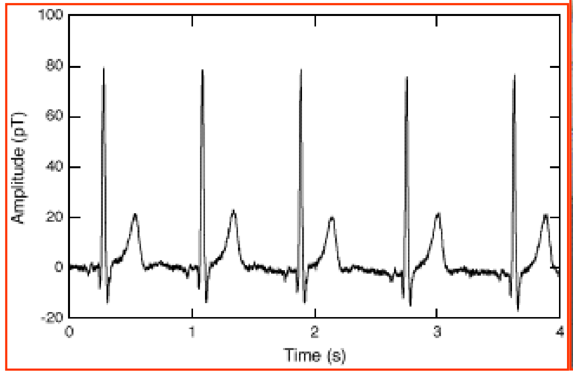

Giant Magneto-Impedance (GMI)

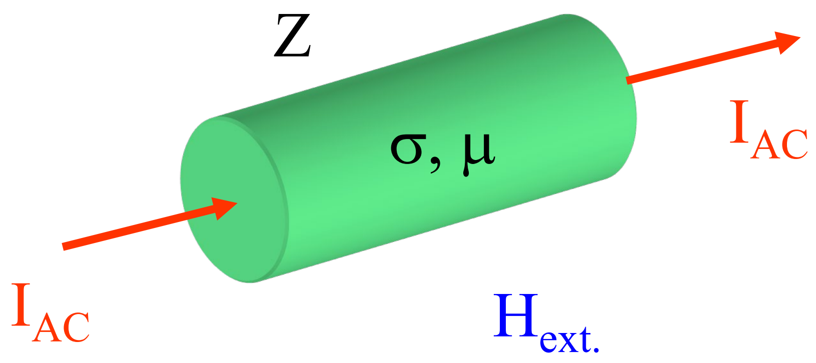

The external field $H_{ext.}$ influences the permeability μ.

The impedance Z depends on the transverse permeability μ_t due to:

- The skin effect: $$\delta \equiv \frac{\sqrt{2}}{\sqrt{\omega \mu_0 \mu_t \sigma}}$$
- The self-inductance. $$L \propto \mu_t$$

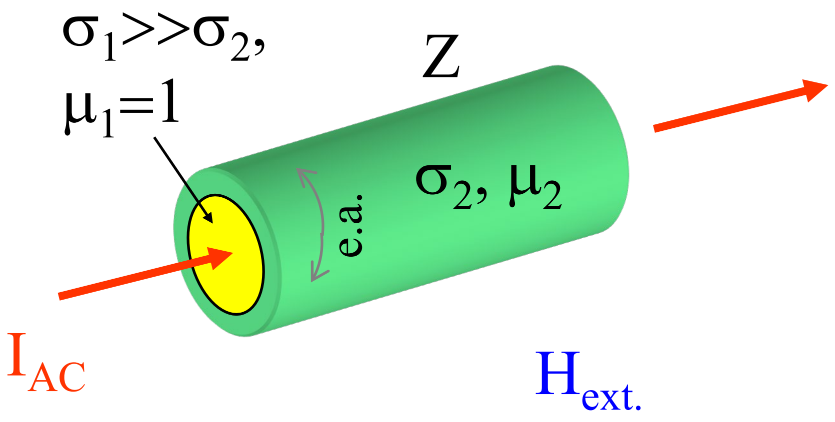

- Easy axis is transverse
- I_{AC} produces H_{var} in transverse direction

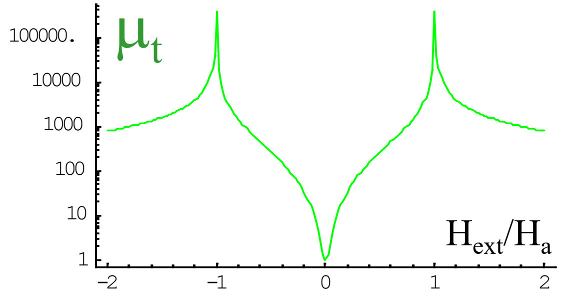

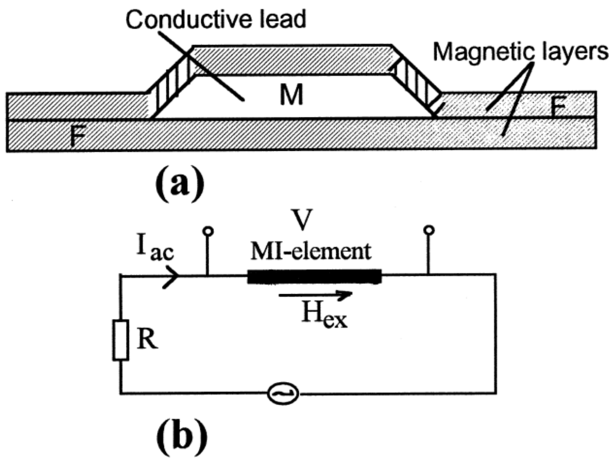

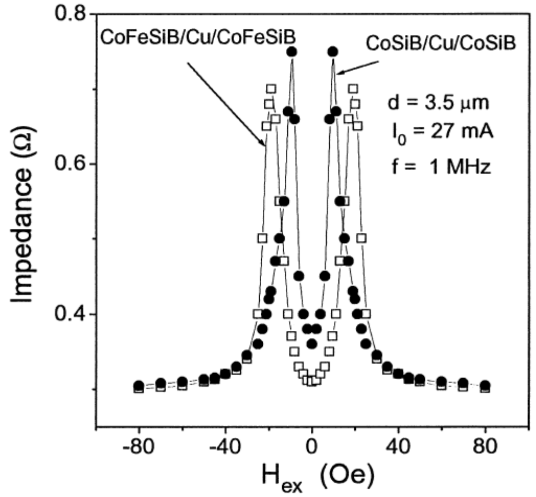

L.V. Panina et al, Sensors and Actuators 81 (2000) 71-77

Cantilever magnetometer

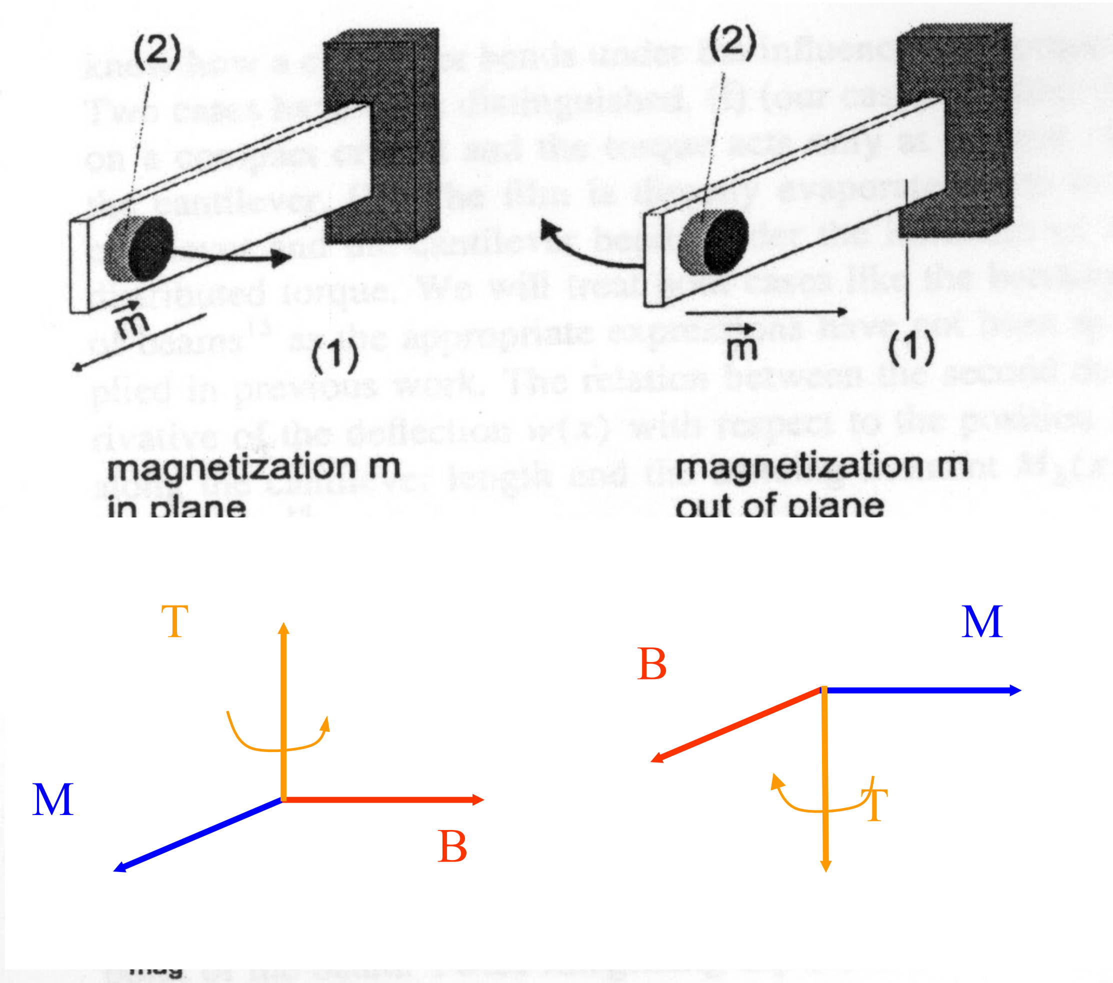

FIG. 1. Principle of the cantilever magnetometer. The cantilever (1) is fixed at one end. At the free end a single crystal (2) is mounted, which is used as a substrate for the ferromagnetic film. The deflection field $\mathbf{B}_{defl}$ and the magnetizing field $\mathbf{B}_{mag}$ are oriented differently for in-plane and out-of-plane magnetized films. The resulting torque **T** leads to a bending of the cantilever that is measured by a laser beam technique.

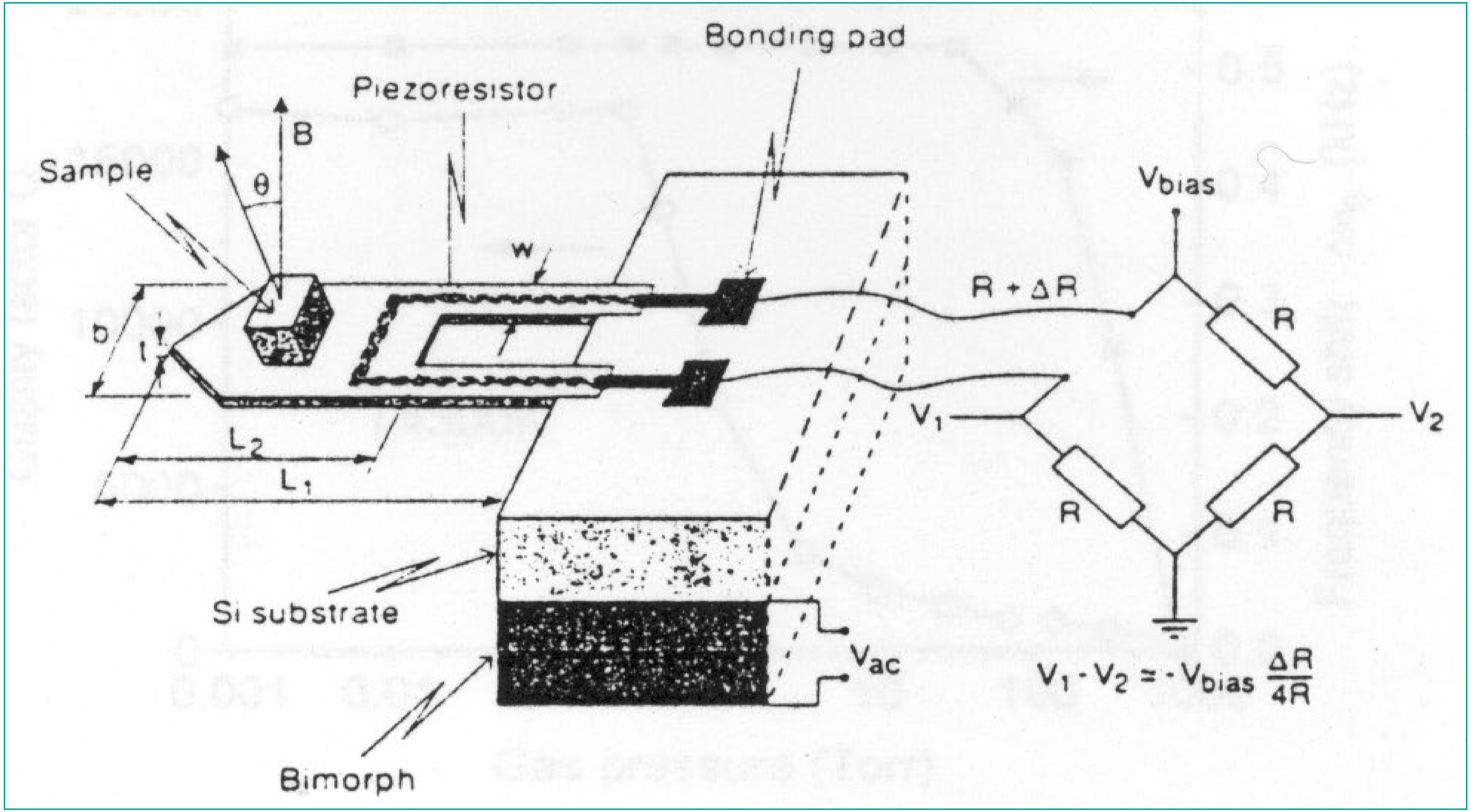

Bonding pad
Piezoresistor
B
Sample
θ
w
b
t
L2
L1
R + ΔR
Vbias
R
V1
V2
R
R
Si substrate
Vac
Bimorph
$V_1 - V_2 \approx -V_{bias}\frac{\Delta R}{4R}$

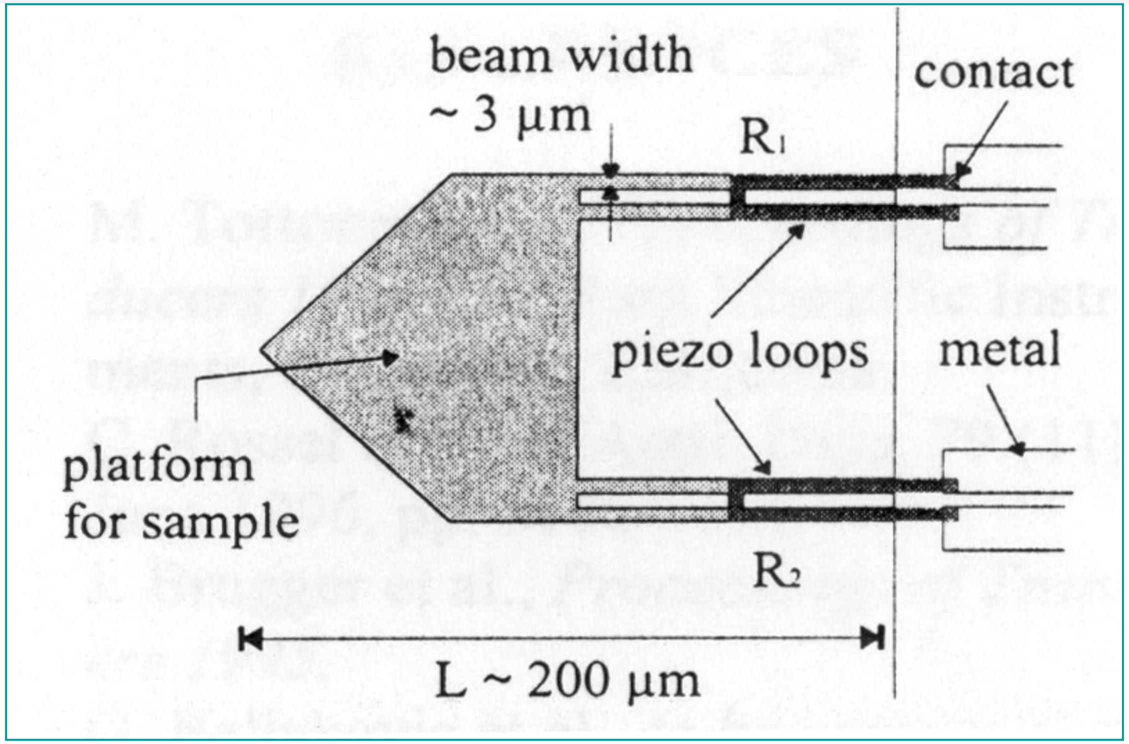
beam width
~ 3 µm
R1
contact
piezo loops
metal
platform
for sample
R2
L ~ 200 µm

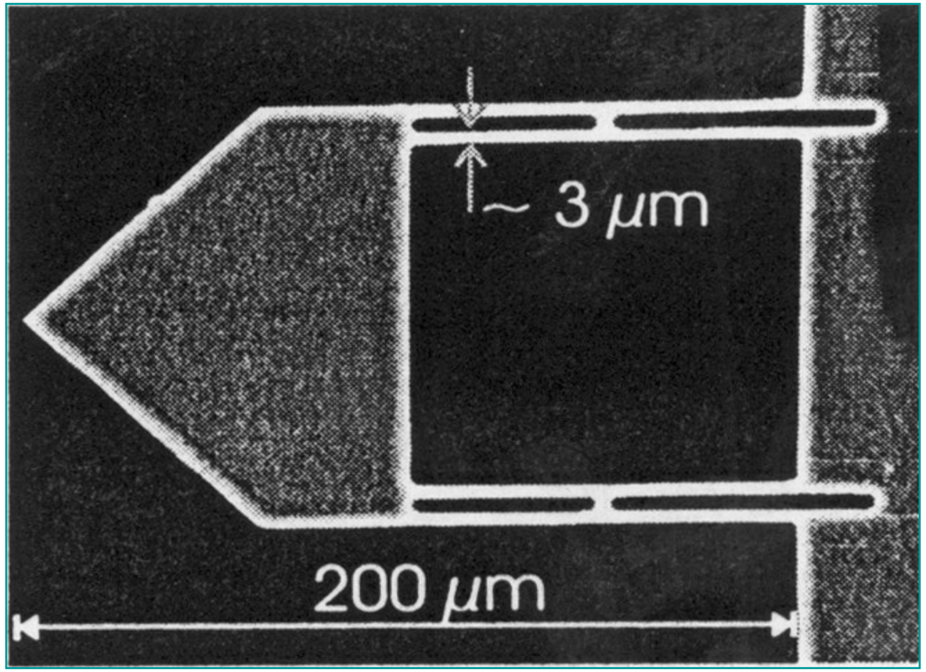
~ 3 µm
200 µm

Torque magnetometers

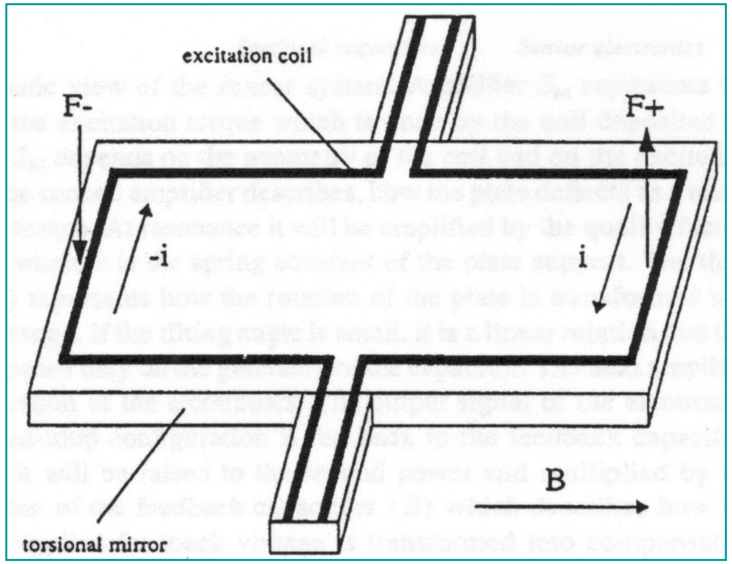

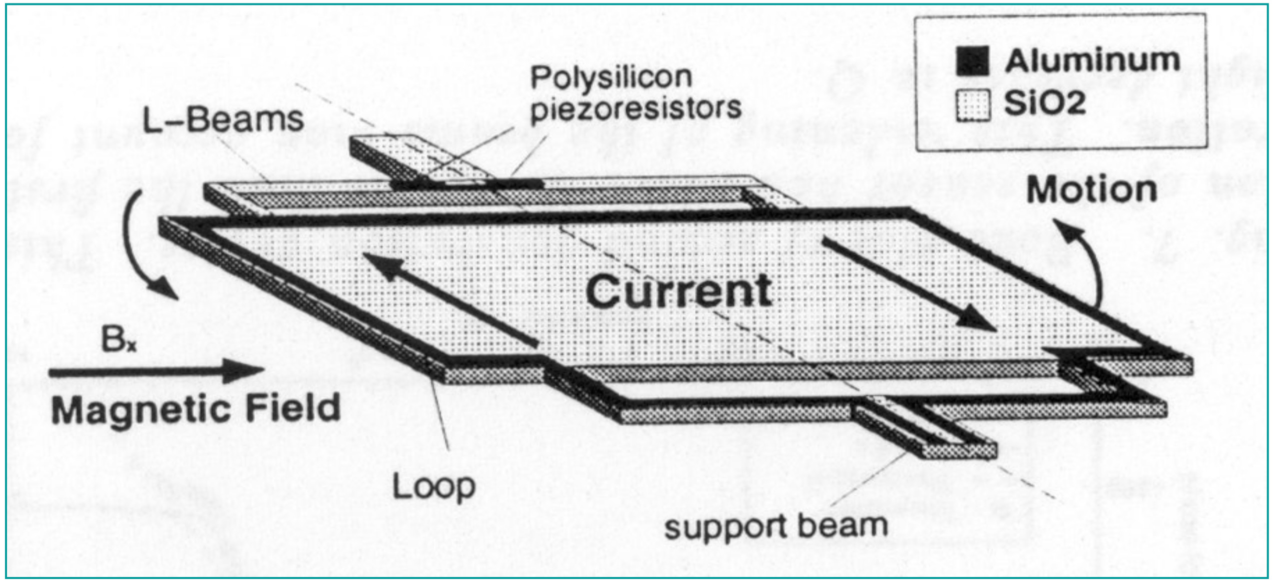

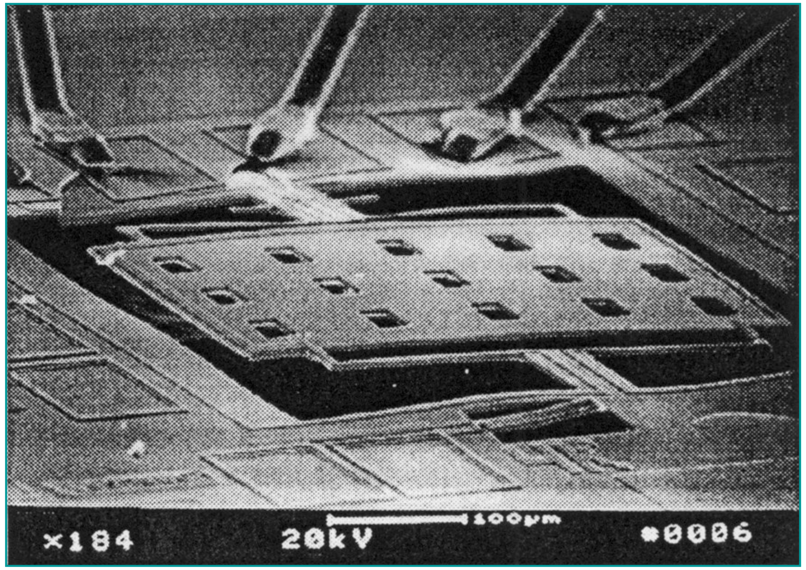

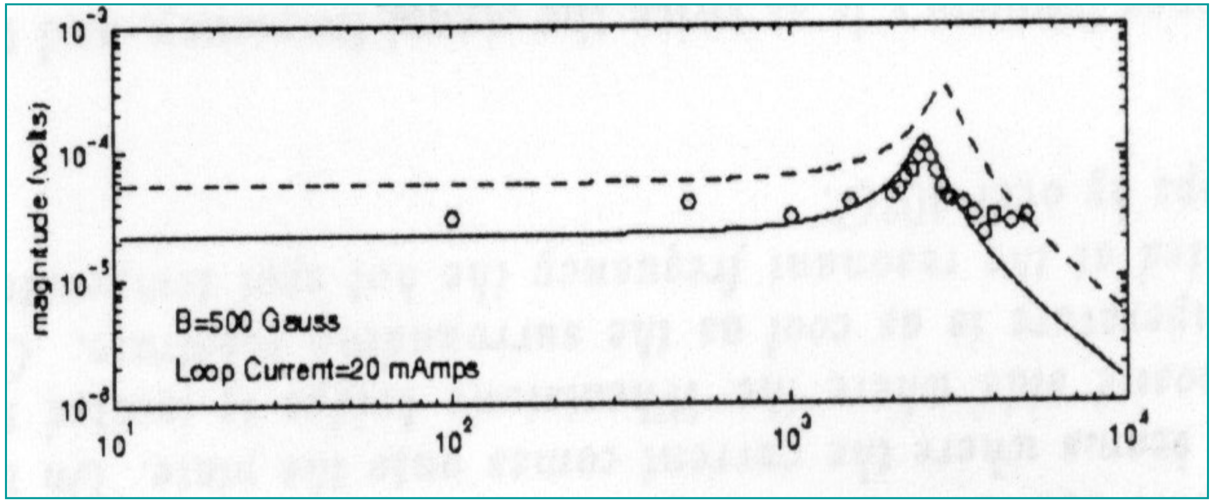

E-beam magnetometers

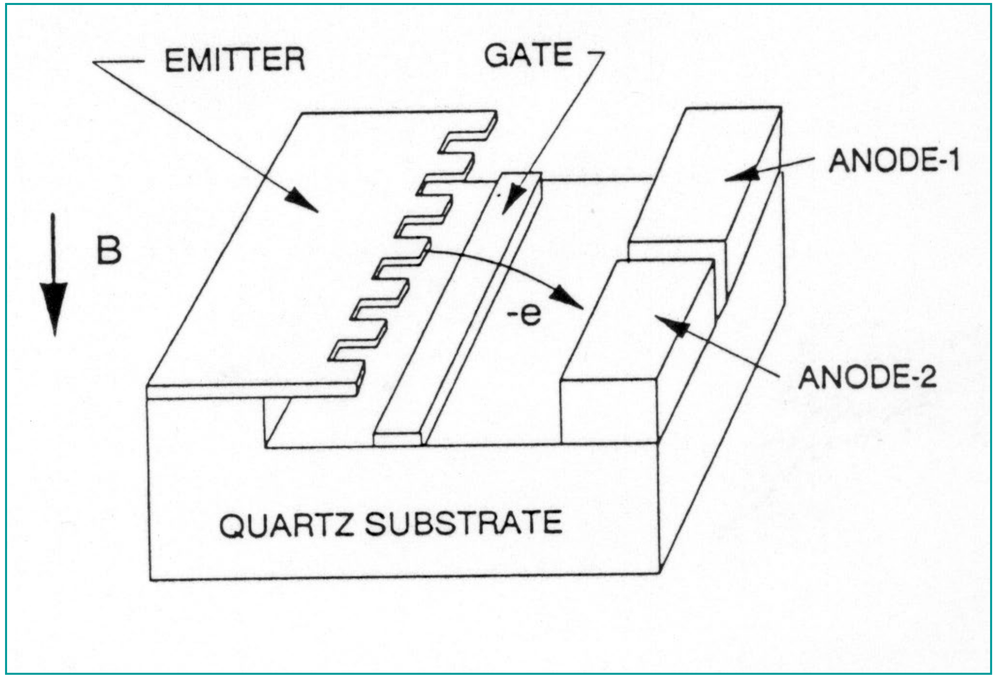

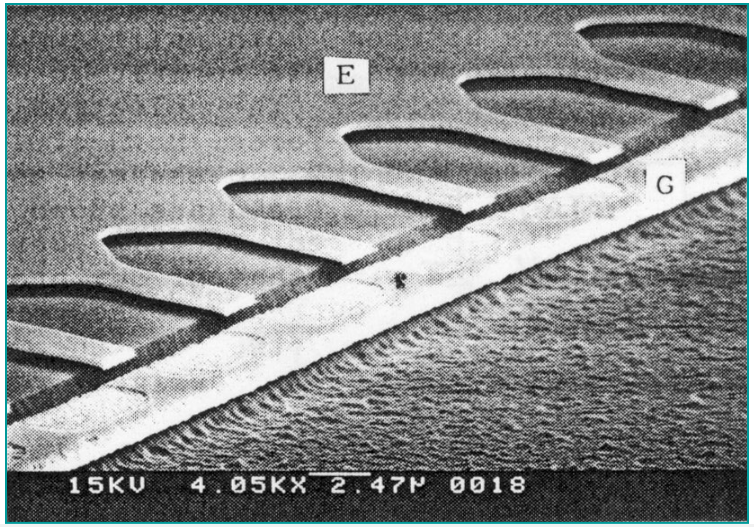

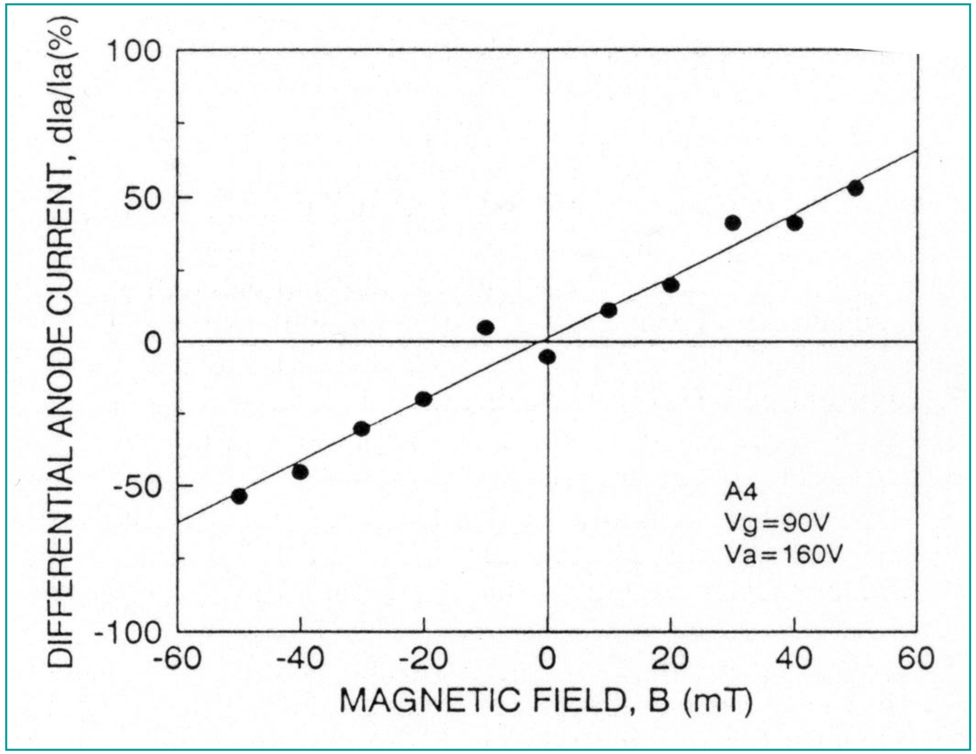

Inductive sensors

Inductance:

Equations générales pour la détermination de l'inductance d'une conducteur (équivalents):

$$L \equiv \frac{1}{\mu_0} \int_V \frac{1}{\mu_r(\mathbf{x})} \left|\mathbf{B}_u(\mathbf{x})\right|^2 d\mathbf{x}^3$$

$$L \equiv \frac{\mu_0}{4\pi} \int_{V_c} d\mathbf{x}'^3 \int_{V_c} \mu_r(\mathbf{x}) \frac{\mathbf{J}_\mathrm{u}(\mathbf{x}') \cdot \mathbf{J}_\mathrm{u}(\mathbf{x})}{\left|\mathbf{x}' - \mathbf{x}\right|} d\mathbf{x}^3$$

$\mathbf{B}_u(\mathbf{x})$: induction magn. produit par un courant unitaire (i=1 A) dans le conducteur.

$\mathbf{J}_u(\mathbf{x})$: densité de courant produit par un courant unitaire (i=1 A) dans le conducteur.

V : volume dans lequel $\mathbf{B}_u(\mathbf{x})$ est significativement différent de zéro.

V_c : volume du conducteur.

Examples of Inductors:

- Solenoidal coil (lenght l, turns N, radius R) : $L \cong \mu_0 \frac{N^2}{l^2} l \pi R^2$ (pour $l >> R$)

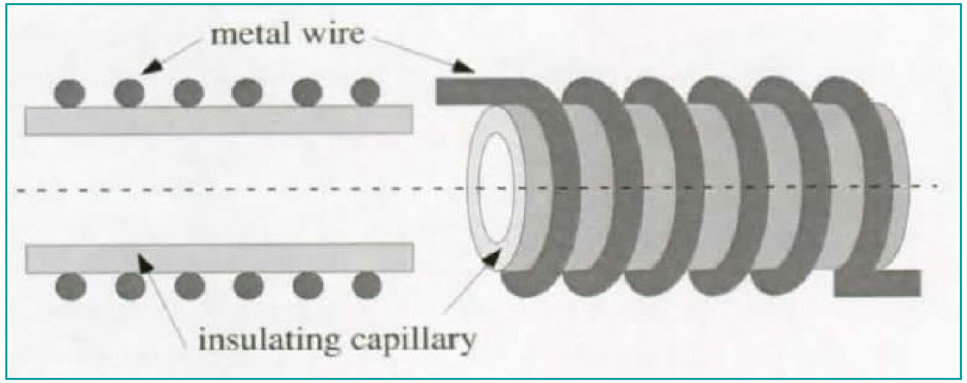

- Planar coil (int. radius R_i, ext. radius R_e, turns N) : $L \cong 1.12 \mu_0 N^2 \frac{(R_e + R_i)^2}{2.14 R_e - R_i}$

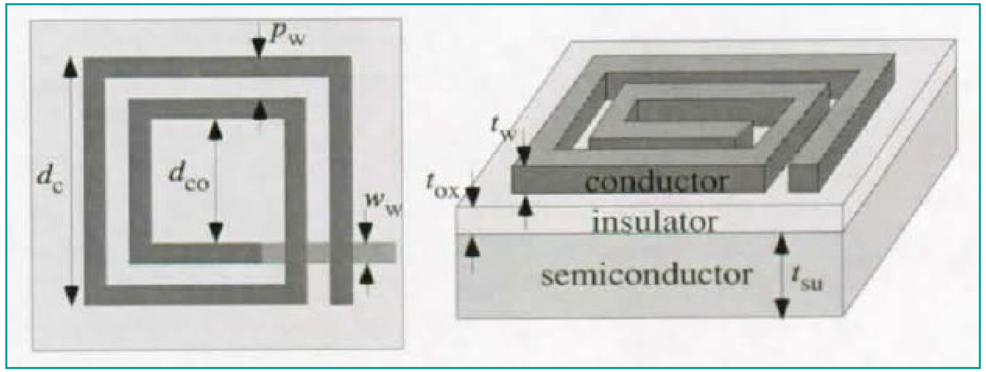

- Wire with circular section (lenght l, radius R) : $L \cong 0.16 \mu_0 \cdot l \cdot \log((2l/R) - 1)$

Inductance et flux du vecteur d'induction magnétique :

$$\Phi(t) = Li(t) \qquad U(t) = -\frac{d\Phi(t)}{dt} = -L\frac{di}{dt} \quad \text{(loi de Lenz)}$$

$\Phi(t)$: flux du vecteur d'induction magnétique **B** [Tm^2]

L : inductance [H] i : courant [A] U: tension [V]

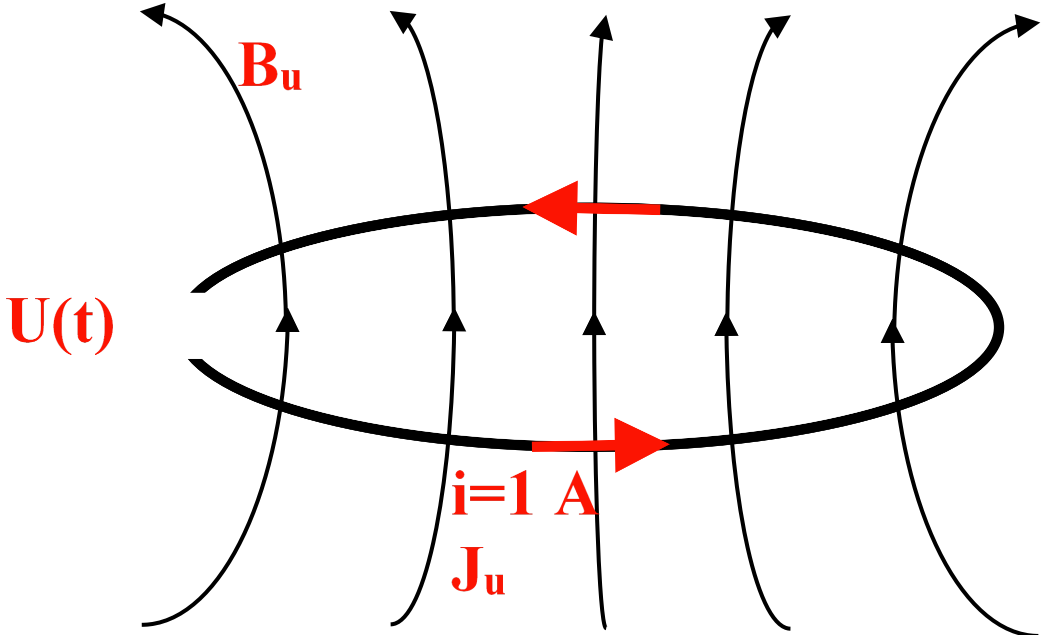

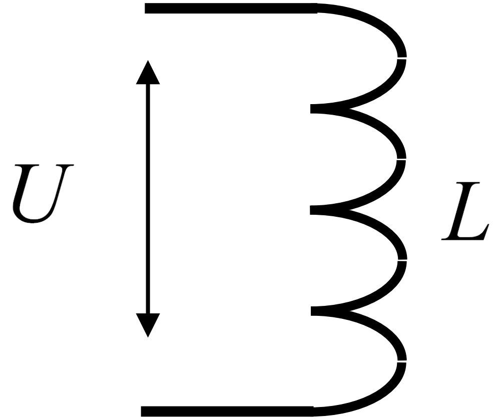

Inductances mutuelles L_{12} et L_{21} :

$$U_1(t) = L_1 \frac{di_1}{dt} + L_{12}\frac{di_2}{dt} \qquad U_2(t) = L_2 \frac{di_2}{dt} + L_{21}\frac{di_1}{dt}$$

- Facteur de couplage k: $$k = \sqrt{\frac{L_{12}^{\;2}}{L_1 \cdot L_2}}$$

k=0 couplage nul

k=1 couplage parfait

- Equation générale: $$L_{12} \equiv \frac{\mu_0}{4\pi}\int_{V_{c2}} d\mathbf{x}'^3 \int_{V_{c1}} \frac{\mathbf{J}_u(\mathbf{x}')\cdot\mathbf{J}_u(\mathbf{x})}{|\mathbf{x}'-\mathbf{x}|} d\mathbf{x}^3$$

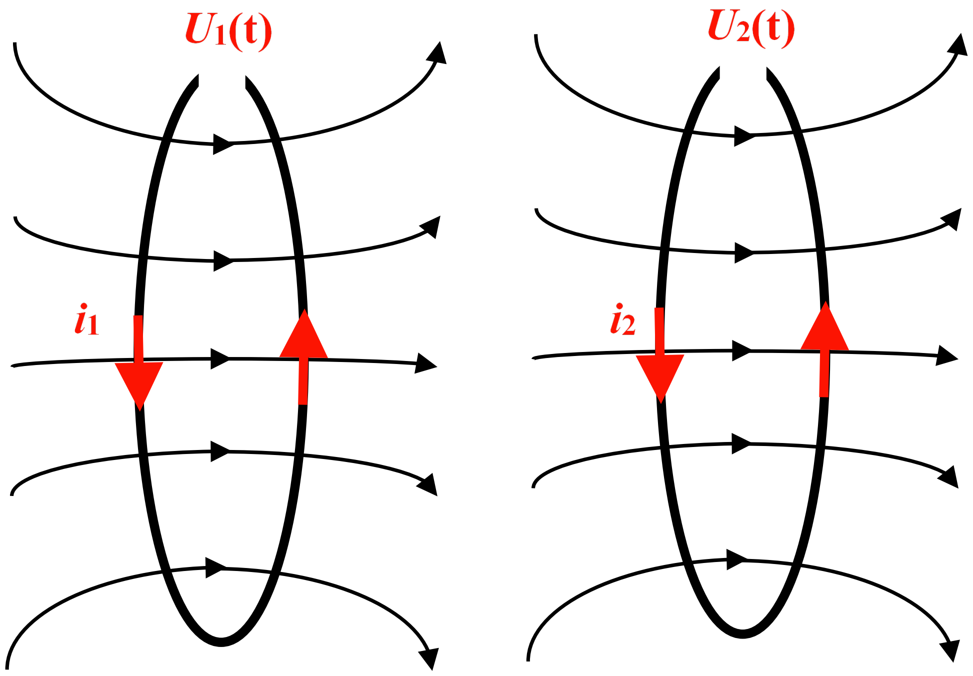

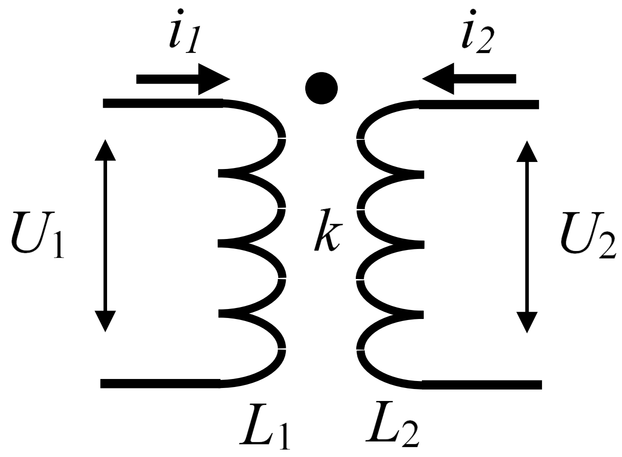

Proximity sensor (based on Foucault currents)

$\Delta x \rightarrow \Delta L$ et ΔR

Principle : Impedance variation (resistance and inductance) of a coil placed in proximity of a conducting surface. Foucault currents induced in the conducting material.

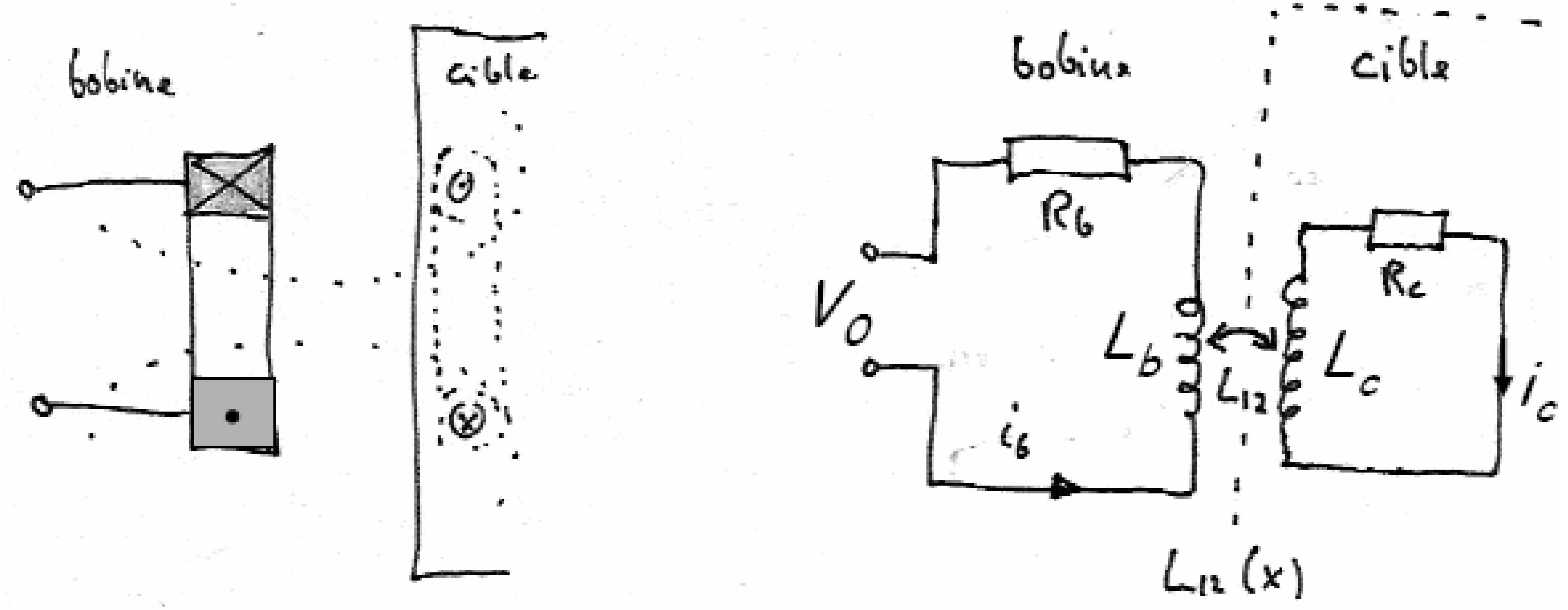

Mutual Inductance : $L_{12}(x) = k(x)\sqrt{L_b \cdot L_c}$

Model (2 equations)

Coil: $V_0 = R_b i_b + j\omega L_b \cdot i_b + j\omega L_{12} \cdot i_c$

Target: $0 = R_c i_c + j\omega L_c \cdot i_c + j\omega L_{12} \cdot i_b$

→

$$V_0 = \left[R_b + \underbrace{\frac{\omega^2 L_{12}^{\ 2}}{R_c^{\ 2} + \omega^2 L_c^{\ 2}} R_c}_{\Delta R(x)} + j\omega \left(L_b - \underbrace{\frac{\omega^2 L_{12}^{\ 2}}{R_c^{\ 2} + \omega^2 L_c^{\ 2}} L_c}_{\Delta L(x)} \right) \right] \cdot i_b$$

If the target is a good conductor : $R_c^{\ 2} << \omega^2 L_c^{\ 2}$

$$\Delta R \cong k^2 \frac{L_b}{L_c} R_c > 0$$

Increase of resistance (losses in the target)

$$\Delta L \cong -\frac{L_{12}^{\ 2}}{L_c} = -k^2 L_b < 0$$

Reduction of inductance (counter field produced by current in the target)

$k = k(x)$, k increses for $x \to 0$

=

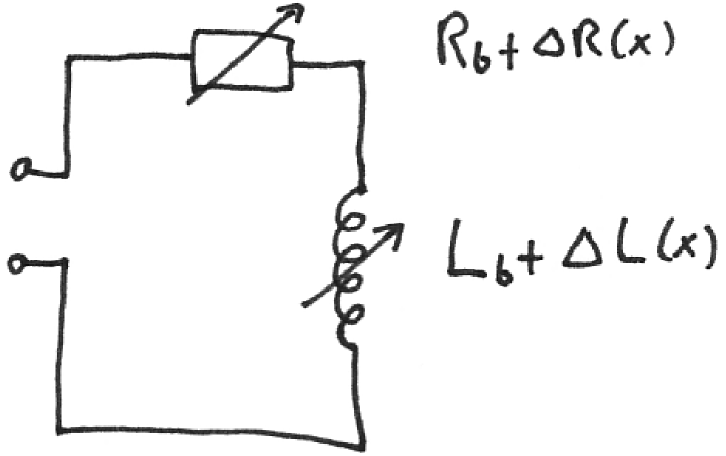

A desplacement towards the target induce:

1. a reduction of the equivalent self inductance : $L_{equiv} = L_b + \Delta L(x) \cong L_b(1-k^2)$
(the magnetic flux produced by i_c is opposite to the magnetic flux produced by i_b)

2. an increase of the equivalent resistance: $R_{equiv} = R_b + \Delta R(x) = R_b + k^2 \frac{L_b}{L_c} R_c$

(the presence of the target increase the losses of the system)

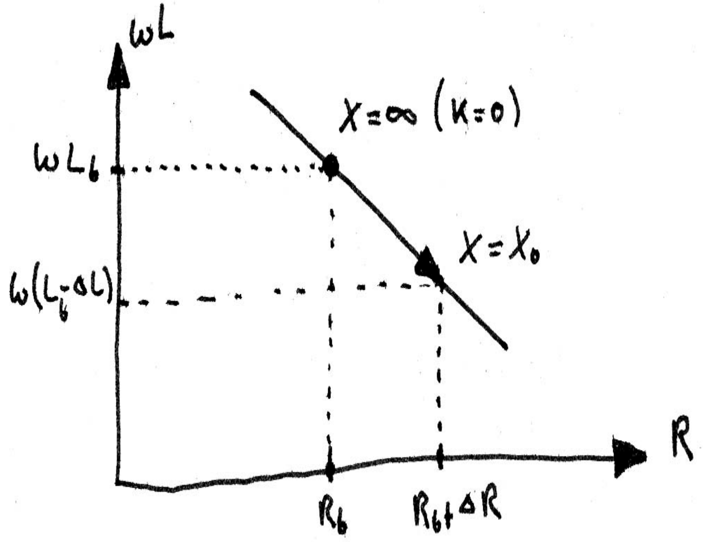

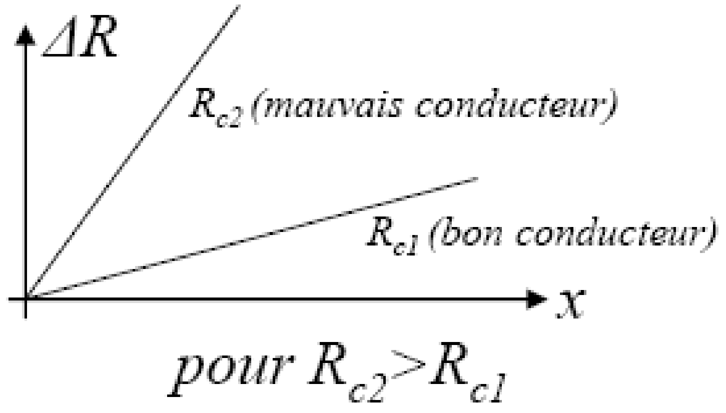

(x = desplacement towards the target)

Bridge and synchronous demodulation:

Signal in phase : $$\left|V_m\right|^0 = \frac{1}{2}\left|V_0\right|\left[\frac{\Delta R}{R_b}\right] = \frac{1}{2}\left|V_0\right| \cdot k^2 \frac{L_b}{L_c}\frac{R_c}{R_b}$$

Signal at 90° : $$\left|V_m\right|^{90} = \frac{1}{2}\left|V_0\right|\left[\frac{\Delta L}{L_b}\right] = -\frac{1}{2}\left|V_0\right| \cdot k^2$$

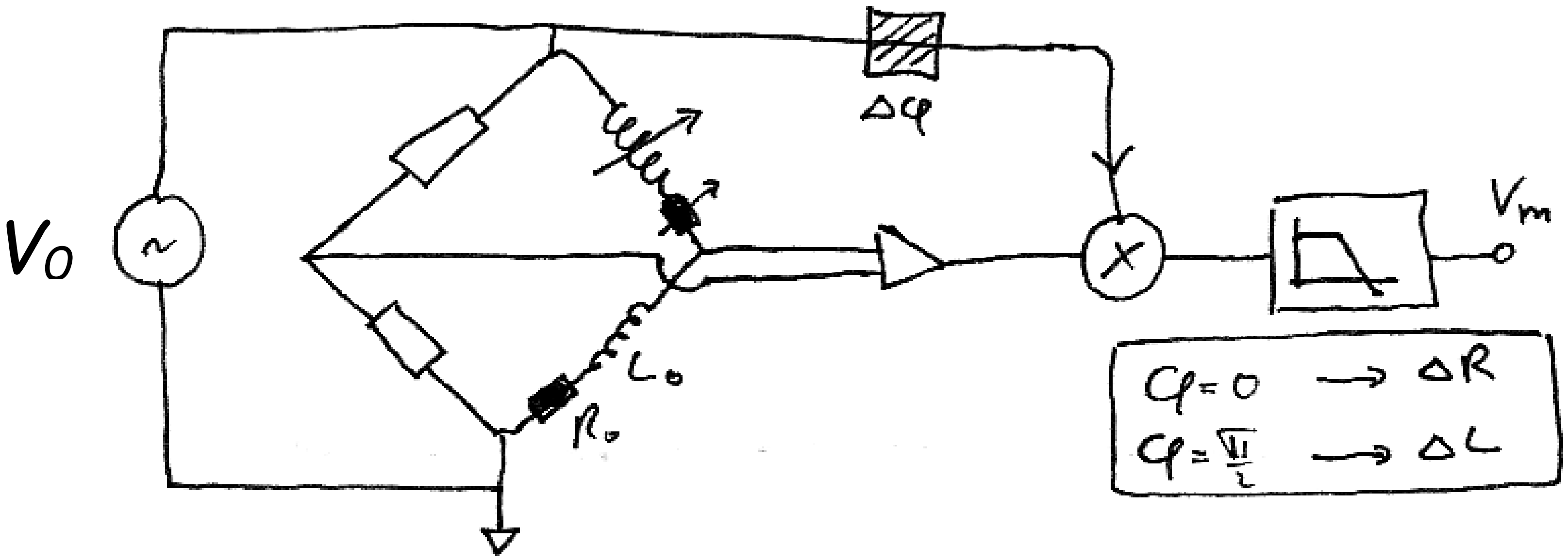

Cracks detection (based on Foucault currents)

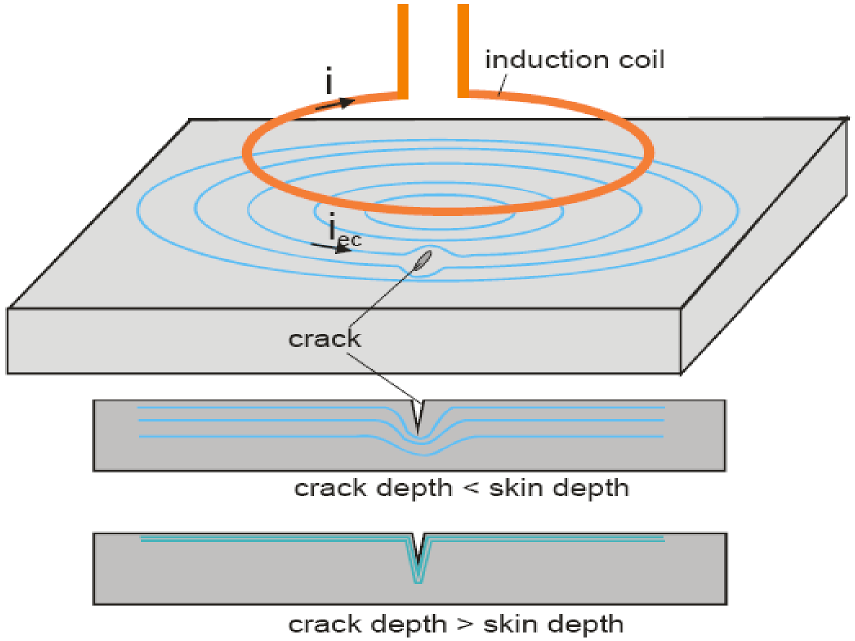

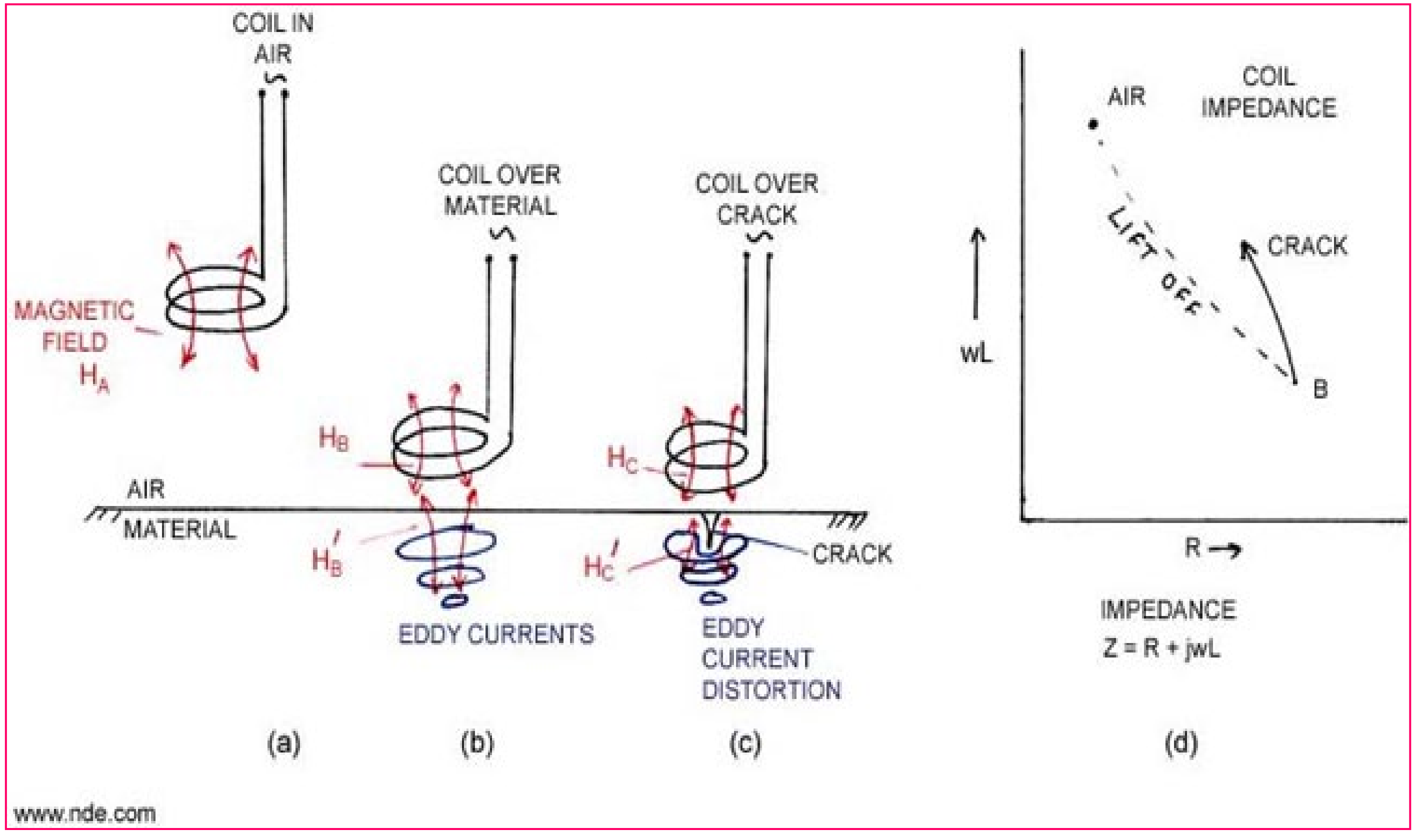

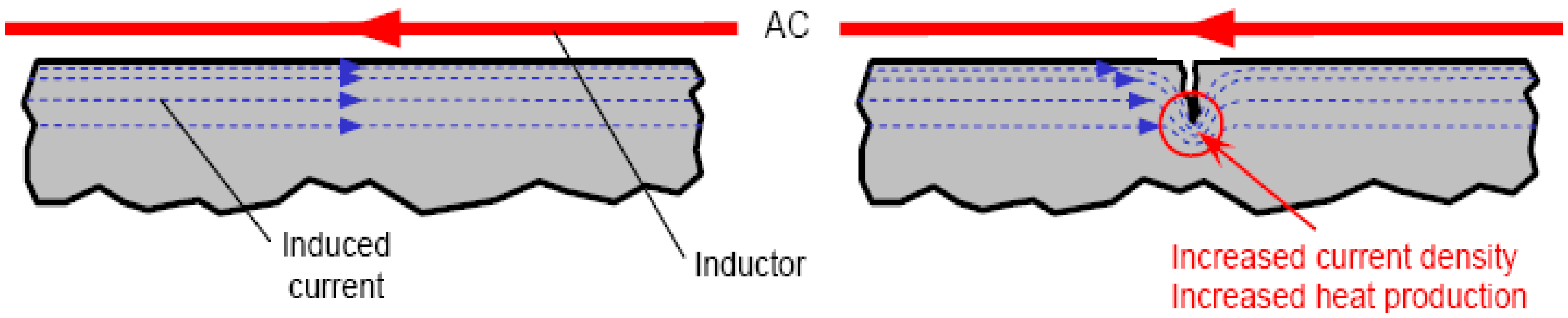

Excitation: AC magnetic field (to induce the eddy currents)

Detection: Thermal

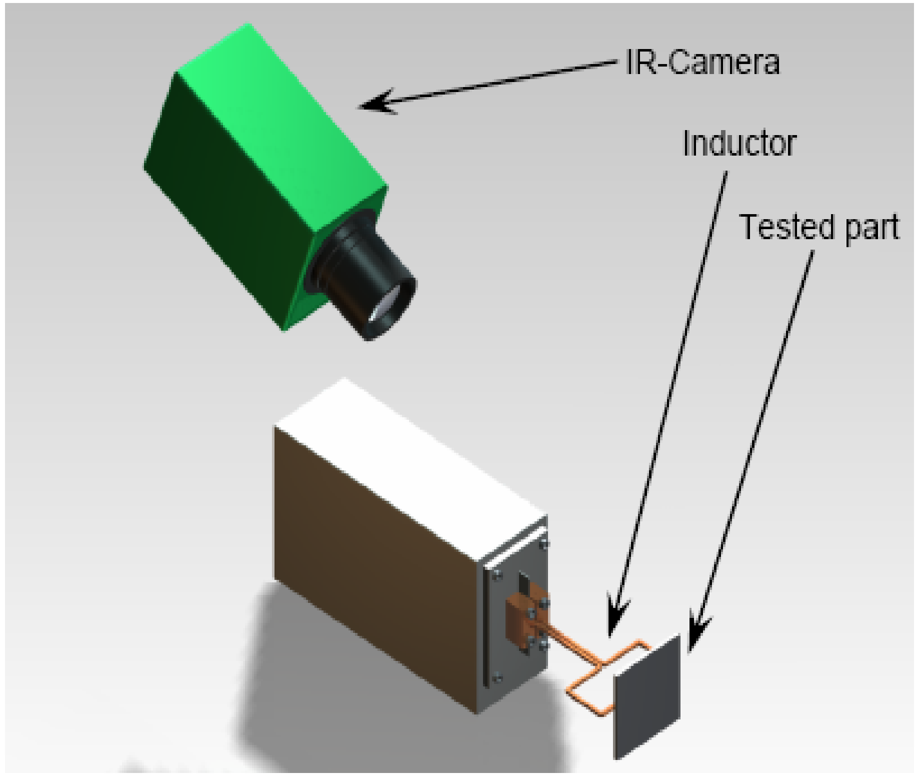

Linear variable differential transformer (LVDT)

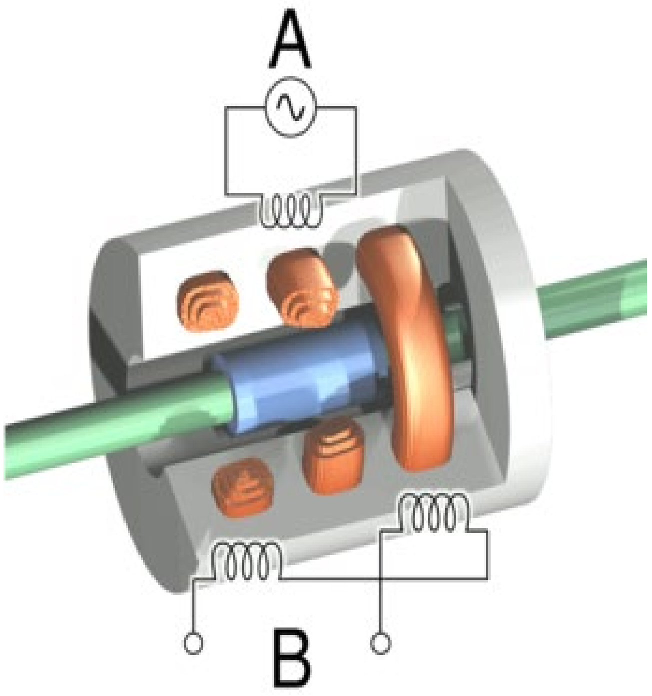

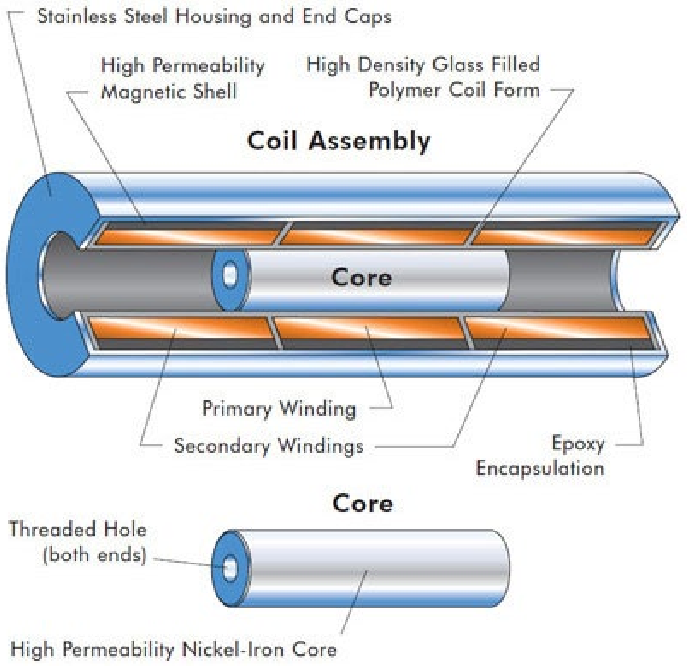

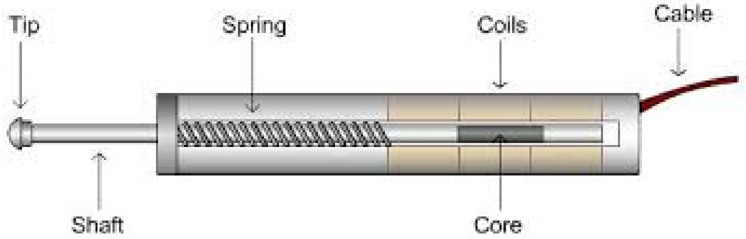

Equivalent circuit:

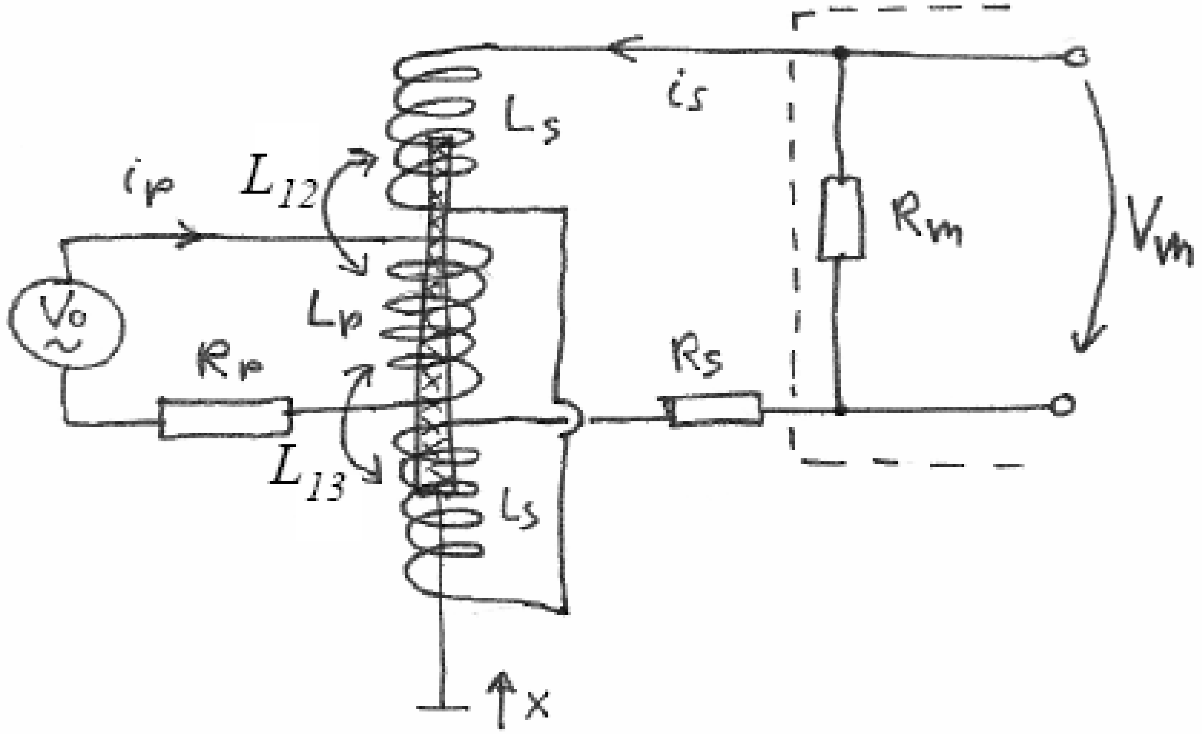

Excitation circuit: $V_0 = R_p i_p + j\omega L_p \cdot i_p + j\omega\left(L_{12} - L_{13}\right)\cdot i_s$

Detection circuit: $0 = R_s i_s + 2 j\omega L_s \cdot i_s + j\omega\left(L_{12} - L_{13}\right)\cdot i_p + V_m$ with $V_m = R_m i_s$

Solution generale :

$$V_m = \frac{j\omega R_m \left[L_{13}(x) - L_{12}(x)\right]}{R_p(R_s + R_m) + j\omega\left[2L_s R_p + L_p\left(R_s + R_m\right)\right] - \omega^2\left[L_p L_s + \left(L_{12}(x) - L_{13}(x)\right)^2\right]} V_0$$

For $R_m \to \infty$ (high input impedence) →

$$V_m \cong \frac{j\omega\left[L_{13}(x) - L_{12}(x)\right]}{R_p + j\omega L_p} V_0$$

For small displacement

$$L_{12}(x) = L_{12}(0) + Ax + Bx^2 + \dots \qquad L_{13}(x) = L_{13}(0) - Ax + Bx^2 - \dots$$

For $x \to 0$

$$L_{12}(x) - L_{13}(x) = 2Ax$$

$$V_m \cong V_0 \frac{-2j\omega A}{R_p + j\omega L_p} x$$

If $j\omega L_p >> R_p$

Amplitude $|V_m| = V_0 \frac{2A}{L_p}|x|$ Phase $\Phi_m = \frac{\pi}{2}\frac{x}{|x|}$

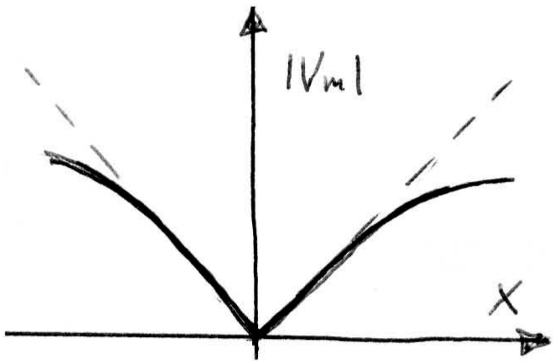

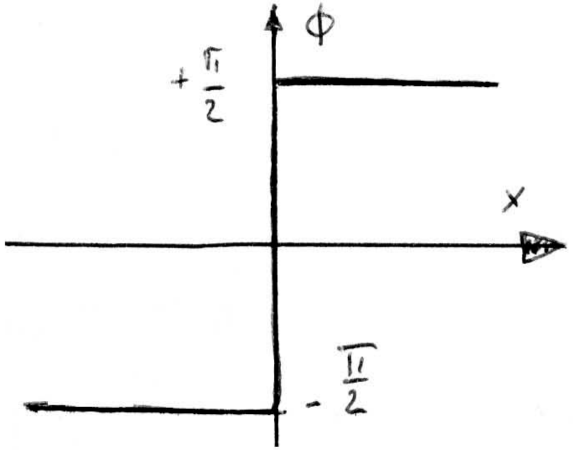

Synchronous demodulation for the LVDT

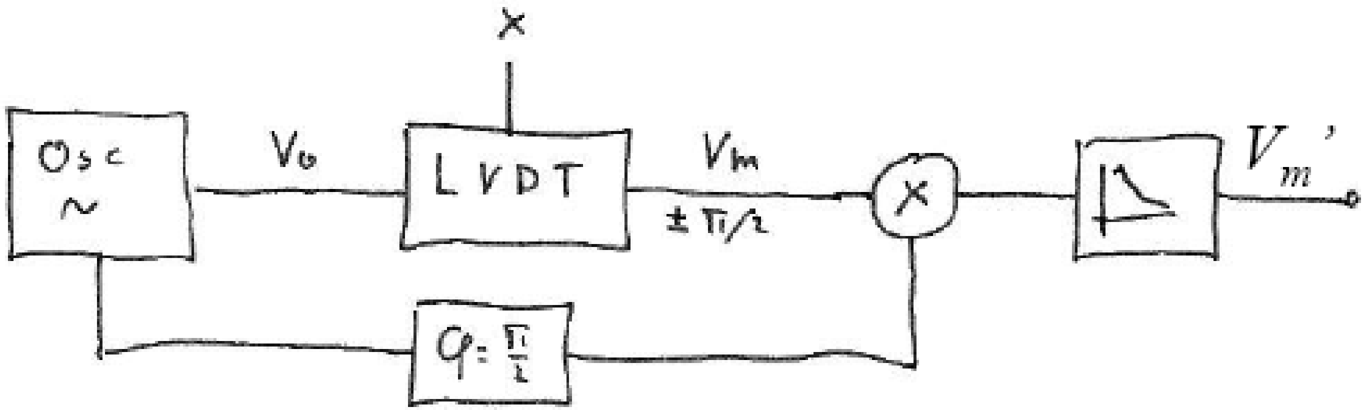

Signal after demodulation :

$$V_m' = V_0 \frac{2A}{L_p} x$$

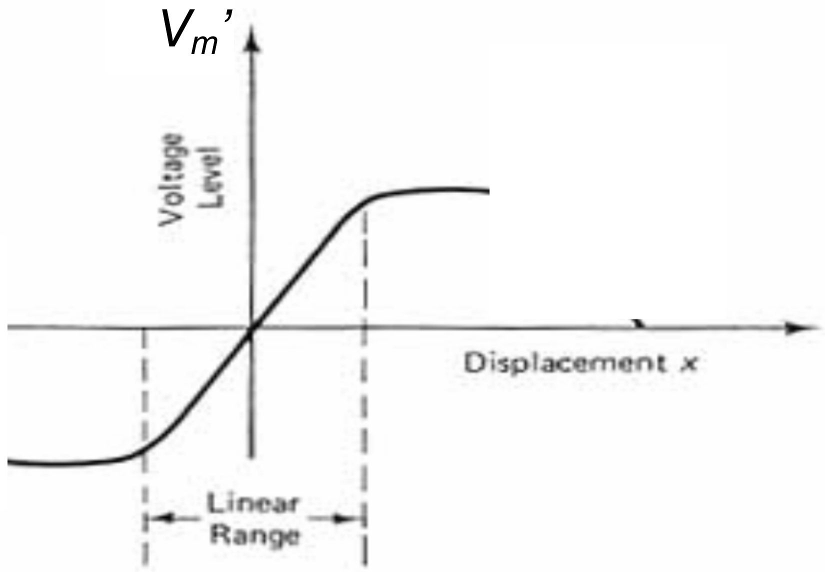

RF tags (chipless RF ID)

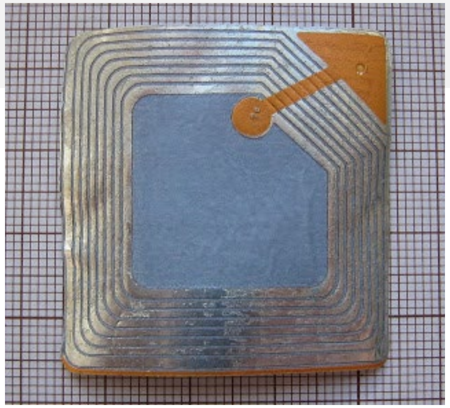

LC resonator:

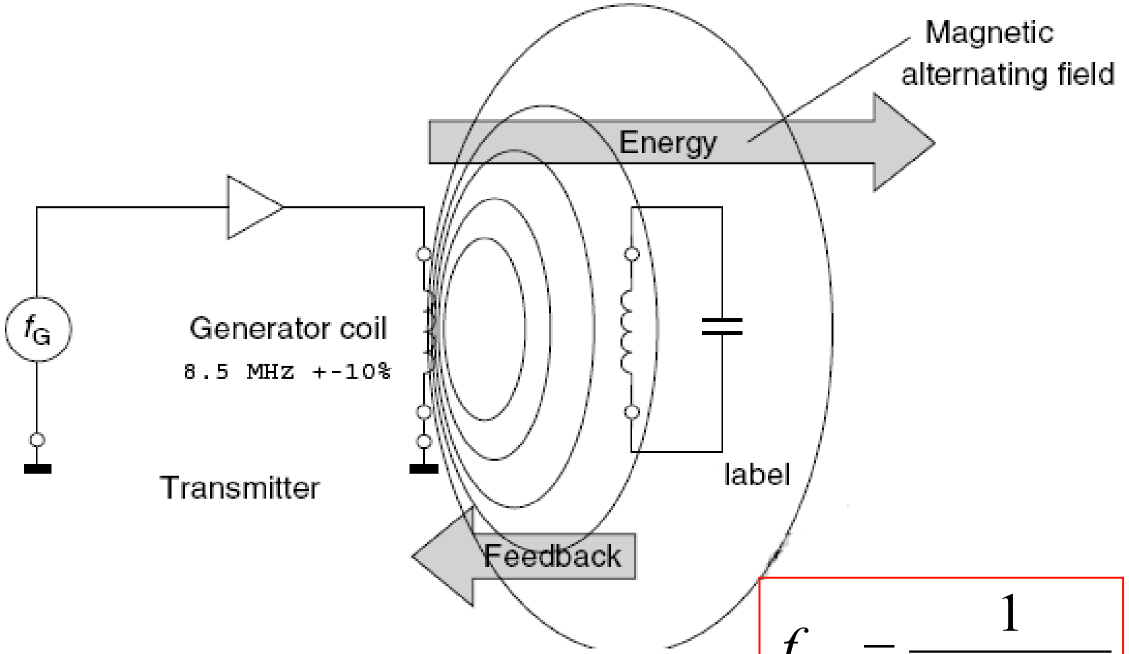

$$f_{rés} = \frac{1}{2\pi\sqrt{LC}}$$

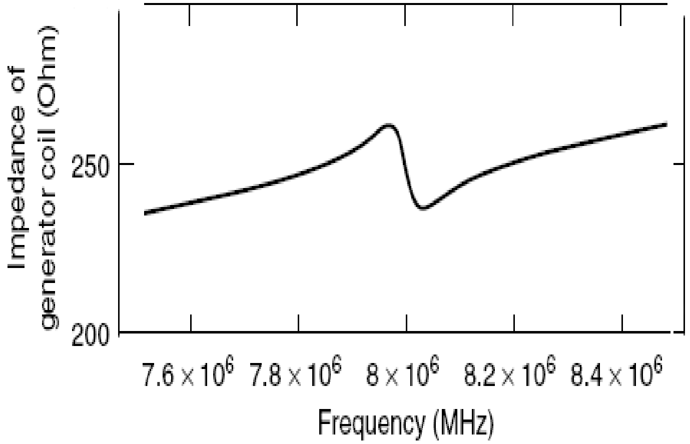

- The presence of the LC-resonator (Label) is detected by measuring the impedence of the transmitter (Generator) coil as a function of the frequency
- Standard frequencies: between 2 MHz and 8 MHz
- The tag can be deactivated by a strong RF pulse that destroy the capacitor of the tag.
- Detection distance: typically 1 m

RF ID

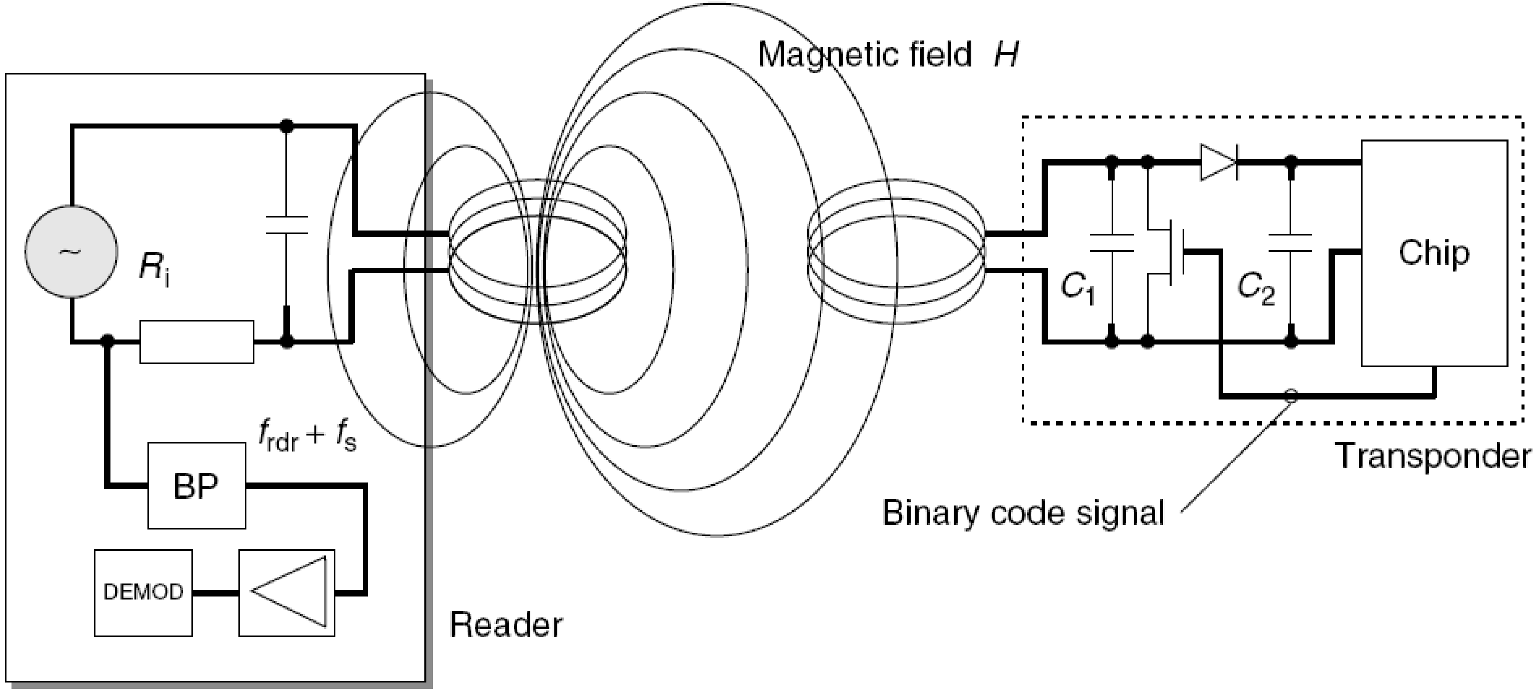
Magnetic field H
~
Ri
frdr + fs
BP
DEMOD
Reader
C1
C2
Chip
Transponder
Binary code signal

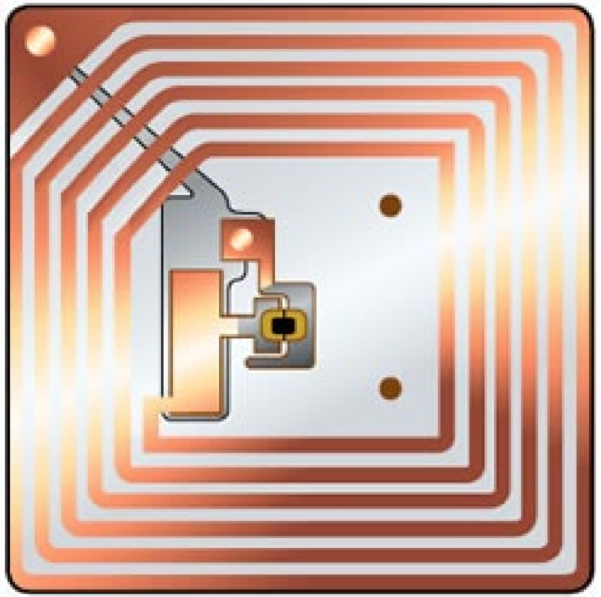

Magnetic tags

- Soft ferromagnet + Semi-Hard ferromagnet.

Enable/Disable :

- Semi-Hard ferromagnet magnetized or demagnetized (with demagnetization loops).

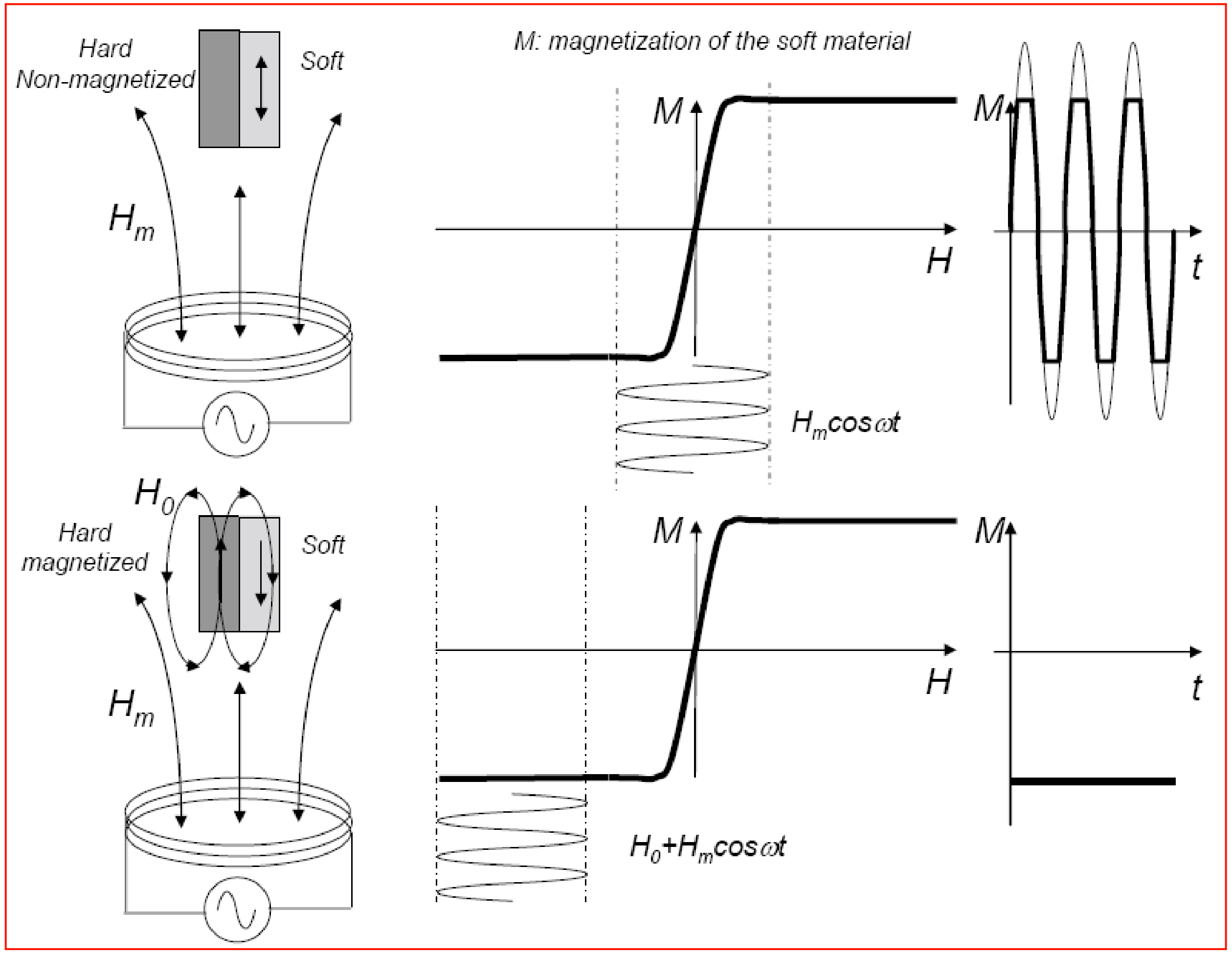

Magneto-acoustic tags

Magnetostrictive material + hard magnetic material

$$F_0 = \frac{1}{2\pi}\sqrt{\frac{E}{\rho}}$$

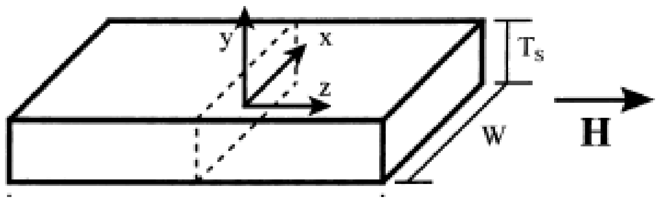

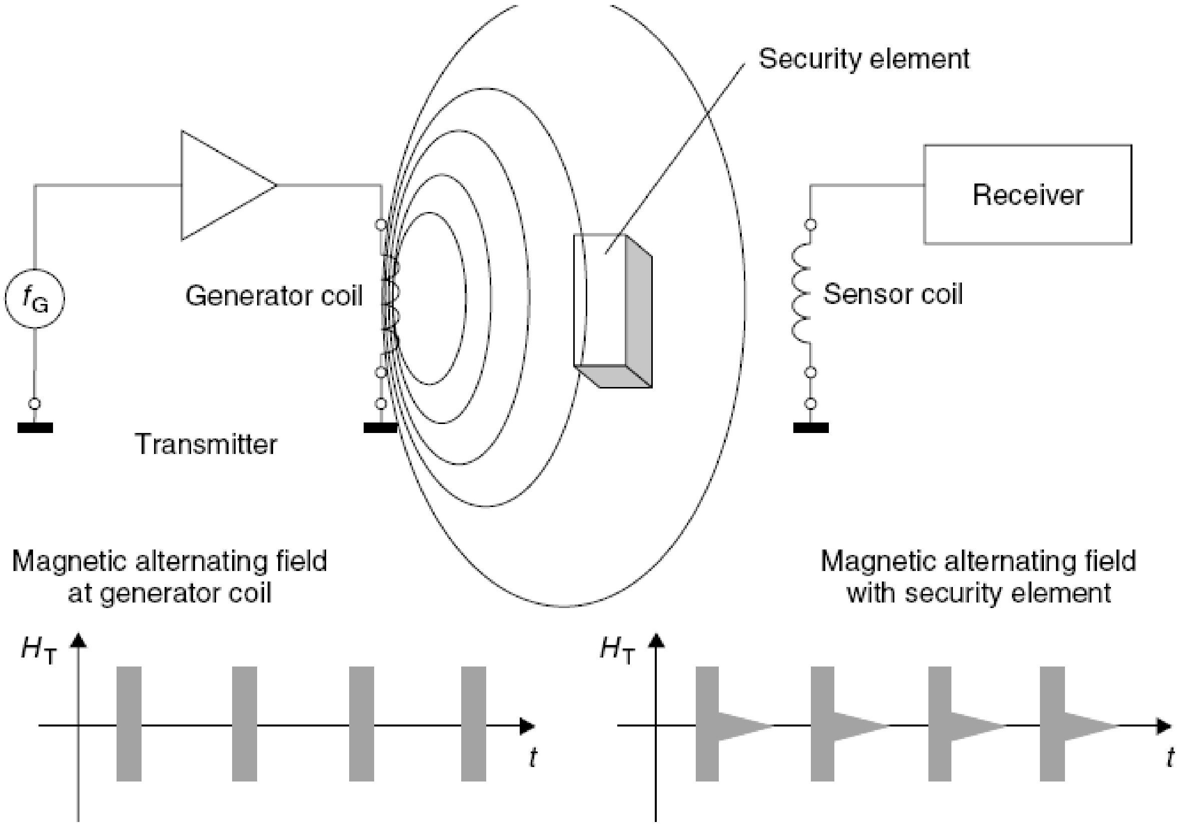

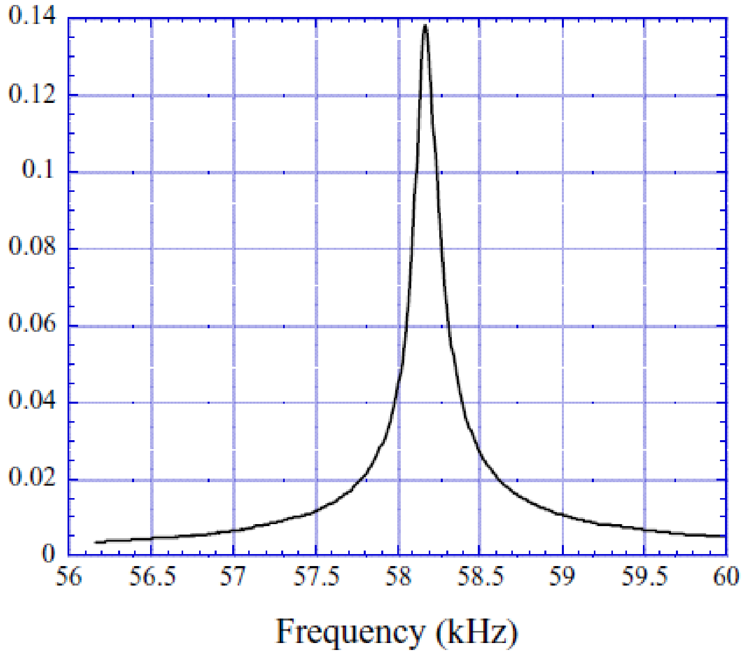

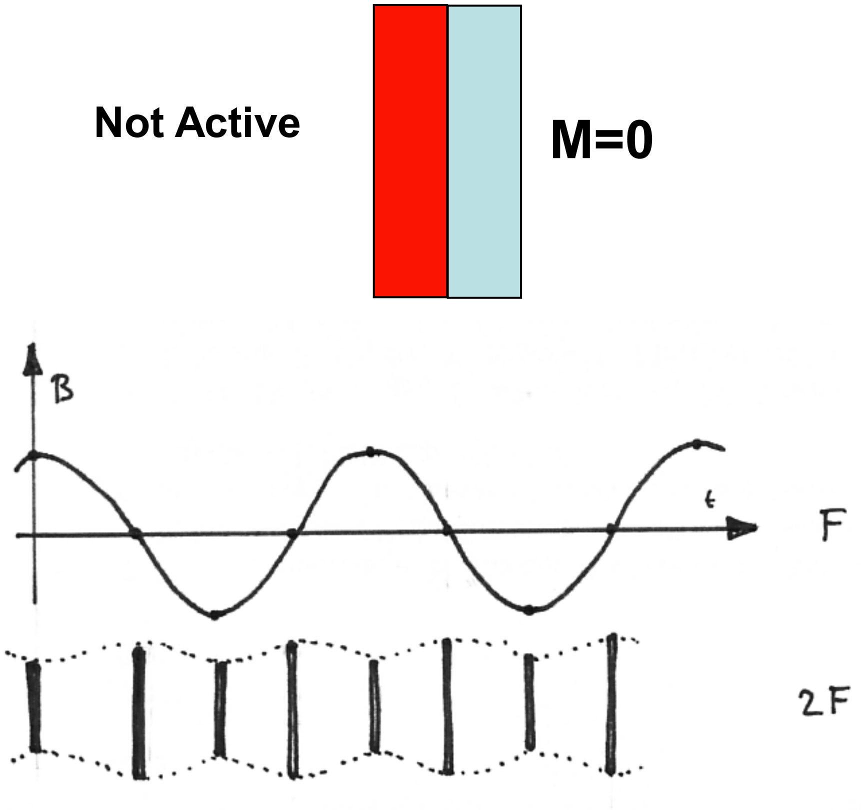

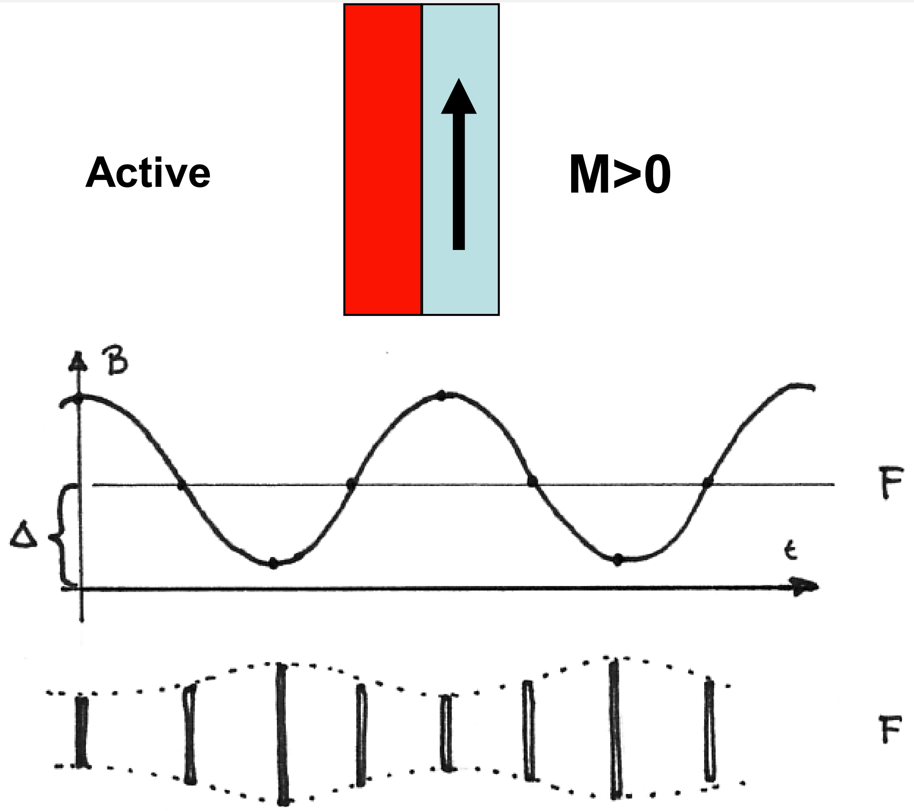

Exitation frequency: F

Mechanical resonance frequency: F_0

$B = B_0 \cos(2\pi F t)$

$F = F_0$